Unraveling the Molecular Mechanisms that Orchestrate Electron Transfer in Anaerobic Respiratory Metabolism of *Shewanella oneidensis* MR-1

Sónia Estêvão Neto

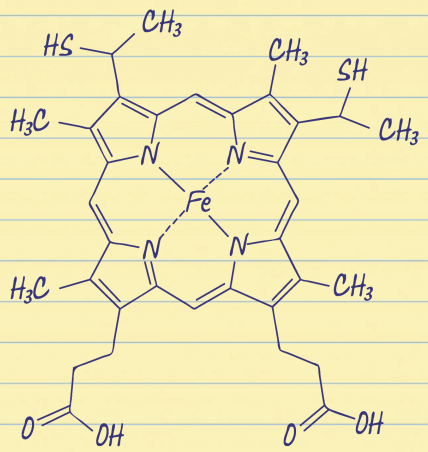

- SOMR-1
- outer-membrane
- electron transfer
- multiheme cytochromes
- periplasm
- NMR
- heme proteins
- iron reduction
- electron shuttles
- microbial fuel cells
- paramagnetic

Dissertation presented to obtain the Ph.D degree in Biochemistry

Instituto de Tecnologia Química e Biológica António Xavier | Universidade Nova de Lisboa

Oeiras,
February, 2017

UNIVERSIDADE NOVA DE LISBOA

Unraveling the Molecular Mechanisms that Orchestrate Electron Transfer in Anaerobic Respiratory Metabolism of *Shewanella oneidensis* MR-1

Sónia Estêvão Neto

Dissertation presented to obtain the Ph.D degree in Biochemistry

Instituto de Tecnologia Química e Biológica António Xavier | Universidade Nova de Lisboa

Oeiras, February, 2017

Ao meu amigo Santos.

Acknowledgments

I always knew that I wanted a PhD. I wanted all the things a person can take out from this experience and the knowledge that we get during the process, not only the scientific one. This thesis and the work here developed was only possible with the help of several people that I would like to thank.

First of all I would like to thank my team of supervisors, Doctor Ricardo Louro and Doctor Catarina Paquete. If one is the “yin” the other one is the “yang”, and it was the complement of both that helped this work to be a success. I was very lucky to have had the opportunity to get the best from both of you.

To Ricardo Louro, for giving me the opportunity to work in his lab, for always believing in me and in my capabilities and most of all, for not giving up on me. Working with him for almost seven years has been quite a ride, but we always manage to have success in the tasks we proposed to do. I have to thank all the “nada temas” that kept me going in several occasions.

To my co-supervisor Catarina Paquete, which is a fundamental piece in this lab and whose practical way of being helped to get the work moving when it seemed that was in a death-end.

To the members of my thesis committee, Doctor Teresa Catarino and Professor Miguel Teixeira, for their advice and dedication during the evolution of the work.

To Professor Maycock, for allowing me to do the synthesis of labelled δ-ALA in his laboratory, leading to a very nice work published in a great magazine.

To Bruno Fonseca, my mentor in the *Shewanella* world. We were kind of a team in this lab and I am very thankful for the support that he gave me in several hard situations. Also thank you for all the joyful times we spend in 3.18.

To Alexandra, because it was always easy to work, and run the lab next to her. Thank you for the talks, the laughs and everything else.

To Ivo Saraiva, I felt very honoured in each conversation we had about complicated theoretical things of the NMR.

To all my colleagues in the Inorganic Biochemistry and NMR group during the time I spend here, that always helped lightning the spirit (most of the times) and to kept the work going.

To Isabel Pacheco for the help in managing the laboratory.

To my friends in the 5th floor that were a support for so many circumstances and to whom I could always count: Marta, Luís, Laura, Ana, Sara, Dusica, Carla, Tiago, Nuno, Paula. To my friends in the other floors. Sónia, Mariana, Inês and all the others that I forgot to mention.

To all the colleagues and workers at ITQB, for the help in several situations.

Finalmente tenho que agradecer às pessoas mais importantes da minha vida, os meus pais. Obrigada por acreditarem em mim, por me apoiarem para lá de tudo o que eu podia imaginar e por me fazerem acreditar que eu sou capaz realizar de qualquer projecto a que me proponha.

Thesis Publications

Rosa, L. F., Neto, S. E., Alves, A. S., and Louro, R. O. (2013). Electrocatálise Microbiana: Uma Plataforma Versátil para Processos Industriais Sustentáveis. *Biotecnol. Soc. Port. Biotecnol.* 3, 33–34.

Neto, S. E., Fonseca, B. M., Maycock, C., and Louro, R. O. (2014). Analysis of the Residual Alignment of a Paramagnetic Multiheme Cytochrome by NMR. *Chem. Commun.* 50, 4561–4563.
doi:10.1039/c3cc49135h.

Alves, M. N., Neto, S. E., Alves, A. S., Fonseca, B. M., Carrêlo, A., Pacheco, I., Paquete, C. M., Soares, C. M., Louro R. O. (2015). Characterization of the Periplasmic Redox Network that Sustains the Versatile Anaerobic Metabolism of *Shewanella oneidensis* MR-1. *Front. Microbiol.* 6, 1–10.
doi:10.3389/fmicb.2015.00665.

Neto, S. E., Paquete, C. M., de Melo-Diogo, D., Correia, I. J., Louro, R. O. (2017) Characterization of OmcA Mutants from *Shewanella oneidensis* MR-1 to Investigate the Molecular Mechanisms Underpinning Electron Transfer Across the Microbe-Electrode Interface
(submitted to Fuel Cells)

TITLE

Unraveling the Molecular Mechanisms that Orchestrate Electron Transfer in Anaerobic Respiratory Metabolism of *Shewanella oneidensis* MR-1

AUTHOR

Sónia Estêvão Neto

COVER IMAGE DESIGN

Raquel Strecht

Printed in Portugal

Contents

Abbreviations and Acronyms

^{13}C	Carbon-13
A, Abs	Absorbance
AQDS	Antraquinone 2,6-disulfonate
Arg	Arginine
β_d, K_d	Dissociation constant
ccm	Cytochrome *c* maturation
$\Delta\delta_{bind}$	Chemical shift perturbation
δ-ALA	δ -aminolevulinic acid
DEAE	Diethylaminoethanol
DMSO	Dimethyl sulfoxide
EPR	Electron paramagnetic resonance
FAD	Flavin adenine dinucleotide
FMN	Flavin mononucleotide
Fw	Forward
GROMOS	GROningen MOlecular Simulation
H	Histidine
His-tag	Histidine tag
HMQC	Heteronuclear multiple-quantum correlation
HTP	Hydroxyapatite
IUPAC-IUB	International union of pure and applied chemistry-International union of biochemistry and molecular biology
LB	Lysogeny broth

M	Methionine
MECs	Microbial electrosynthesis cells
METs	Microbial electrochemical technologies
MFCs	Microbial fuel cells
MQ	Menaquinone
MQH_2	Menaquinol
NMR	Nuclear magnetic resonance
NOESY	Nuclear Overhauser effect spectroscopy
OMC	Outer-membrane cytochrome
OTR	Octaheme tetrathionate reductase
PDB	Protein data bank
PMS	Phenazine methosulfate
Pro	Proline
RDC	Residual dipolar coupling
Rev	Reverse
RF	Riboflavine
SAXS	Small- angle X-ray scattering
SDS-PAGE	Sodium dodecyl sulphate-polyacrylamide gel electrophoresis
Ser	Serine
SOMR-1	*Shewanella oneidensis* MR-1
STC	Small tetraheme cytochrome
TB	Terrific broth
Thr	Threonine
TMAO	Trimethylamine N-oxide

TPPI	Time-proportional phase incrementation
UV-Vis	Ultraviolet-visible spectroscopy
wt	Wild type

Abstract

Among the portfolio of proposals for sustainable industrial processes, Microbial Electrochemical Technologies (METs) are emerging as a versatile option with multiple potential applications, such as bioremediation of metal contamination, wastewater treatment, and electricity production in microbial fuel cells (MFC). Such systems rely on microorganisms with the ability to transfer or receive electrons from electrodes, enabling the operation of these bioelectrochemical systems.

Shewanella oneidensis MR-1 (SOMR-1) is a sedimentary Gram-negative bacterium with a highly versatile metabolism, uniquely suited for the operation of METs. This bacterium has the ability to link its bioenergetic metabolism through the periplasm to reduce extracellular electron acceptors, like electrodes. SOMR-1 was shown to reduce a wide variety of soluble and insoluble compounds, such as metals, like iron or small molecules such as DMSO, nitrite or fumarate. However, the pathways leading to the reduction of those compounds are not completely clarified.

The present work proposes to understand specific electron transfer pathways orchestrated by this bacterium, from inside the cells to the final electron acceptors, with the goal is to clarify if the electron transfer across the periplasm is specific for each terminal electron acceptor, or if it is common for the different respiratory processes. This information will guide efforts to optimize electron transfer in METs.

The two most abundant cytochromes of SOMR-1, the small tetraheme cytochrome (STC) and FccA, are found in the periplasmic space and are responsible for two non-mixing pathways for metal reduction. Both cytochromes can transfer electrons to the membrane complex, MtrCAB, which is the major responsible for extracellular iron reduction. Interactions, followed by NMR, showed that these two proteins bind to the cytochrome facing the periplasm, MtrA, in the same or at least closely related locations, given that saturation of MtrA with FccA prevents the binding of STC.

The two existing periplasmic pathways for the reduction of iron suggested the hypothesis that both STC and FccA work as shuttles in the periplasm and may be involved in other respiratory processes. Interactions between STC or FccA with nitrite reductases and DMSO reductases, showed that STC is a promiscuous mobile redox protein responsible for the periplasmic electron transfer to iron-, nitrite- and DMSO-reductases, in contrast with FccA that does not participate in these reduction pathways.

Iron reduction by SOMR-1 is mainly associated with outer membrane cytochromes (OMC) that perform this activity by two mechanisms: a) direct contact (OMCs or nanowires), and b) indirect contact (using soluble electron shuttles that transport electrons from the cells to final electron acceptors). Among SOMR-1 OMCs, the decaheme cytochromes MtrC and OmcA from the complex MtrCAB-OmcA were shown to be essential in metal reduction. These cytochromes are located in the same

operon but they have distinct localizations and functions in the cells. OmcA is a lipoprotein found in the external part of the outer-membrane, is the most abundant cytochrome located on the outer surface of SOMR-1 cells, and is the major responsible for extracellular electron transfer to terminal electron acceptors and electron shuttles and cells attachment to electrodes.

Characterization of the interactions between OmcA and its physiological partners (iron oxides and/or mobile electron shuttles) was performed using NMR spectroscopy and stopped-flow experiments followed spectrophotometrically. Using site-directed mutagenesis, axial ligands of the hemes of OmcA were modified to investigate the effect of that change on the interaction and reactivity of OmcA with electron shuttles. The kinetics of oxidation of mutant of heme VII of OmcA by redox shuttles was different when compared with the wtOmcA, with the thermodynamic equilibrium of the reaction being established with less cytochrome oxidized. This suggests a change in the reduction potential of that heme of OmcA. Moreover, NMR spectroscopy showed that the perturbation in the heme VII is the one that most affects interaction between the cytochrome and the redox shuttle FMN. The dissociation constant for the binding between FMN and the mutant of heme VII axial ligand increase almost 5 times. However, the stoichiometry of binding was not affected, 1:2 (OmcA:FMN), remaining equal to that observed between FMN and native OmcA.

Altogether, the results indicate that mutation of heme VII changes the driving force of electron transfer towards electron shuttles and disturbs the flavin binding site near heme VII.

In order to better understand electron transfer pathways within SOMR-1, a detailed thermodynamic characterization of these complex multiheme cytochromes is needed. Although the cytochromes under study are paramagnetic, a feature that facilitates their characterization using spectroscopic methods, the majority of these multiheme cytochromes display a high number of hemes making functional characterization very difficult. With the goal to develop an effective strategy to study and characterize multiheme cytochromes, a technique was developed to assess the hemes' organization inside the structure of cytochromes. STC, which is well characterized structurally, was used as a model protein to determine the relative orientation of the hemes within the cytochrome. Since STC hemes are low-spin paramagnetic in the oxidized state, the whole cytochrome tends to adopt a preferential orientation with respect to an external magnetic field, due to the unpaired electrons in the hemes. This enables the use of nuclear magnetic resonance (NMR) to measure residual dipolar couplings (RDCs) between NMR active nuclei in the cytochrome. The RDCs revealed that the rhombicity of the electronic structure of low-spin paramagnetic hemes determines how much each heme contributes to the preferential orientation of protein when placed in a strong magnetic field. Since the rhombicity of the electronic structure of low-spin paramagnetic hemes can be determined from the paramagnetic chemical shifts of the heme

signals, the RDCs enable the determination of the relative orientation of hemes in multiheme proteins and enzymes for which structures are not available, provided that the heme signals are assigned.

Overall, the work presented in this thesis clarified the electron transfer pathways across the periplasm of SOMR-1 towards soluble and insoluble terminal electron acceptors such as iron, nitrite and DMSO. Finally, new methodologies were developed for the characterization of complex multiheme cytochromes. This knowledge is essential to understand the electron transfer processes performed by SOMR-1 and fully profit from its ability to reduce a wide diversity of compounds in its application in METs.

Resumo

As Tecnologias Electroquímicas Microbianas (METs) têm surgido como uma opção versátil no desenvolvimento de processos industriais sustentáveis. A biorremediação de locais contaminados com metais, o tratamento de águas residuais e a produção de eletricidade em células de combustível microbiano, são alguns dos exemplos deste tipo de tecnologias. Para funcionar, estes sistemas dependem de microorganismos que possuam a capacidade de transferir ou receber electrões de e para eléctrodos.

Shewanella oneidensis MR-1 (SOMR-1) é uma bactéria sedimentar, Gram-negativa, que tem um metabolismo energético bastante versátil, sendo por isso adequada para a operação em METs. Esta bactéria consegue ligar o seu metabolismo bioenergético desde o interior da célula até ao meio extracelular, através do periplasma, de modo a reduzir aceitadores de electrões extracelulares, como por exemplo eléctrodos. SOMR-1 tem a capacidade de reduzir uma grande variedade de compostos solúveis e insolúveis, tais como metais (p.e. ferro) ou moléculas pequenas como DMSO, nitrito ou fumarato. No entanto, as vias de transferência electrónica que conduzem à redução desses compostos não estão completamente esclarecidas.

O trabalho desenvolvido nesta tese propõe-se a elucidar as vias de transferência electrónica usadas por SOMR-1, desde o interior das células, até aos aceitadores finais de electrões. O objetivo é perceber se a transferência electrónica no periplasma é específica para cada

aceitador final de electrões ou se é comum entre diferentes processos respiratórios.

Os dois citocromos mais abundantes de SOMR-1 são o STC (um pequeno citocromo tetrahémico) e o FccA. Ambos co-existem no espaço periplásmico e são responsáveis pela redução de metais através de duas vias de transferência electrónica independentes. Ambos os citocromos transferem electrões para o complexo membranar MtrCAB, o principal responsável pela redução extracelular de ferro. Interacções, seguidas por ressonância magnética nuclear (RMN), mostraram que estas duas proteínas se ligam ao MtrA no mesmo local ou em dois locais próximos, uma vez que a saturação de MtrA com FccA impede a ligação de STC.

O facto de existirem duas vias de transferência electrónica independentes no periplasma, envolvidas na redução de ferro, deu origem à hipótese de que o STC e o FccA poderão funcionar como transportadores de electrões no periplasma e estarem envolvidos em outras vias respiratórias. Interações entre o STC ou o FccA com duas nitrito-reductases e uma DMSO reductase mostraram que o STC pode de facto funcionar como um transportador de electrões no periplasma uma vez que está envolvido na transferência electrónica para ferro, nitrito e DMSO-reductases. Contrariamente ao FccA que participa apenas na redução de ferro e fumarato.

A redução de ferro por SOMR-1 depende de citocromos associados à membrana externa (OMC) que reduzem os substratos através de dois mecanismos: a) contato directo (OMCs ou “nanowires”) e b) contato indirecto (transportadores solúveis de electrões transportam os

electrões das células para os aceitadores finais). Entre os OMCs de SOMR-1, os citocromos decahémicos MtrC e OmcA, do complexo MtrCAB-OmcA mostraram ser essenciais na redução de metais. Estes citocromos são codificados pelo mesmo operão mas têm localizações e funções distintas na célula. O OmcA é uma lipoproteína que se encontra na superfície extracelular da membrana externa, é o citocromo mais abundante à superfície das células e o principal responsável pela transferência electrónica para aceitadores finais e transportadores de electrões.

A caracterização das interações entre o OmcA e seus parceiros fisiológicos (óxidos de ferro e/ou transportadores de electrões) foi seguida usando RMN e experiências de fluxo interrompido. Através de mutagénese dirigida, os ligandos axiais dos hemos do OmcA foram modificados, e verificou-se o efeito dessa modificação na interacção e na reactividade do OmcA com vários transportadores de electrões. Verificou-se que a cinética de oxidação do mutante do hemo VII é diferente da observada para o wtOmcA., sendo o equilíbrio termodinâmico da reacção estabelecido com uma maior fracção de citocromo reduzido. Isto sugere uma mudança no potencial de redução do OmcA. Usando espectroscopia de RMN mostrou que a mutação no hemo VII é a que mais afeta a interacção entre o citocromo e o transportador de electrões FMN. Apesar da constante de dissociação da reacção de formação do complexo entre o FMN e o OmcA com a mutação no hemo VII aumentar aproximadamente 5 vezes, a estequiometria do complexo não foi afectada, permanecendo igual ao

observado entre o FMN e OmcA nativo (1:2 (OmcA:FMN)). Em suma, os resultados indicam que a mutação do hemo VII altera a força motriz da transferência electrónica para transportadores de electrões e afecta o local de ligação de flavinas existente perto do hemo VII.

Para melhor perceber os mecanismos de transferência electrónica orquestrados por SOMR-1, é necessária uma caracterização termodinâmica detalhada dos citocromos multihémicos envolvidos nesses porcessos. Apesar dos citocromos em estudo neste trabalho serem paramagnéticos, uma característica que facilita a sua caracterização através de métodos espectroscópicos, a maioria deles possui um elevado número de hemos, o que torna a sua caracterização funcional muito difícil. Com o objetivo de desenvolver uma estratégia eficaz para estudar e caracterizar citocromos multihémicos, foi desenvolvida uma técnica para avaliar a organização dos hemos dentro da estrutura tridimensional dos citocromos. O STC, um citocromo tetrahémico caracterizado, estrutural e funcionalmente em detalhe, foi usado como proteína modelo para determinar a orientação relativa dos hemos dentro do citocromo. Como os hemos do STC são paramagnéticos e de baixo spin no estado oxidado, o citocromo tende a adotar uma orientação preferencial quando sujeito a um campo magnético externo, devido à presença dos electrões desemparelhados nos hemos. Isto permite medir acoplamentos dipolares residuais (RDCs) entre os núcleos activos no RMN que existam no citocromo. Os RDCs revelaram que a rombicidade da estrutura electrónica dos hemos de baixo spin pode ser usada para determinar a contribuição de cada hemo

para a orientação preferencial das proteínas quando colocadas sob um campo magnético forte. Uma vez que a rombicidade da estrutura electrónica dos hemos paramagnéticos de baixo spin pode ser determinada a partir das mudanças dos desvios químicos dos sinais dos hemos, é possível, a partir dos valores dos RDCs determinar a orientação relativa dos hemos em proteínas multihémicas para as quais as estruturas não estão ainda disponíveis. Isto desde que os sinais dos hemos estejam atribuídos.

Em conclusão, o trabalho apresentado nesta tese permite esclarecer as vias de transferência electrónica ao longo do periplasma de SOMR-1 para aceitadores de electrões solúveis e insolúveis, como por exemplo ferro, nitrito e DMSO. Adicionalmente, foi desenvolvida uma nova metodologia para caracterizar citocromos multihémicos. Este conhecimento é essencial para compreender os processos de transferência electrónica realizados por SOMR-1 de modo a aproveitar plenamente a sua capacidade para ser aplicada em METs.

Chapter I

Introduction

Contents

Chapter I is adapted from my contributions to the paper

Rosa, L. F., Neto, S. E., Alves, A. S., and Louro, R. O. (2013). Electrocatálise Microbiana: Uma Plataforma Versátil para Processos Industriais Sustentáveis. *Biotecnol. Soc. Port. Biotecnol.* 3, 33–34.

1. Introduction

The energy needs of the world are increasing due to the evolution of the quality of life in the developed world. Current energy generation methods are unsustainable because they consume non-renewable resources and produce greenhouse gases that are causing global warning.

A sustainable production of energy must include a carbon-neutral and renewable technology. There is a portfolio of technologies based on solar, wind and biomass that are being explored in order for the Earth to be more sustainable.

Among the several options available biomass is very promising because is a cheap resource that is used in microbial electrochemical systems with diverse purposes that will be highlighted further.

2. Microbial Electrochemical Technologies (METs)

Microbial electrochemical technologies (METs) are unique technologies in the field of clean environmental technologies nowadays. The working principle behind METs is the same as an electrochemical cell, but METs uses microorganisms to catalyse the electrochemical reaction. The electrons involved in that reaction can be transferred to an anode by the microorganisms and used directly for electricity production (microbial fuel cells), or can be obtain from the bioremediation of contaminants

(microbial remediation cells), or used in the cathode for chemical synthesis (microbial electrolysis cells, microbial electrosynthesis) (Gregory and Lovley, 2005; Liu et al., 2004, 2010; Rabaey and Rozendal, 2010). The development of these systems combines a wide diversity of scientific areas, such as microbiology, electrochemistry, materials science and engineering.

METs can work either with microorganisms growing in the anode compartment (bioanode), in the cathode compartment (biocathode) or can work with a combination of bioanode and biocathode in a dual chamber or a single chamber device. In METs with bioanodes the microorganisms are used to oxidize an electron donor that can be organic matter, sediments, photosynthetic microorganisms, or *in situ* photosynthesized plant rhizodeposits (Hamelers et al., 2010) and transfer the electrons to the electrode. In biocathodes, microorganisms catalyse the oxidation of the electrode and the electrons are used by the microorganisms for example, for nitrate reduction and hydrogen production (Clauwaert et al., 2007; Rozendal et al., 2008). The phenomenon of electrons being released and accepted by microorganisms shed light into the possibility of such processes occurring naturally (Logan, 2009) and brought into light the idea for the first MET created (Potter, 1911).

In a METs the anode is maintained in anoxic conditions and a culture of the microorganisms oxidize organic or inorganic electron donors (usually waste waters or waste materials) transferring the electrons to the

electrode. The first applications were the implementation of microbial fuel cells (MFCs) for direct production of electric energy (Logan et al., 2006). MFCs have been optimized specially for the use of wastewaters, both domestic or from the industry, where the substrate and the microorganisms used were the ones naturally present in those waters (Logan and Regan, 2006). Although these MFCs could produce energy, the value of the production was not considered economically viable (Logan and Rabaey, 2012). Microorganisms used in the anode compartment of METs are called exoelectrogens, because of their ability to transfer electrons from their intracellular metabolism to extracellular acceptors using redox proteins that span across the cell membrane, delivering the electrons to the final electron acceptor.

Microbial electrosynthesis cells (MEC) are devices that use microorganisms in the cathode compartment, where they are responsible for the production of organic or inorganic chemical compounds with high market value using low value material as starting material (Rabaey and Rozendal, 2010). MEC first applications were towards the production of hydrogen, nowadays called microbial electrolysis cells (Liu et al., 2010). It will be expected that such approach, which combines microbial activity with the use of low value matter leads to a decrease in the energy spent by the system, when compared with the classic form of production, leading to more efficient synthetic processes.

Figure 1 summarizes the reactions that may occur in anodes and cathodes of METs.

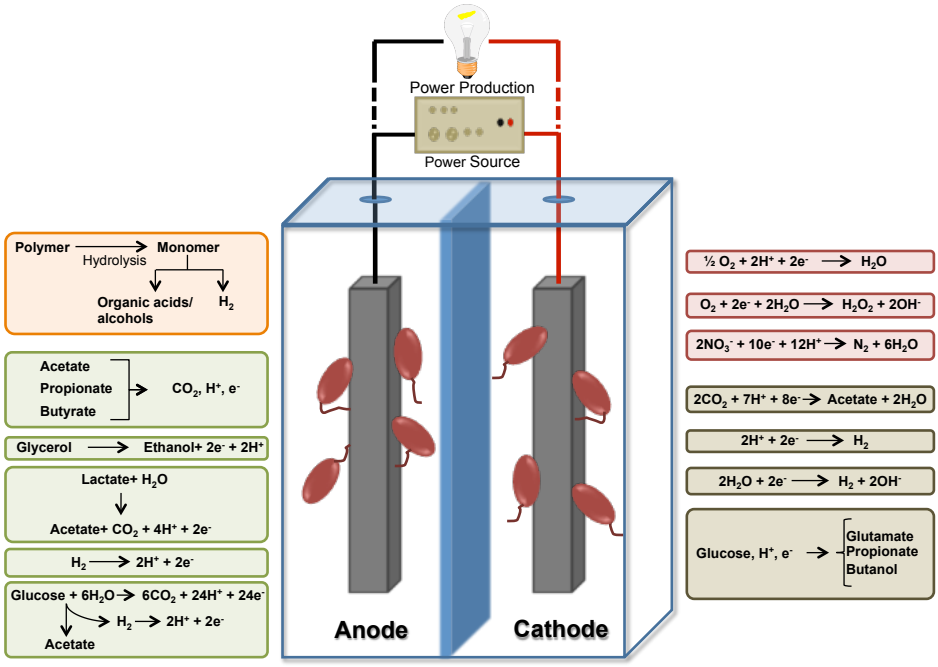

Figure 1. Anodic and catodic reactions possible to occur in METs, in a dual chamber cell. Reactions on the electrodes can be performed by planktonic cells or biofilms attached to the electrodes or by electrochemical catalysis. In the anode compartment, polymeric compounds can be degraded in more simple molecules, with an external energy source that can then be use as energy source (orange) and organic compounds can be converted generating current (green). In the cathode compartment reactions can produce energy or high value compouds, occuring spontaneously (red) or not spontaneous and have the need of an external energy source (grey). Adapted from (Logan and Rabaey, 2012).

The interest in METs has been increasing everyday (Wang and Ren, 2013) because when compared with abiotic fuel cells they are much more economic and safe (Lovley, 2006). Operations in METs generally occur at room temperature and the fuel is often of low-value and safe.

Opposite to abiotic fuel cells that work with fuels that are normally explosive and toxic, and need expensive catalysts to induce oxidation of the electron donor at high temperatures (Lovley, 2006).

Considering the opportunities and challenges in the development of METs, one can considered two different approaches:

1) Applications focused in the treatment of large amounts of substrate, such as wastewater, for production of electricity, hydrogen production, or desalinization of sea water. These systems have a large dependence with the size and distances between the electrodes. Scale up of this type of cells can strongly influence its performance (Logan and Rabaey, 2012). Moreover, the microorganisms need to be able to grow inside the anode compartment, attached to the electrode, making essential the development of electrodes and membranes with a good cost/area relation and that are biocompatible (Schroder, 2012). The other point that should be taken into consideration is the reaction with atmospheric oxygen in the cathode compartment. Cheap catalysts with high efficiency and durability and membranes that do not leak oxygen to the anode are fundamental to construct efficient systems (Rosa et al., 2013).

2) Applications towards the production of high value compounds, during consumption of low value substrates.

Such applications are a challenge because normally the goal is a pure high quality product, which often needs extra steps of production and purification, increasing the costs of the production. To overcome this challenge, there is the need to identified strains able to synthesize the desired product in proper quantity and quality, minimizing the purification steps.

The use of METs in the future has several challenges ahead. However, there is no doubt about the advantages of the use of these technologies in order to close the life cycle of materials. In fact the fuels for METs are residues that otherwise would need to be treated, this way are being used to be converted in electric energy or high value compounds. Therefore introduction of METs in industrial process can strongly diminish the ecological impact of the wide diversity of electrochemical processes.

Research has been concentrating efforts in understanding microbial metabolism towards electrodes of METs with special attention to dissimilatory metal reducing organisms.

3. Dissimilatory Metal Reducing Organisms

Biochemical and microbiological knowledge regarding microorganism metabolism directs the efforts to implement METs using bacteria isolated from marine environments. The proof of concept of METs has

been shown mainly with power generation in MFC using organisms from Proteobacteria, Firmicutes, Acidobacteria phyla and also organisms from the Archaea and Eukarya domains of life (Logan, 2009).

Among the Proteobacteria group, *Shewanella oneidensis* MR-1 (SOMR-1) was the first organism that showed electrical current production in a MFC, using lactate as electron donor and the electrode as electron acceptor in the absence of soluble redox mediators (Kim et al., 2002). Years later, SOMR-1 mutants have produced more current than the wild type (Bretschger et al., 2007), showing that either electron flow in this bacteria can redirect towards specific electron acceptors or biofilms can be induced to increase adhesion of bacteria to electrodes.

Geobacter strains, also from the Proteobacteria group, have been widely used in MFCs for current production (Bond et al., 2002; Bond and Lovley, 2003). *Geobacter* oxidize organic electron donors to carbon dioxide, normally combined with respiration of insoluble final electron acceptors.

Desulfuromonas acetoxidans, *Pseudomonas aeruginosa*, *Escherichia coli*, *Rhodopseudomonas palustris* and *Desulfovibrio desulfuricans* are other examples of Proteobacteria that showed the ability to transfer electrons extracellularly and were used in electrochemical systems (Logan, 2009).

Clostridium butyricum EG3 was the first Gram-positive shown to produce electrical current in a MFC (Park et al., 2001). Several years latter *Thermincola* sp. strain JR, also a Gram-positive bacteria, was identified as the dominant organism in a MFC working in thermophilic

conditions, when acetate was used as electron donor (Wrighton et al., 2008).

Organisms from the domains Archaea and Eukarya also showed electric current production in MFCs (Prasad et al., 2007; Abrevaya et al., 2011).

Although there is a wide diversity of microorganisms able to be used in efficient METs, a marine, or salt tolerant organism like *Shewanella* is more adequate. *Shewanella oneidensis* MR-1 is the most versatile microorganism, able to use a diversity of final electrons acceptors (Logan, 2009), and therefore will be the object of study in this work.

3.1. *Shewanella oneidensis* MR-1

Species from the genus *Shewanella* are facultative Gram-negative bacteria, belonging to the γ-Proteobacteria *pylum* (MacDonell and Colwell, 1985). There are sixty-three different *Shewanella* species recognized until now (accordingly to LPSN; http://www.bacterio.net, September 2016, Appendix 1- Figure 1) and the majority are found in aquatic and sedimentary environments, where organic matter is actively degraded. Such environments vary in nutrient composition, salinity, temperature, redox potential and pressure and these differences in growth conditions produce evolutionary pressure that results in different genotypes between the species (Venkateswaran et al., 1999; Hau and Gralnick, 2007). Among the ones with the genome sequenced, a core genome of 2137 genes is common to all of them (Fredrickson et

al., 2008). Several organisms from this genus have demonstrated preferential metabolism towards metallic electron acceptors, rather than sugars and aminoacids (Nealson et al., 1995), and in fact, the metal reductase containing locus is conserved among several strains of *Shewanella* (Figure 2).

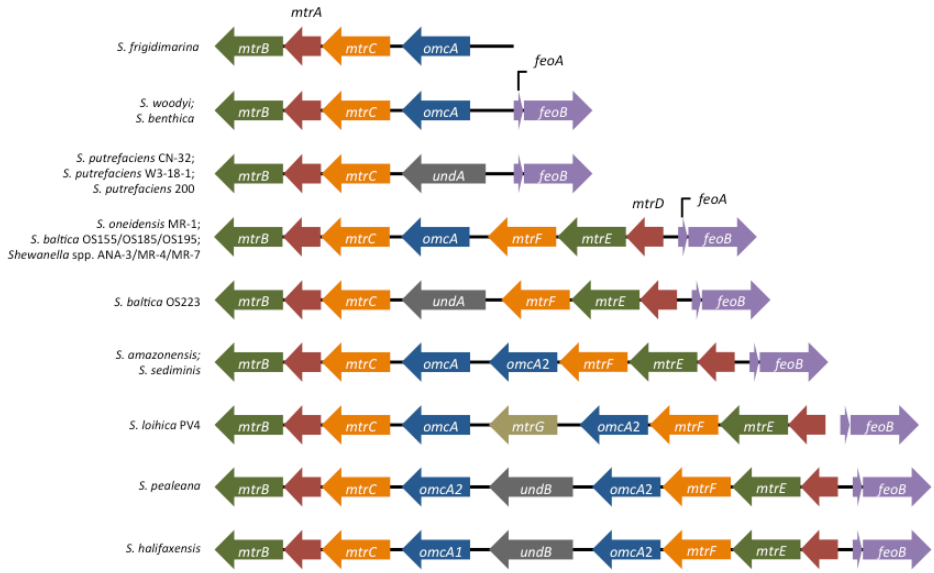

Figure 2. Locus encoding the genes responsible for metal reduction in *Shewanella* species. Adapted from (Fredrickson et al., 2008).

Shewanella oneidensis MR-1 (SOMR-1), formerly known as *Alteromonas putrefaciens* MR-1, was isolated from anaerobic sediments of Oneida Lake (New York) and it was discovered due to an increase in the accumulation of Mn(II) during summer months (Myers and Nealson, 1988) in opposition to the deposition of Mn(IV) during the winter. SOMR-1 was identified as the microorganism present in the sediments responsible for the reduction of manganese during the summer, as a

consequence of the optimal growth temperature for this microorganism.

SOMR-1 has a very versatile metabolism and its genome suggests multiple pathways for catabolism of organic acids, fatty acids, aminoacids, peptides and nucleotides, strongly suggesting the ability of this microorganism to consume a variety of organic matter (Fredrickson et al., 2008). Genome sequencing identified 41 possible *c*-type cytochromes, based on the heme binding motif (CXXCH) (Meyer et al., 2004), which are strongly connected with the versatile metabolism observed in SOMR-1. Electron transfer pathways in SOMR-1 occur towards a wide variety of final electron acceptors, such as oxygen, fumarate, nitrate, nitrite, thiosulfate, sulphur, selenium, trimethylamine N-oxide, dimethyl sulfoxide, anthraquinone-2,6-disolfunate, and soluble and insoluble metals, such as iron, manganese, uranium, chromium, cobalt, technetium and vanadium (Nealson and Saffarini, 1994; Liu et al., 2002; Carpentier et al., 2003; Hau et al., 2008). Moreover, SOMR-1 was the first microorganism shown to perform direct electron transfer to glassy carbon electrodes in MFC (Kim et al., 1999).

Extracellular electron transfer mechanisms were shown to rely on *c*-type cytochromes that are either located in the cytoplasmic membrane, soluble in the periplasm or attached to the outer-membrane, allowing SOMR-1 to reduce extracellular compounds (Meyer et al., 2004; Shi et al., 2007). Electron transfer processes can occur in the periplasmic space, towards the reduction of soluble electron acceptors (Leys et al.,

1999; Gao et al., 2009), or extracellular towards the reduction of insoluble electron acceptors, and are linked to the activity of multiheme cytochromes that shuttles electrons between the cytoplasmic membrane and the external cell wall (Table 1).

Table 1. Multiheme cytochromes involved in electron transfer pathways in SOMR-1.

Cytochrome	Nº of hemes	MW/ kDa	Location	Activity
CymA	4	21	Cytoplasmic membrane	Electron transfer
STC	4	12	Periplasm	Electron transfer
FccA	4	64	Periplasm	Fumarate reduction
MtrA	10	35	Periplasm	Iron reduction
MtrC	10	71	Outer membrane	Iron reduction
OmcA	10	83	Outer membrane	Iron reduction
MtrD	10	38	Periplasm	Iron reduction
MtrF	10	73	Outer membrane	Iron reduction
ccNir	5	58	Periplasm	Nitrite reduction
OTR	8	55	Periplasm	Nitrite reduction
DmsE	10	35	Periplasm	DMSO reduction

3.1.1. Reduction of Soluble Electron Acceptors in the Periplasm

Electrons from the intracellular metabolism enter the periplasmic space, from the inner membrane, via a tetraheme *c*-type cytochrome called CymA. This cytochrome shares similarity with members from the quinol dehydrogenases family and is reduced by taking electrons from the quinone pool in the inner membrane (Myers and Myers, 1997). Deletion of CymA from SOMR-1 genome disables this microorganism to use

several substrates as final electron acceptors, including soluble (fumarate, nitrate, nitrite, selenium) and insoluble (Fe(III)/Mn(IV) oxides and DMSO) compounds (Shi et al., 2007). Although there are some genes in SOMR-1 genome that share homology with the one of CymA, the ability of the proteins encoded by them to substitute CymA is very low, with the exception of SirCD that can recover the microorganism ability to reduce fumarate and DMSO (Cordova et al., 2011). CymA is known to interact with a wide variety of proteins involved in reduction of several compounds, such as, nitrate, nitrite, fumarate and iron (Cordova et al., 2011), and Figure 3 shows the interactions already studied between CymA and physiological partners.

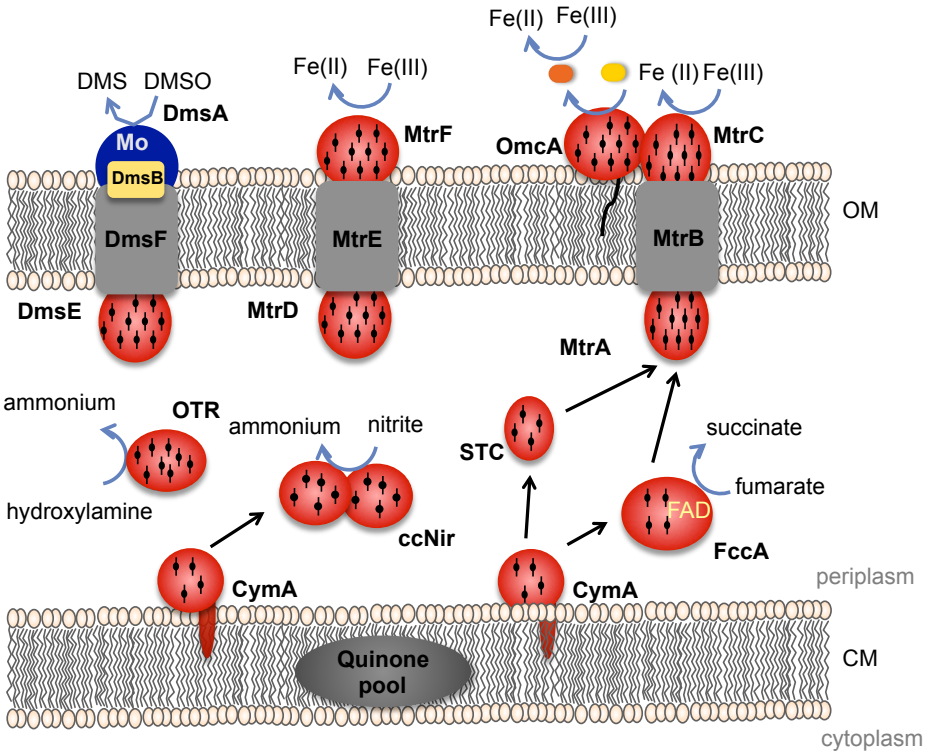

Figure 3. Schematic representation of electron transfer pathways of *Shewanella oneidensis* MR-1.

The two most abundant *c*-type cytochromes found in the periplasmic space of SOMR-1 are FccA, which is responsible for the catalytic reduction of fumarate (Leys et al., 1999) and a small tetraheme cytochrome (STC) that works as a electron carrier across the periplasm (Fonseca et al., 2013; Sturm et al., 2015).

3.1.1.1. Fumarate Reduction

FccA was identified as the unique fumarate reductase of this organism (Taylor et al., 1999). This enzyme performs the reduction of fumarate to

succinate in a two-electron/two-proton reaction. Structural studies showed that FccA is composed by three domains: a heme domain with four bis-histidine coordinated hemes; a domain with a non-covalently bound flavin adenine dinucleotide group (FAD) where the fumarate reduction occurs; and a clamp domain, that links the two domains. It was proposed that this clamp domain contributes to the formation of two different conformations depending on the presence and absence of the substrate (Leys et al., 1999). Previous work on FccA showed that hemes I and II are the ones that receive electrons from the electron donor, whereas the fourth heme that is buried within the protein close to the FAD domain is proposed to be responsible to transfer electrons to the catalytic site (Rothery et al., 2003). The *in vitro* activity of FccA to reduce fumarate to succinate was studied with the enzyme from *S. frigidimarina* where two aminoacids were described as having a crucial role in this process: Histine 61 that is the distal axial ligand of the heme IV, and Arg402 (Rothery et al., 2003; Pankhurst et al., 2006). Histidine 61 is highly conserved in the family of fumarate/succinate dehydrogenases, and kinetic and electrochemical characterization of H61A and H61M mutant forms of FccA showed that these mutations affect the catalytic activity of the enzyme and proved that the electron transfer for the FAD is rate-limiting (Rothery et al., 2003; Pankhurst et al., 2006). Moreover, kinetic and structural evidence showed that Arg402, located near the active site acid/base catalyst for fumarate reduction is vital for the enzyme activity in *S. frigidimarina.* Since Arg402 is also a well conserved residue among fumarate reductases, it is believed to fulfil the same role in all the members of this family (Pankhurst et al., 2006).

3.1.1.2. Nitrogen Compounds Reduction

Reduction of nitrogen compounds occurs in the periplasmic space and two different enzymes were identified to perform this type of reactions: the octaheme tetrathionate reductase (OTR) and the cytochrome-*c* nitrite reductase (ccNir) (Mowat et al., 2004; Youngblut et al., 2014). OTR was originally identified as a soluble tetrathionate reductase, but activity assays showed that this protein has the ability to reduce a wide range of nitrogen substrates (Atkinson et al., 2007). It is composed by a chain of seven low spin hemes, that provide efficient electron transfer to the catalytic heme, which is a penta-coordinated high-spin heme axially coordinated by a lysine (Mowat et al., 2004). Coordination of the catalytic heme is unique among these types of enzymes because the lysine is not part of the heme-binding motif of that heme.

ccNir is a soluble periplasmic cytochrome, which is a dimeric pentaheme nitrite reductase. It has a catalytic heme in each monomer that is, like OTR, lysine coordinated. The penta-coordination of the catalytic heme allows the substrate to bind to the open position and the six-electron reduction of nitrite to ammonia occurs with the substrate and intermediates, always bound to the catalytic heme during catalysis (Youngblut et al., 2012).

Studies of OTR and ccNir showed that these two cytochromes are biased towards similar electron acceptors and have similarities in the coordination of the catalytic hemes and in the catalytic mechanism. The 3D crystal structures of the two cytochromes are considerably different,

however the heme arrangement is similar between the two proteins. Previous work showed that ccNir can be reduced by CymA (Gao et al., 2009), but is not yet clear how electrons reach OTR.

3.1.2. Reduction of Insoluble Electron Acceptors

The known pathways for reduction of insoluble electron acceptors, outside of the cells, also start with electrons entering the periplasmic space via CymA. Recent findings suggest the existence of two separate pathways of electron flow across the periplasm to the outside of the cell, which rely on the two most abundant cytochromes of SOMR-1, the small tetraheme cytochrome (STC) and FccA (Fonseca et al., 2013). These two pathways seem to be redundant for extracellular reduction by the outer-membrane complex MtrCAB-OmcA, since both STC and FccA can transfer electrons to MtrA, the decaheme cytochrome of the complex facing the periplasmic space (Figure 3) (Fonseca et al., 2013). The MtrCAB-OmcA complex is encoded by the operon *mtrCAB-omcA* and contains three homologues in SOMR-1 genome. These are the complexes encoded by the operons *mtrDEF* (proposed to have a similar role to MtrCAB–OmcA complex due to its high similarity), *dmsEFABGH* (responsible for the extracellular respiration of DMSO) and the third containing the genes SO_4360 and SO_4359 (Coursolle and Gralnick, 2010). The OMCs MtrC and OmcA from the complex MtrCAB-OmcA were shown to be essential for metal reduction (Coursolle and Gralnick,

2010). Although they are located in the same operon, they have distinct localizations and functions: MtrC is part of the complex, being buried in the membrane beta-barrel (MtrB), and receives electrons from the periplasmic cytochrome MtrA; OmcA is a lipoprotein found in the external part of the outer-membrane and receives electrons from MtrC (Lower et al., 2009). Both MtrC and OmcA interact with the same electron shuttles, but with different stoichiometry, one molecule of MtrC binds only one molecule of FMN and one molecule of OmcA can bind 2 molecules of FMN (Paquete et al., 2014a). This phenomenon is probably related with the functionality of these OMC that were shown to exist with different stoichiometry in SOMR-1 membranes 1:1 or 2:1 of OmcA:MtrC (Ross et al., 2007; Zhang et al., 2009). This two possible stoichiometry ratios between the two OMCs along with studies showing different distribution patterns of OmcA and MtrC at the cell surface (Lower et al., 2009) support the idea that OmcA has the ability to move in the surface of SOMR-1, receiving electrons from MtrC and transferring them to electron shuttles (Paquete et al., 2014a). This movement contributes to the discharge of electrons, and allows the modulation of the charge of cell surface patches, controlling cell adhesion to electrode surfaces or to other cells (Lower et al., 2009; Paquete et al., 2014a).

The extracellular respiration of SOMR-1 to insoluble compounds relies on these outer-membrane cytochromes and may occur through two mechanisms: a) direct contact via OMC or nanowires that are extensions of the outer-membrane of SOMR-1, and b) indirect contact through

soluble electron shuttles that transport electrons from cells to final electron acceptors (Figure 4) (Gralnick and Newman, 2007).

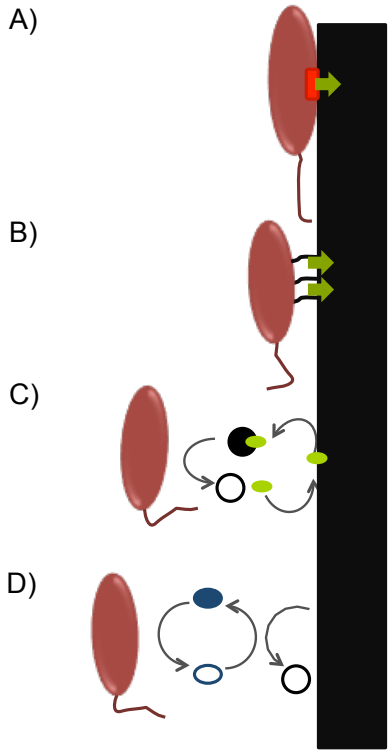

Figure 4. Mechanisms for extracellular respiration. From top: A) The substrate (solid black rectangle) is reduced directly by the outer-membrane cytochrome (red rectangle) in the cell surface; B) Conductive nanowires form a bridge from the cell to the solid electron acceptor that is reduced. C) and D) Indirect electron transfer. Small molecules, such as metal chelators C) in which the substrate is brought to the cell by the chelators (green oval) to be reduced and electron shuttles D) in which the electron shuttle (blue oval) transfer the electrons between the cell and the substrate. Adapted from (Gralnick and Newman, 2007).

4. Final Remarks

Bacteria that have the ability to populate the electrodes in METs take advantage of the several strategies they can use, such as versatility towards electron donors, ability to reduce several electron acceptors, and secondary metabolites production, in order to increase electric current production. The understanding of the mechanisms sustaining this phenomenon is essential to increase biocompatibility, design and proper materials for the construction of efficient electrodes.

The work of this thesis aims to study in detail several cytochromes involved in electron transfer towards soluble and insoluble electron acceptors, with the goal to improve their role in METs for electricity production or in the synthesis of high value products. The advantage in the implementation of such systems is a progressive integration of METs in industrial environment towards a more sustainable use of resources.

5. References

Abrevaya, X. C., Sacco, N., Mauas, P. J. D., and Cortón, E. (2011). Archaea-based Microbial Fuel Cell Operating at High Ionic Strength Conditions. *Extremophiles* 15, 633–642. doi:10.1007/s00792-011-0394-z.

Alves, M. N., Neto, S. E., Alves, A. S., Fonseca, B. M., Carrêlo, A., Pacheco, I., et al. (2015). Characterization of the periplasmic redox

network that sustains the versatile anaerobic metabolism of Shewanella oneidensis MR-1. *Front. Microbiol.* 6, 1–10. doi:10.3389/fmicb.2015.00665.

Atkinson, S. J., Mowat, C. G., Reid, G. A., and Chapman, S. K. (2007). An Octaheme c-type Cytochrome From Shewanella oneidensis Can Reduce Nitrite and Hydroxylamine. *FEBS Lett.* 581, 3805–3808. doi:10.1016/j.febslet.2007.07.005.

Bond, D. R., Holmes, D. E., Tender, L. M., and Lovley, D. R. (2002). Electrode-Reducing Microorganisms That Harvest Energy from Marine Sediments. *Science (80-.).* 295, 483–485. doi:10.1126/science.1066771.

Bond, D. R., and Lovley, D. R. (2003). Electricity Production by Geobacter sulfurreducens Attached to Electrodes. *Appl. Environ. Microbiol.* 69, 1548–1555. doi:10.1128/AEM.69.3.1548.

Bretschger, O., Obraztsova, A., Sturm, C. A., In, S. C., Gorby, Y. A., Reed, S. B., et al. (2007). Current Production and Metal Oxide Reduction by Shewanella oneidensis MR-1 Wild Type and Mutants. *Appl. Environ. Microbiol.* 73, 7003–7012. doi:10.1128/AEM.01087-07.

Carpentier, W., Sandra, K., Smet, I. De, Brigé, A., Smet, L. De, and Beeumen, J. Van (2003). Microbial Reduction and Precipitation of Vanadium by Shewanella oneidensis. *Appl. Environ. Microbiol.* 69, 3636–3639. doi:10.1128/AEM.69.6.3636.

Clauwaert, P., Rabaey, K., Aelterman, P., De Schamphelaire, L., Pham, T. H., Boeckx, P., et al. (2007). Biological Denitrification in Microbial Fuel Cells. *Environ. Sci. Technol.* 41, 3354–3360. doi:10.1021/es062580r.

Cordova, C. D., Schicklberger, M. F. R., Yu, Y., and Spormann, A. M. (2011). Partial Functional Replacement of CymA by SirCD in Shewanella oneidensis MR-1. *J. Bacteriol.* 193, 2312–2321. doi:10.1128/JB.01355-10.

Coursolle, D., and Gralnick, J. A. (2010). Modularity of the Mtr Respiratory Pathway of Shewanella oneidensis Strain MR-1. *Mol. Microbiol.* 77, 995–1008. doi:10.1111/j.1365-2958.2010.07266.x.

Fonseca, B. M., Paquete, C. M., Neto, S. E., Pacheco, I., Soares, C. M., and Louro, R. O. (2013). Mind the Gap: Cytochrome Interactions Reveal Electron Pathways Across the Periplasm of Shewanella oneidensis MR-1. *Biochem. J.* 449, 101–108. doi:10.1042/BJ20121467.

Fredrickson, J. K., Romine, M. F., Beliaev, A. S., Auchtung, J. M., Driscoll, M. E., Gardner, T. S., et al. (2008). Towards Environmental Systems Biology of Shewanella. *Nat. Rev. Microbiol.* 6, 592–603. doi:10.1038/nrmicro1947.

Gao, H., Yang, Z. K., Barua, S., Reed, S. B., Romine, M. F., Nealson, K. H., et al. (2009). Reduction of Nitrate in Shewanella oneidensis Depends on Atypical NAP and NRF Systems with NapB as a

Preferred Electron Transport Protein from CymA to NapA. *ISME J.* 3, 966–976. doi:10.1038/ismej.2009.40.

Gralnick, J. A., and Newman, D. K. (2007). Extracellular respiration. *Mol. Microbiol.* 65, 1–11. doi:10.1111/j.1365-2958.2007.05778.x.

Gregory, K. B., and Lovley, D. R. (2005). Remediation and Recovery of Uranium from Contaminated Subsurface Environments with Electrodes. *Environ. Sci. Technol.* 39, 8943–8947. doi:10.1021/es050457e.

Hamelers, H. V. M., Ter Heijne, A., Sleutels, T. H. J. A., Jeremiasse, A. W., Strik, D. P. B. T. B., and Buisman, C. J. N. (2010). New Applications and Performance of Bioelectrochemical Systems. *Appl. Microbiol. Biotechnol.* 85, 1673–1685. doi:10.1007/s00253-009-2357-1.

Hau, H. H., Gilbert, A., Coursolle, D., and Gralnick, J. A. (2008). Mechanism and Consequences of Anaerobic Respiration of Cobalt by Shewanella oneidensis strain MR-1. *Appl. Environ. Microbiol.* 74, 6880–6886. doi:10.1128/AEM.00840-08.

Hau, H. H., and Gralnick, J. A. (2007). Ecology and Biotechnology of the Genus Shewanella. *Annu. Rev. Microbiol.* 61, 237–258. doi:10.1146/annurev.micro.61.080706.093257.

Kim, B. H., Ikeda, T., Park, H. S., Kim, H. J., Hyun, M. S., Kano, K., et al. (1999). Electrochemical Activity of an Fe(III)-Reducing Bacterium, Shewanella putrefaciens MR-1, in the Presence of Alternative

Electron Acceptors. *Biotechnol. Tech.* 13, 475–478. doi:10.1023/A:1008993029309.

Kim, H. J., Park, H. S., Hyun, M. S., Chang, I. S., Kim, M., and Kim, B. H. (2002). A mediator-less microbial fuel cell using a metal reducing bacterium, Shewanella putrefaciens. *Enzyme Microb. Technol.* 30, 145–152. doi:10.1016/S0141-0229(01)00478-1.

Leys, D., Tsapin, A. S., Nealson, K. H., Meyer, T. E., Cusanovich, M. A., and van Beeumen, J. J. (1999). Structure and Mechanism of the Flavocytochrome c Fumarate Reductase of Shewanella putrefaciens MR-1. *Nat. Struct. Biol.* 6, 1113–1117. Available at: http://www.nature.com/nsmb/journal/v6/n12/abs/nsb1299_1113.html [Accessed November 18, 2013].

Liu, C., Gorby, Y. A., Zachara, J. M., Fredrickson, J. K., and Brown, C. F. (2002). Reduction Kinetics of Fe(III), Co(III), U(VI), Cr(VI), and Tc(VII) in Cultures of Dissimilatory Metal-Reducing Bacteria. *Biotechnol. Bioeng.* 80, 637–649. doi:10.1002/bit.10430.

Liu, H., Hu, H., Chignell, J., and Fan, Y. (2010). Microbial Electrolysis: Novel Technology for Hydrogen Production From Biomass. *Biofuels* 1, 129–142. doi:10.4155/bfs.09.9.

Liu, H., Ramnarayanan, R., and Logan, B. E. (2004). Production of Electricity During Wastewater Treatment Using a Single Chamber Microbial Fuel Cell. *Environ. Sci. Technol.* 38, 2281–2285. doi:10.1021/es034923g.

Logan, B. E. (2009). Exoelectrogenic Bacteria that Power Microbial Fuel Cells. *Nat. Rev. Microbiol.* 7, 375–381. doi:10.1038/nrmicro2113.

Logan, B. E., Hamelers, B., Rozendal, R., Schröder, U., Keller, J., Freguia, S., et al. (2006). Microbial Fuel Cells: Methodology and Technology. *Environ. Sci. Technol.* 40, 5181–5192. doi:10.1021/es0605016.

Logan, B. E., and Rabaey, K. (2012). Conversion of Wastes into Bioelectricity and Chemicals by Using Microbial Electrochemical Technologies. *Science (80-.).* 337, 686–690. doi:10.1126/science.1217412.

Logan, B. E., and Regan, J. M. (2006). Microbial Fuel Cells- Challenges and Applications. *Environ. Sci. Technol.* 40, 5172–5180. doi:10.1021/es0627592.

Lovley, D. R. (2006). Bug Juice: Harvesting Electricity with Microorganisms. *Nat. Rev. Microbiol.* 4, 497–508. doi:10.1038/nrmicro1442.

Lower, B. H., Yongsunthon, R., Shi, L., Wildling, L., Gruber, H. J., Wigginton, N. S., et al. (2009). Antibody Recognition Force Microscopy Shows that Outer Membrane Cytochromes OmcA and MtrC Are Expressed on the Exterior Surface of Shewanella oneidensis MR-1. *Appl. Environ. Microbiol.* 75, 2931–2935. doi:10.1128/AEM.02108-08.

MacDonell, M. T., and Colwell, R. R. (1985). Phylogeny of the

Vibrionaceae, and Recommendation for Two New Genera, Listonella and Shewanella. *Syst. Appl. Microbiol.* 6, 171–182. doi:10.1016/S0723-2020(85)80051-5.

Meyer, T. E., Tsapin, A. I., Vandenberghe, I., de Smet, L., Frishman, D., Nealson, K. H., et al. (2004). Identification of 42 Possible Cytochrome c Genes in the Shewanella oneidensis Genome and Characterization of Six Soluble Cytochromes. *Omi. A J. Integr. Biol.* 8, 57–77. doi:10.1089/153623104773547499.

Mowat, C. G., Rothery, E., Miles, C. S., McIver, L., Doherty, M. K., Drewette, K., et al. (2004). Octaheme Tetrathionate Reductase is a Respiratory Enzyme with Novel Heme Ligation. *Nat. Struct. Mol. Biol.* 11, 1023–1024. doi:10.1038/nsmb827.

Myers, C. R., and Myers, J. M. (1997). Cloning and Sequence of cymA, a Gene Encoding a Tetraheme Cytochrome c Required for Reduction of Iron(III), Fumarate, and Nitrate by Shewanella putrefaciens MR-1. *J. Bacteriol.* 179, 1143–1152.

Myers, C. R., and Nealson, K. H. (1988). Bacterial Manganese Reduction and Growth with Manganese Oxide as the Sole Electron Acceptor. *Science (80-.).* 240, 1319–1321. Available at: http://science.sciencemag.org/content/240/4857/1319.abstract.

Nealson, K. H., Moser, D. P., and Saffarini, D. A. (1995). Anaerobic Electron Acceptor Chemotaxis in Shewanella putrefaciens. *Appl. Environ. Microbiol.* 61, 1551–1554.

Nealson, K. H., and Saffarini, D. (1994). Iron and Manganese in Anaerobic Respiration: Environmental Significance, Physiology, and Regulation. *Annu. Rev. Microbiol.* 48, 311–343. doi:10.1146/annurev.micro.48.1.311.

Pankhurst, K. L., Mowat, C. G., Rothery, E. L., Hudson, J. M., Jones, A. K., Miles, C. S., et al. (2006). A Proton Delivery Pathway in the Soluble Fumarate Reductase from Shewanella frigidimarina. *J. Biol. Chem.* 281, 20589–20597. doi:10.1074/jbc.M603077200.

Paquete, C. M., Fonseca, B. M., Cruz, D. R., Pereira, T. M., Pacheco, I., Soares, C. M., et al. (2014a). Exploring the Molecular Mechanisms of Electron Shuttling Across the -Microbe/Metal Space. *Front. Microbiol.* 5, 318–330. doi:10.3389/fmicb.2014.00318.

Paquete, C. M., Saraiva, I. H., and Louro, R. O. (2014b). Redox Tuning of the Catalytic Activity of Soluble Fumarate Reductases from Shewanella. *Biochim. Biophys. Acta* 1837, 717–725. doi:10.1016/j.bbabio.2014.02.006.

Park, H. S., Kim, B. H., Kim, H. S., Kim, H. J., Kim, G. T., Kim, M., et al. (2001). A Novel Electrochemically Active and Fe (III)-reducing Bacterium Phylogenetically Related to Clostridium butyricum Isolated from a Microbial Fuel Cell. *Anaerobe* 7, 297–306. doi:10.1006/anae.2001.0399.

Potter, M. C. (1911). Electrical Effects Accompanying the Decomposition of Organic Compounds. *Proc. R. Soc. London. Ser. B, Contain. Pap. a*

Biol. Character 84, 260–276. Available at: http://rspb.royalsocietypublishing.org/content/84/571/260.abstract.

Prasad, D., Arun, S., Murugesan, M., Padmanaban, S., Satyanarayanan, R. S., Berchmans, S., et al. (2007). Direct Electron Transfer With Yeast Cells and Construction of a Mediatorless Microbial Fuel Cell. *Biosens. Bioelectron.* 22, 2604–2610. doi:10.1016/j.bios.2006.10.028.

Rabaey, K., and Rozendal, R. A. (2010). Microbial Electrosynthesis-Revisiting the Electrical Route for Microbial Production. *Nat. Rev. Microbiol.* 8, 706–716. doi:10.1038/nrmicro2422.

Rosa, L. F., Neto, S. E., Alves, A. S., and Louro, R. O. (2013). Electrocatálise Microbiana: Uma Plataforma Versátil para Processos Industriais Sustentáveis. *Biotecnol. Soc. Port. Biotecnol.* 3, 33–34.

Ross, D. E., Ruebush, S. S., Brantley, S. L., Hartshorne, R. S., Clarke, T. A., Richardson, D. J., et al. (2007). Characterization of Protein-Protein Interactions Involved in Iron Reduction by Shewanella oneidensis MR-1. *Appl. Environ. Microbiol.* 73, 5797–5808. doi:10.1128/AEM.00146-07.

Rothery, E. L., Mowat, C. G., Miles, C. S., Walkinshaw, M. D., Reid, G. A., and Chapman, S. K. (2003). Histidine 61: An Important Heme Ligand in the Soluble Fumarate Reductase from Shewanella frigidimarina. *Biochemistry* 42, 13160–13169. doi:10.1021/bi030159z.

Rozendal, R. A., Jeremiasse, A. W., Hamelers, H. V. M., and Buisman, C. J. N. (2008). Hydrogen Production with a Microbial Biocathode. *Environ. Sci. Technol.* 42, 629–634. doi:Doi 10.1021/Es071720+.

Schroder, U. (2012). Microbial fuel cells and microbial electrochemistry: Into the next century! *ChemSusChem* 5, 959–961. doi:10.1002/cssc.201200319.

Shi, L., Squier, T. C., Zachara, J. M., and Fredrickson, J. K. (2007). Respiration of Metal (Hydr)Oxides by Shewanella and Geobacter: A Key Role for Multihaem c-type Cytochromes. *Mol. Microbiol.* 65, 12–20. doi:10.1111/j.1365-2958.2007.05783.x.

Sturm, G., Richter, K., Doetsch, A., Heide, H., Louro, R. O., and Gescher, J. (2015). A Dynamic Periplasmic Electron Transfer Network Enables Respiratory Flexibility Beyond a Thermodynamic Regulatory Regime. *ISME J.*, 1–10. doi:10.1038/ismej.2014.264.

Taylor, P., Pealing, S. L., Reid, G. A., Chapman, S. K., and Walkinshaw, M. D. (1999). Structural and Mechanistic Mapping of a Unique Fumarate Reductase. *Nat. Struct. Biol.* 6, 1108–1112. doi:10.1038/70045.

Venkateswaran, K., Moser, D. P., Dollhopf, M. E., Lies, D. P., Saffarini, D. A., MacGregor, B. J., et al. (1999). Polyphasic Taxonomy of the Genus Shewanella and Description of Shewanella oneidensis sp. nov. *Int. J. Syst. Bacteriol.* 49, 705–724. doi:10.1099/00207713-49-2-705.

Wang, H., and Ren, Z. J. (2013). A Comprehensive Review of Microbial Electrochemical Systems as a Platform Technology. *Biotechnol. Adv.* 31, 1796–1807. doi:10.1016/j.biotechadv.2013.10.001.

Wrighton, K. C., Agbo, P., Warnecke, F., Weber, K. A., Brodie, E. L., DeSantis, T. Z., et al. (2008). A Novel Ecological Role of the Firmicutes Identified in Thermophilic Microbial Fuel Cells. *ISME J.* 2, 1146–1156. doi:10.1038/ismej.2008.48.

Youngblut, M., Judd, E. T., Srajer, V., Sayyed, B., Goelzer, T., Elliott, S. J., et al. (2012). Laue Crystal Structure of Shewanella oneidensis Cytochrome c Nitrite Reductase from a High-yield Expression System. *J. Biol. Inorg. Chem.* 17, 647–662. doi:10.1007/s00775-012-0885-0.

Youngblut, M., Pauly, D. J., Stein, N., Walters, D., Conrad, J. A., Moran, G. R., et al. (2014). Shewanella oneidensis Cytochrome c Nitrite Reductase (ccNiR) Does Not Disproportionate Hydroxylamine to Ammonia and Nitrite, Despite a Strongly Favorable Driving Force. *Biochemistry* 53, 2136–2144. doi:10.1021/bi401705d.

Zhang, H., Tang, X., Munske, G. R., Tolic, N., Anderson, G. A., and Bruce, J. E. (2009). Identification of Protein-Protein Interactions and Topologies in Living Cells with Chemical Cross-linking and Mass Spectrometry. *Mol. Cell. Proteomics* 8, 409–420. doi:10.1074/mcp.M800232-MCP200.

Chapter II

Characterization of the Periplasmic Redox - Network that Sustains the Versatile Anaerobic Metabolism of *Shewanella oneidensis* MR-1

Chapter II has been published in

Alves, M. N., Neto, S. E., Alves, A. S., Fonseca, B. M., Carrêlo, A., Pacheco, I., Paquete, C. M., Soares, C. M., Louro, R. O. (2015). Characterization of the periplasmic redox network that sustains the versatile anaerobic metabolism of Shewanella oneidensis MR-1. *Front. Microbiol.* 6, 1–10. doi:10.3389/fmicb.2015.00665.

Author contributions:

Sónia E. Neto performed the cloning of OTR and expression and purification of OTR, MtrA, STC and FccA.

Sónia E. Neto performed titrations, followed by ^{1}H-NMR, of OTR with STC or FccA, and the competition titration of MtrA with STC and FccA, together with the data analysis.

Sónia E. Neto performed the spectroscopic assays of inter-protein electron transfer.

Sónia E. Neto contributed to the planning of the experiments and to the writing of the original paper.

Abstract

The versatile anaerobic metabolism of the Gram-negative bacterium *Shewanella oneidensis* MR-1 (SOMR-1) relies on a multitude of redox proteins found in its periplasm. Most are multiheme cytochromes that carry electrons to terminal reductases of insoluble electron acceptors located at the cell surface, or *bona fide* terminal reductases of soluble electron acceptors. In this study, the interaction network of several multiheme cytochromes was explored by a combination of NMR spectroscopy, activity assays followed by UV-visible spectroscopy and comparison of surface electrostatic potentials. From these data the small tetraheme cytochrome (STC) emerges as the main periplasmic redox shuttle in SOMR-1. It accepts electrons from CymA and distributes them to a number of terminal oxidoreductases involved in the respiration of various compounds. STC is also involved in the electron transfer pathway to reduce nitrite by interaction with the octaheme tetrathionate reductase (OTR), but not with cytochrome *c* nitrite reductase (ccNiR). In the main pathway leading the metal respiration, STC pairs with flavocytochrome *c* (FccA), the other major periplasmic cytochrome, which provides redundancy in this important pathway. The data reveals that the two proteins compete for the binding site at the surface of MtrA, the decaheme cytochrome inserted on the periplasmic side of the MtrCAB–OmcA outer-membrane complex. However, this is not observed for the MtrA homologues. Indeed, neither STC nor FccA interact with MtrD, the best replacement for MtrA, and only STC is able to interact with the decaheme cytochrome DmsE of the outer-

membrane complex DmsEFABGH. Overall, these results shown that STC plays a central role in the anaerobic respiratory metabolism of SOMR- 1. Nonetheless, the trans-periplasmic electron transfer chain is functionally resilient as a consequence of redundancies that arise from the presence of alternative pathways that bypass/compete with STC.

Introduction

Shewanella oneidensis MR-1 is a Gram-negative bacterium that can use a wide range of terminal electron acceptors in the absence of oxygen, including fumarate, nitrite, nitrate, trimethylamine oxide (TMAO), dimethyl sulfoxide (DMSO), sulfur compounds and a variety of metal compounds including radionuclides (Myers and Nealson, 1988; Nealson and Saffarini, 1994; Myers and Myers, 2000; Gralnick and Newman, 2007; Burns and DiChristina, 2009). This metabolic versatility has made SOMR-1 a target of biotechnological research for the development of novel bioremediation processes and generation of electricity in MFC (Lovley, 2006; Logan and Rabaey, 2012). Electron transfer from SOMR-1 to extracellular substrates relies on the conduction of electrons from the cytoplasm to the cell surface via a periplasmic network of redox proteins dominated by *c*-type cytochromes (Heidelberg et al., 2002; Hau and Gralnick, 2007). With the exception of thiosulfate and TMAO reduction, all forms of anaerobic respiration described in SOMR-1 are routed via the tetraheme *c*-type cytochrome CymA, anchored to the inner-membrane of the cell (Myers and Myers, 1997; Saffarini et al., 2002).

This protein collects electrons from the menaquinone pool in the cytoplasmic membrane and distributes them among periplasmic proteins. These proteins can be either terminal reductases or periplasmic redox shuttles that transfer electrons to outer-membrane reductases (Myers and Myers, 1997; Saffarini et al., 2002; Schwalb et al., 2003). Nevertheless, the detailed organization of the trans-periplasmic redox network remains to be completely elucidated (Hartshorne et al., 2009). In anaerobic conditions, the most abundant periplasmic *c*-type cytochromes in SOMR-1 are the STC and the FccA (Tsapin et al., 2001). It was recently shown that both STC and FccA can accept electrons from CymA and transfer them to outer-membrane metal reductases, which lead to the identification of two independent redox pathways across the periplasm (Fonseca et al., 2013). Although this finding confirmed the functional redundancy already observed for other multiheme cytochromes (Coursolle and Gralnick, 2010; Richardson et al., 2012), the physiological reason for this is still unknown. One of the most explored and well described anaerobic respiratory pathways in SOMR-1 is Fe(III) reduction, which involves the outer-membrane MtrCAB–OmcA complex (Myers and Nealson, 1988; Myers and Myers, 1997, 2000; Pitts et al., 2003). However, less is known about the periplasmic electron transfer network that delivers electrons to the homologous complexes, MtrDEF and DmsEFABGH. While the DmsEFABGH complex is responsible for the extracellular respiration of DMSO, the specific physiological function of MtrDEF is still unclear. It appears to play a similar role to MtrCAB–OmcA complex

because of their high similarity (Fredrickson et al., 2008; Coursolle and Gralnick, 2010).

Another important respiratory process carried out by SOMR-1 is the conversion of nitrogen compounds to ammonia (Myers and Nealson, 1988; Nealson and Saffarini, 1994). This respiratory pathway involves the OTR and the cytochrome *c* nitrite reductase (ccNiR). OTR is described as an efficient nitrite and hydroxylamine reductase and ccNiR catalyzes the reduction of nitrite (Einsle et al., 2002; Atkinson et al., 2007). It was previously demonstrated that CymA is essential for nitrite reduction (Schwalb et al., 2003), but nothing is known about the routes of electron transfer to OTR and ccNiR. In order to determine if STC and FccA mediate the electron transfer from CymA to the outer-membrane complexes MtrDEF and DmsEFABGH, protein interactions studied by nuclear magnetic resonance (NMR) and UV-visible spectroscopy were performed. NMR spectroscopy together with protein electrostatic surface potential calculations was also used to explore the ability of STC and FccA transfer electrons to OTR and ccNiR (Mowat et al., 2004; Youngblut et al., 2012). These results showed that the functional redundancy between STC and FccA appears to be restricted to the interaction with the MtrCAB–OmcA complex. Furthermore, the data showed that STC plays the major role in connecting CymA with the DmsEFABGH complex and OTR, but is not involved in interactions neither with ccNiR nor with MtrD.

Materials and Methods

Cloning and Expression of the Genes of Interest

The vectors containing *dmsE* and *mtrD* genes were kindly provided by Dr. Liang Shi from the Pacific Northwest National Laboratory (Richland, WA, U.S.A.). A stop codon was inserted at the 3' end of each gene, allowing the removal of the V5 epitope and the 6xHis-tag sequence at the C-terminus of the proteins. The lack of these sequences eliminated concerns about proper folding of the protein in the presence of the 6xHis-tag at the C-terminus. The cloning vector pHSG298 (Takara Bio), containing the *ccnir* gene with the wild-type N-terminal signal peptide replaced by the signal peptide from the SOMR-1 protein STC, was gently provided by Dr. Sean J. Elliott from Boston University. The *otr* gene was amplified from genomic DNA of SOMR-1 and cloned into the pBAD202/D-TOPO vector following the instructions from the supplier (pBAD202 directional TOPO Expression Invitrogen KIT) and according to the work of Shi et al. (2005). The primers used are reported in Table 1.

Table 1. Primers used in this study.

Primers	**Sequence (5'-3')**
DmsE_Stop_Forw	GCGGCAGCAATTTTGCCCGTTGAGGCGAGCTCAAGCTTGAAGG TAAGCC
DmsE_Stop_Rev	GGCTTACCTTCAAGCTTGAGCTCGCCTCAACGGGCAAAATTGCT GCCGC
MtrD_Stop_Forw	AAGTTGCTGCAGAGATAAGGCGAGCTCAAGCTTGA
MtrD_Stop_Rev	TCAAGCTTGAGCTCGCCTTATCTCTGCAGCAACTT
OTR_Stop_Forw	CACCTAAGAAGGAGATATACATCCCATGAA
OTR_Stop_Rev	TTATTGCTTATGTTTAGGGCCTTGTTTGTT

Bacterial Strains and Growth Conditions

Shewanella oneidensis JG207 strain (knockout strain of the *fccA* gene), kindly provided by Prof. Dr. Johannes Gescher from Karlsruher Institut für Technologie (Karlsruher, Germany), was transformed with the vector containing the *otr* gene. The vectors containing the *dmsE* and *mtrD* genes were separately transformed in SOMR-1. *S. oneidensis* cells were grown at 30 °C in Terrific Broth (TB) containing 50 µg/mL kanamycin in 5 L Erlenmeyer flasks containing 2 L of medium and 1:100 inoculum volume, at 130 rev./min. Protein expression was induced by addition of L-arabinose: 1 mM (for the strains over-expressing DmsE and OTR) and 2 mM (for the strain over-expressing MtrD) after 6–8 h of growth. After induction, cells continued to grow for 16 h, until harvesting. Bacterial cells were harvested by centrifugation at 11,325 *g* for 10 min, at 4 °C. In this study the strain SOMR-1 was used to express ccNiR employing the growth conditions previously reported in the literature (Judd et al., 2012). The vectors, strains and growth conditions to express MtrA, STC, FccA, and CymA were as previously described (Fonseca et al., 2009, 2013).

Protein Purification

The cell pellets were resuspended in 20 mM Tris-HCl (pH 7.6) containing protease inhibitor cocktail (Roche) and DNase I (Sigma). The disruption of the cells was achieved by a passage through a

French Press at 1000 psi. Membranes and cell debris were removed by centrifugation at 219,000 *g* for 1 h, at 4°C, and the supernatant containing the soluble protein fraction was dialyzed overnight against 4 L of 20 mM Tris-HCl (pH 7.6). These fractions were concentrated in ultrafiltration cells, using a 10 kDa cut-off membrane. The fractions containing each of the target proteins were loaded onto a diethylaminoethyl (DEAE) column (GE Healthcare) pre-equilibrated with 20 mM Tris-HCl (pH 7.6). A gradient from 0 to 1 M NaCl was applied. The fractions containing MtrD were eluted at 150 mM NaCl, while DmsE and OTR were eluted at 200 mM NaCl. The fractions containing DmsE and MtrD were concentrated and loaded onto a HTP (hydroxyapatite) column (Bio-Rad Laboratories) pre-equilibrated with 10 mM potassium phosphate buffer (pH 7.6) and gradient from 10 mM to 1 M. DmsE and MtrD were eluted at 100 and 150 mM of potassium phosphate buffer (pH 7.6), respectively. The final purification step used a Superdex 75 column (GE Healthcare) pre-equilibrated with 20 mM potassium phosphate buffer (pH 7.6) and 100 mM NaCl. The fraction resulting from the DEAE column containing OTR was concentrated and loaded onto a Q-Sepharose column (GE Healthcare) previously equilibrated with 20 mM Tris-HCl (pH 7.6). A salt gradient from 0 to 1 M NaCl was applied and this protein was eluted at 150 mM NaCl. The fraction containing OTR was concentrated and loaded onto a HTP column pre-equilibrated with 10 mM potassium phosphate buffer (pH 7.6). A gradient from 10 mM to 1 M of potassium phosphate buffer (pH 7.6) was applied, and pure OTR was eluted at 100 mM. The purification of

STC, FccA, CymA, and ccNiR cytochromes was performed as described in the literature (Judd et al., 2012; Fonseca et al., 2013). The recombinant TEV protease was removed from the fraction containing ccNiR using a Superdex 75 column pre-equilibrated with 20 mM potassium phosphate buffer (pH 7.6) with 150 mM KCl. All the chromatographic fractions were analyzed by SDS-PAGE stained for heme proteins (Francis and Becker, 1984) and by UV-visible spectroscopy to select those containing the target proteins. Proteins were considered pure when having an absorbance ratio Soret peak/A_{280nm} higher than 3.5, and when showing a single band in Coomassie staining SDS/PAGE gels. The identity of DmsE, MtrD, and OTR was confirmed by mass spectrometry and N-terminal sequencing.

NMR Sample Preparation and Titrations

Stock samples of DmsE, MtrD, OTR, ccNiR, STC, and FccA in 20 mM potassium phosphate (pH 7.6) with an ionic strength of 100 mM (adjusted by addition of potassium chloride) were lyophilized and dissolved in $^{2}H_2O$ (99.9 atom%, Spectra Stable Isotopes). NMR spectra obtained before and after lyophilization were identical, demonstrating that the proteins were not affected by this procedure. The protein concentration was determined by UV-visible spectroscopy using ε_{410nm} of 125,000 $M^{-1}cm^{-1}$ per heme for the oxidized state of the protein (Massey, 1959; Hartshorne et al., 2007).

Samples containing 50 or 100 µM of STC and FccA were titrated against increasing concentrations of DmsE, MtrD, OTR, and ccNiR. The competition titration was performed with a sample of MtrA (50 µM) incubated with sufficient amount of FccA to have at least 90% of MtrA bound to FccA. Subsequently, increasing amounts of STC were added to the NMR tube, in order to detect any perturbation in STC signals. ^{1}H-1D-NMR spectra were recorded after each addition. The chemical shifts of the signals corresponding to the methyl substituents of the hemes of STC and FccA were measured in each spectrum. These signals have been previously assigned to specific hemes in the structure, allowing the identification of the docking sites with its redox partners (Fonseca et al., 2009; Pessanha et al., 2009).

Nuclear magnetic resonance experiments were performed at 25 °C on a Bruker Avance II spectrometer operating at 500 MHz equipped with a TXI probe. The proton spectra were calibrated using the water signal as an internal reference (Banci et al., 1995).

Data Analysis and Binding Affinities

Chemical shift perturbations equal to or larger than 0.025 ppm were considered significant (Diaz-Moreno et al., 2005b). The chemical shift perturbations (Δδbind) of the NMR signals from a cytochrome resulting from the complex formation with another cytochrome were plotted against the molar ratio (R) of [CytB]/[CytA]. The data were

fitted using least squares minimization to a 1:1 binding model using equations 1 and 2 (Worrall et al., 2003):

$$\Delta\boldsymbol{\delta_{bind}} = \frac{\mathbf{1}}{\mathbf{2}}\Delta\boldsymbol{\delta^{\infty}_{bind}}\left(\boldsymbol{A} - \sqrt{(\boldsymbol{A^2} - \mathbf{4}\boldsymbol{R})}\right) \quad \textbf{Equation 1}$$

$$\boldsymbol{A} = \mathbf{1} + \boldsymbol{R} + \frac{\boldsymbol{K_d}([\boldsymbol{Cyt_A}]_0\boldsymbol{R} + [\boldsymbol{Cyt_B}]_0)}{[\boldsymbol{Cyt_A}]_0[\boldsymbol{Cty_B}]_0} \quad \textbf{Equation 2}$$

where $\Delta\boldsymbol{\delta^{\infty}_{bind}}$ is the maximal chemical shift perturbation of the NMR signals resulting from the complex formation between CytA and CytB, K_d is the dissociation constant, $[\boldsymbol{CtyA}]_0$ is the initial concentration of CytA and $[\boldsymbol{CtyB}]_0$ is the stock concentration of CytB. When several methyl signals belonging to an individual heme were visible, the data obtained for all methyls were used to define the dissociation constant. Experimental uncertainty was estimated from the spectral resolution of the NMR data acquired.

Spectroscopic Assay of Interprotein Electron Transfer

Electron transfer involving FccA from SOMR-1 was measured spectrophotometrically inside an anaerobic chamber using an UV–visible spectrophotometer (Shimadzu model UV-1800) to collect spectra in the range of 300–800 nm as previously described (Fonseca et al., 2013). Briefly, an approximate final concentration of 1 µM of each target protein was prepared in a 1 ml cuvette. Dilutions were made from stock solutions of DmsE, MtrD, OTR, ccNiR, and FccA in degassed 20 mM potassium phosphate buffer (pH 7.6) with 100 mM

KCl. Each protein was reduced by addition of small amounts of a concentrated solution of sodium dithionite. The absorbance was monitored at 314 nm to avoid excess of reducing agent. Fumarate was added to the reduced protein solutions to a final concentration of ~1 mM. Only when no change was observed in absorbance at 552 nm, the reaction would be initiated by the addition of 1 nM FccA. The spectral changes were monitored over time. Experiments were performed with constant stirring and the temperature was kept at 25°C using an external thermostatic bath.

Protein Electrostatic Surface Potential Calculations

The structures of ccNiR (PDB code 3UBR; Youngblut et al., 2012) and the OTR (PDB code 1SP3; Mowat et al., 2004), were used to calculate the electrostatic potential at the surface of both proteins. Both proteins were set in their fully oxidized states, which were the experimental conditions used to study their interactions. The GROMOS 43A1 force field (Scott et al., 1999) was used to set the partial charges of the proteins and co-factors. The MEAD package (Bashford and Karplus, 1990), which solves the Poisson–Boltzmann equation for a system, was used to calculate the electrostatic potentials. The ionic strength used was 0 mM and the internal and external dielectric constants were set at 2 and 80, respectively. The electrostatic potential was mapped at the surface of the proteins using PyMOL (DeLano, 2003).

Results

NMR Titrations and Binding Affinities

For electron transfer to occur at physiologically relevant rates between two cytochromes, the heme groups of donor and acceptor must be in close proximity (Zhang et al., 2008; Gray and Winkler, 2010). Therefore, when multiheme cytochromes bind in a configuration that is relevant for interprotein electron transfer, NMR spectroscopy can be used to detect this binding through observation of changes in the chemical shifts of signals belonging to the hemes near to the binding sites (Fonseca et al., 2013). This technique is thus highly suited to study interactions between the redox proteins found in the periplasmic space of SOMR-1, revealing the detailed organization of its trans-periplasmic redox network. Figure 1 illustrates spectral changes for the 18^{1} methyl signal (IUPAC-IUB nomenclature) from heme IV ($18^{1}CH_3{}^{IV}$) of STC in the presence of increasing amounts of OTR.

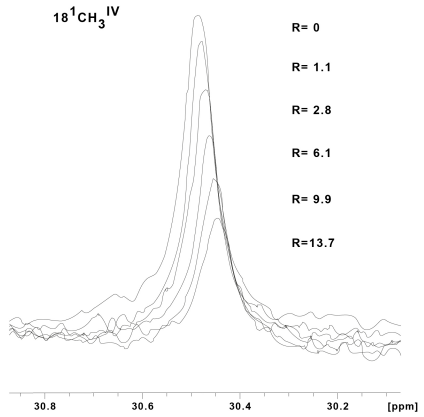

Figure 1. ^{1}H-1D NMR spectral changes of the signal from methyl 18^{1} belonging to heme IV of small tetraheme cytochrome (STC) in the presence of increasing amounts of octaheme tetrathionate reductase (OTR), illustrating the data used in the chemical shift perturbation analysis. The samples were prepared in 20 mM phosphate buffer pH 7.6, with 100 mM KCl, at 25°C. The methyl group is labeled using the IUPAC-IUB nomenclature for hemes. The Roman numeral corresponds to the order of heme binding to the polypeptide chain. The R values correspond to the molar ratios of [OTR]/[STC].

Chemical shift perturbations of the STC and FccA signals, resulting from binding to putative redox partners, were plotted against the molar ratio of redox partner:STC and redox partner:FccA (Figure 2). All the periplasmic pairs of proteins tested and K_d values of proteins that showed interactions are reported in Table 2. In some cases, such as the signals of the 2^{1} methyl of heme III or the 18^{1} methyl of hemes II and IV of STC during interaction with DmsE, the chemical shift perturbation of their signals is smaller than 0.025 ppm. These are therefore of insufficient magnitude for a confident estimation of binding parameters as indicated in the Section “Materials and Methods” and were not used in the calculations. The K_d values calculated are typical of weakly transient interactions as reported for

other cytochromes (Diaz-Moreno et al., 2005a; Perkins et al., 2010; Bashir et al., 2011; Meschi et al., 2011; Fonseca et al., 2013).

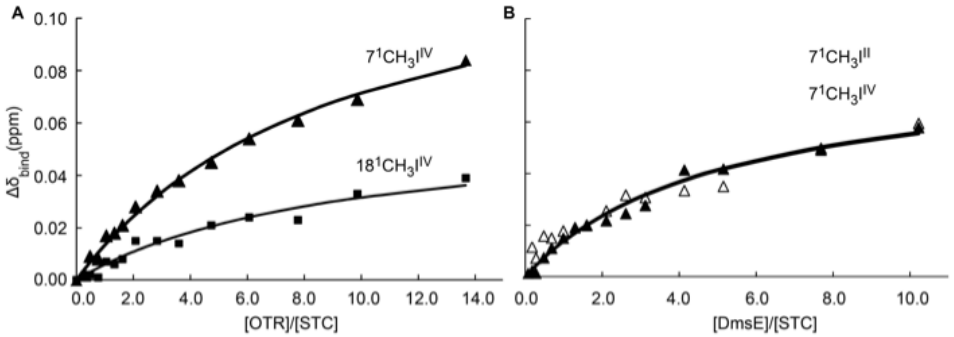

Figure 2. Binding curves of periplasmic cytochromes from SOMR-1 that show interactions monitored by ^{1}H-1D-NMR spectra: OTR and STC (A) and DmsE and STC (B). The chemical shift perturbations of the heme methyl signals are plotted as a function of the molar ratio of the interacting proteins. Solid triangles and solid squares represent the 7^1 methyl and 18^1 methyl of heme IV of STC, respectively; open triangles represent the 7^1 methyl of heme II of STC. The solid lines represent the best global fit to the 1:1 binding model [Equation 1].

Table 2. Pairwise interactions tested for cytochromes found in the periplasm of SOMR-1.

Cytochrome Complex	K_d (μM)	Docking Site
FccA and MtrA	35 (14)	Heme II
FccA and DmsE	–	
FccA and MtrD	–	
FccA and OTR	–	
FccA and ccNiR	–	
STC and MtrA	572 (5)	Heme IV
STC and DmsE	783 (227)	Hemes II,III, and IV
STC and MtrD	–	
STC and OTR	1600 (400)	Heme IV
STC and ccNiR	–	

The "–" symbol indicates no interaction detected. Values in parenthesis are standard errors obtained from the diagonal of the covariance matrix arising from the fitting of the binding model to the experimental data.

Previous studies showed that both STC and FccA interact with the decaheme cytochrome MtrA and that the affinity between FccA and MtrA is much stronger than the affinity between STC and MtrA (Fonseca et al., 2013). Given that the three-dimensional structure of MtrA is not yet available, a competition binding assay monitored by ^{1}H-1D-NMR was performed to study the docking place of STC and FccA with MtrA. In conditions where more than 90% of MtrA is bound to FccA, the chemical shift of the STC signals are not perturbed when the molar ratio of MtrA:STC is changed (Figure 3). This result shows that the presence of FccA bound to MtrA prevents the interaction between MtrA and STC, suggesting that the binding of STC and FccA at the surface of MtrA occurs in the same place or in close proximity.

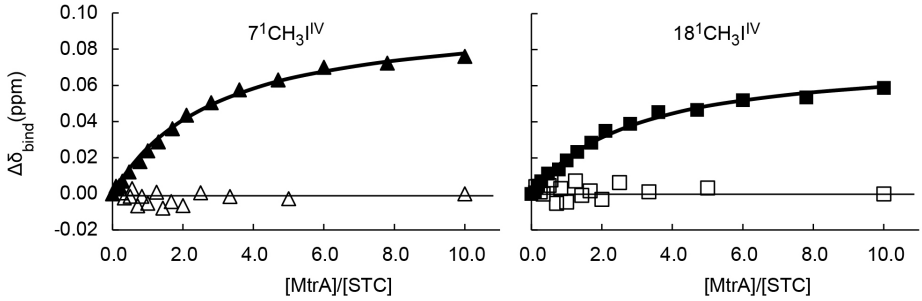

Figure 3. Competition binding curves between STC and FccA with MtrA monitored by ^{1}H-1D NMR spectra. The chemical shift perturbations of the heme methyl signals are plotted as a function of the molar ratio of the interacting proteins. Filled symbols represent the experiment performed in the absence of FccA (Fonseca et al., 2013), whereas open symbols represent the experiment in the presence of 360 µM of FccA to ensure that more than 90% of MtrA is bound to FccA. The solid lines represent the best global fit to the 1:1 binding model [equation 1] as reported by Fonseca et al. (2013).

The inverse competition binding assay with MtrA saturated with bound STC in the presence of increasing amounts of FccA added to the sample is not experimentally feasible. To reach more than 90% saturation of a sample with 50 µM of MtrA with STC would require concentrations of STC above 5 mM. Likewise, a similar experiment exploring the interactions of STC and FccA with CymA, another key protein for which a structure has not been reported in the literature, is not also experimentally feasible. The large dissociation constants reported for the interaction between STC and CymA or FccA and CymA (Fonseca et al., 2013) mean that achieving more than 90% saturation of 50 µM CymA with any of the partners would require concentrations of STC and FccA of 2.2 and 3.5 mM, respectively.

Spectroscopic Assay of Interprotein Electron Transfer

UV-visible experiments were performed to confirm the interaction data obtained from NMR experiments involving FccA. The fumarate reductase activity of FccA was used to measure the re-oxidation of possible partner cytochromes. These experiments showed that FccA cannot re-oxidize MtrD, DmsE, OTR, and ccNiR (Figure 4), which is in agreement with the data obtained from NMR titrations.

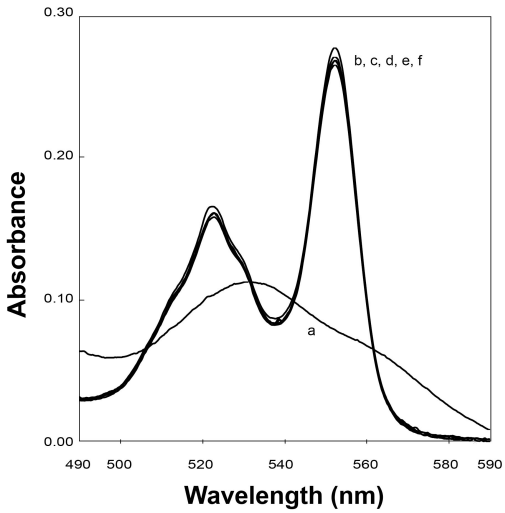

Figure 4. UV–visible spectroscopy of reduced periplasmic cytochromes in the presence of excess fumarate and catalytic amounts of FccA illustrating the absence of electron transfer between OTR with FccA. UV-visible spectrum of the cytochrome as purified (a), after reduction with sodium dithionite (b) and subsequent addition of fumarate (c). After addition of FccA to the mixture, spectra were acquired at 0 min (d), 2.5 min (e), and 5 min (f). The samples were prepared in 20 mM phosphate buffer pH 7.6, with 100 mM KCl, at 25°C

Electrostatic Calculations

The electrostatic potential at the surfaces of the enzymes ccNiR and OTR were calculated using the same procedure as previously used for STC and FccA (Fonseca et al., 2013). OTR presents an overall negative surface, with the exception of two regions, one near heme II (the catalytic heme) and the other one near heme VIII. In the case of ccNiR, the surface potential does not show a clear cut trend as in the case of OTR, with the exception of the region near heme I, which

is the catalytic heme. The region around this heme is strongly negative (Figure 5).

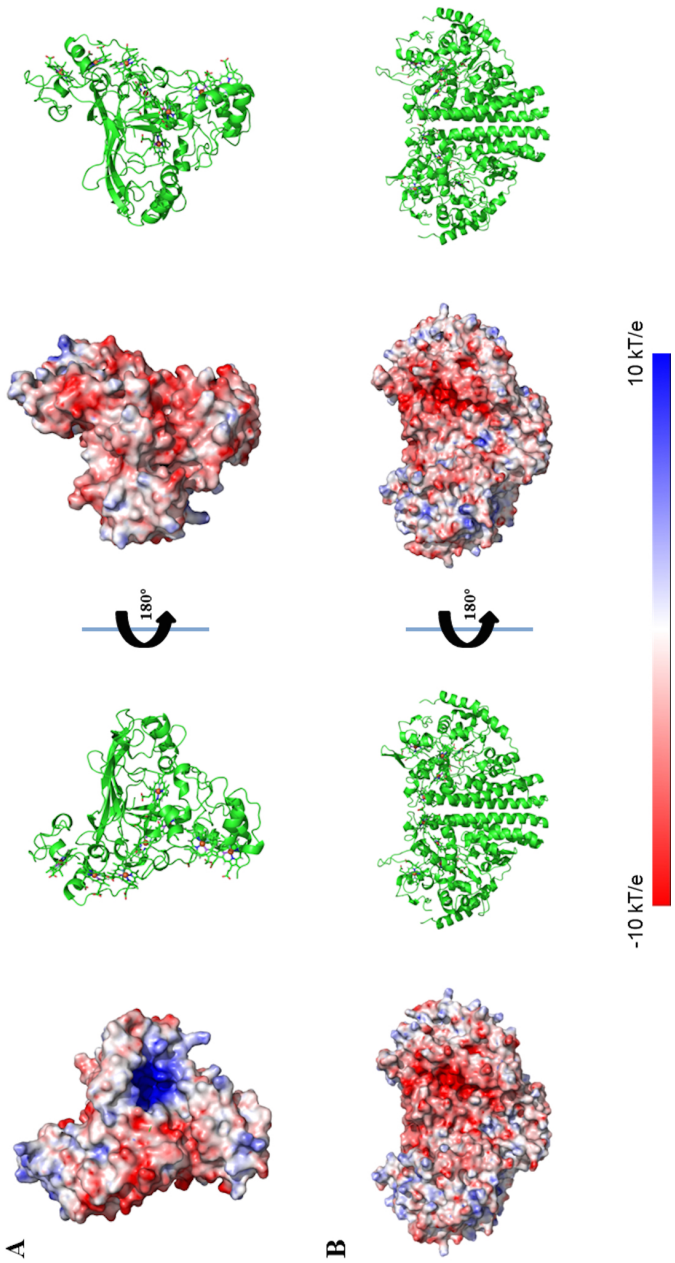

Figure 5. Electrostatic potential mapping on the protein's surface of (A) OTR (PDB code 1S3P) and (B) ccNiR (PDB code3UBR) from SOMR-1. Electrostatic potentials were calculated considering a fully oxidized state for these cytochromes.

Discussion

The electron transfer pathways of the SOMR-1 to reduce Fe(III), DMSO, fumarate and nitrite are established by a variety of multiheme *c*-type cytochromes located at the inner-membrane, periplasm and outer-membrane. Biochemical studies showed that all of these routes have the common feature of being initiated by the oxidation of the quinone pool at the inner-membrane by the tetraheme *c*-type cytochrome, CymA (Schwalb et al., 2003; Marritt et al., 2012). The detailed understanding of the organization of the trans-periplasmic redox network has been compounded by two factors: spectroscopic signatures of *c*-type cytochromes are often overlapping or identical (Firer-Sherwood et al., 2011), and they form low-affinity complexes with fast dissociation rates (Crowley and Ubbink, 2003; Rudolph, 2007; Abresch et al., 2009). Nevertheless, recent studies have demonstrated that NMR spectroscopy is an effective technique to identify transient interactions between redox partners by monitoring the perturbation of the chemical shifts of heme signals (Fonseca et al., 2013). This method does not disturb the protein conformation because it is a soluble assay. Furthermore, it has the unique advantage of allowing the determination of docking regions between redox partners when resonance assignments of the interacting proteins are available.

A previous study revealed that STC and FccA can independently mediate electron transfer between CymA and MtrA leading to

extracellular electron transfer (Fonseca et al., 2013). Since the three-dimensional structure of MtrA was only characterized at low resolution using SAXS (Firer-Sherwood et al., 2011), the docking with its redox partners STC and FccA cannot be modeled at this point. Notwithstanding, in this work the interaction of STC and FccA with MtrA was further characterized by a competition binding assay between STC and FccA. It revealed that these two proteins bind MtrA in the same or at least closely related locations, given that saturation of MtrA with FccA prevents the binding of STC.

This study also reveals that STC interacts transiently with DmsE and that the signals of hemes II, III, and IV are perturbed. Clearly, the interaction between STC and DmsE is different from that between STC and MtrA, which affects only signals of the heme IV of STC. Given the bracket shape of the structure of STC, if one considers the hemes ordered sequentially from top to bottom it can be envisaged that interaction with DmsE occurs via the lower external face of the bracket (Appendix 2- Figure 1).

The genome of SOMR-1 contains three homologues of the MtrCAB–OmcA complex, the MtrDEF complex, the DmsEFABGH complex and the complex coded by the genes SO_4357-62. Studies involving MtrA knockout strains showed that two of these complexes constitute alternative routes of electron flow to Fe(III) respiration (Coursolle and Gralnick, 2010). MtrA can be functionally replaced in ferric citrate reduction in the order MtrD > DmsE (Coursolle and Gralnick, 2012). Despite the high homology of SO4360 with MtrA, this

decaheme cytochrome cannot functionally replace MtrA and requires its own porin SO4359 to function in metal reduction (Schicklberger et al., 2013). This hierarchy in the capacity for functional replacement of MtrA matches the sequence homology among these decaheme cytochromes (Table 3) but does not match the observed interactions with the major trans-periplasmic redox shuttles. MtrA interacts with STC and FccA that compete for the same binding site on the surface of MtrA. DmsE interacts with STC but not FccA, and MtrD does not interact with STC or FccA. Altogether, these data give strong indications that the dominant factor in the capacity of other periplasmic decaheme cytochromes to functionally replace MtrA is the matching with the MtrB porin to establish contact with the outer-membrane MtrC cytochrome, since neither STC nor FccA interact with MtrD.

Table 3. Sequence identity matrix for the periplasmic decaheme cytochromes from SOMR-1.

	MtrA	MtrD	DmsE	SO4360
MtrA	100	72	69	54
MtrD	++	100	60	49
DmsE	+		100	51
SO4360	-			100

Sequences of the four decaheme cytochromes were retrieved from Pubmed-NCBI database and aligned using the Clustal 2.1 Multiple Sequence Alignment website. Values are presented in percentage. Below the diagonal is an indication of the relative ability to functionally replace MtrA according to Coursolle and Gralnick (2010).

Studies recently published by Sturm et al. (2015) showed that single mutants of STC and FccA have only minor phenotypic changes in their ability to reduce DMSO. However, the double mutant strain is

unable to grow using this electron acceptor (Sturm et al., 2015). Those results suggest that both STC and FccA have a key role in the respiration of DMSO in SOMR-1 and the data reported in this work indicates that FccA does not interact directly with DmsE.

In this study, interactions involving two major terminal reductases involved in pathways for dissimilatory nitrate ammonification of SOMR-1, ccNiR, and OTR, were also explored (Berks et al., 1995; Simon, 2002; Einsle and Kroneck, 2004). While the pentaheme ccNiR catalyzes the reduction of nitrite (NO_2^-) to ammonium ($NH4^+$), the octaheme OTR can reduce nitrite (NO_2^-) and hydroxylamine (NH_2OH), as well as the sulfur compound tetrathionate ($S_4O_6^{2-}$) (Atkinson et al., 2007). The results showed that heme IV of STC is perturbed upon interaction with OTR. The region around heme IV of STC displays the strongest negative surface, making it a good candidate to interact with OTR that displays positively charged potentials in various regions of its surface (Figure 5). By contrast, no interaction was observed between ccNiR and STC or FccA. The surface of ccNiR is predominantly weakly negative with a strongly negative region near the catalytic center, therefore discouraging interactions with the negatively charged STC or heme domain of FccA. This result is also consistent with a previous study showing that both wild-type SOMR-1 and the Δ*stc*Δ*fccA* mutant strain reduce nitrite at similar rates (Sturm et al., 2015).

Interestingly, all protein–protein interactions reported between STC and its putative physiological partners involve heme IV (Fonseca et

al., 2013). Given that to perform its function of shuttling electrons between redox partners STC needs to charge and discharge, clearly this protein does not operate as a molecular wire. It functions more like an electronic cul-de-sac that forces electrons to enter and leave the cytochrome by the same heme. This enables *Shewanella* to transfer electrons in a controlled and efficient manner (maximum of four electrons can be transferred by STC) to specific proteins in the periplasmic space, rather than transfer randomly to any protein that may interact with STC. This minimizes the risk of diverting electrons to side redox pathways and production of radical species.

Conclusion

We have elucidated the organization of the multi-branched periplasmic respiratory network of SOMR-1. NMR studies revealed that STC not only contributes to extracellular respiration of metals via interaction with MtrCAB–OmcA, but also to the reduction of nitrogen compounds and DMSO by interacting with OTR and DmsE, respectively (Figure 6). These results demonstrate that STC is a promiscuous periplasmic electron shuttle with a variety of redox partners. Notwithstanding, STC is clearly selective in the mode of interaction with its multiple partners that always appears to involve the participation of heme IV. Interestingly, in contrast to STC, no interaction was observed between FccA with MtrD, DmsE, OTR, and ccNiR. These results contrast with the functional redundancy that FccA provides for STC revealed by delayed or no growth with ferric

citrate, DMSO or nitrite as electron acceptors (Sturm et al., 2015) in double deletion mutant studies. Further studies will reveal whether the differences arise from different metabolic regulation in the mutant strains or if FccA interacts indirectly with partners in those metabolic pathways.

Acknowledgments

We thank Dr. Liang Shi from the Pacific Northwest National Laboratory (Richland, WA, USA) for providing the cloning vectors (pBAD202/D-TOPO) containing the *dmsE* and *mtrD* genes. We thank Dr. Sean J. Elliott from Boston University for providing with the cloning vector pHSG298 containing the *ccnir* gene, and Prof. Dr. Johannes Gescher from Karlsruhe Institut für Technologie for providing the *S. oneidensis* JG207 strain. This work was supported by Fundação para a Ciência e a Tecnologia (FCT)—Portugal [Grants REEQ/336/BIO/2005, PTDC/BIA-PRO/117523/2010, SFRH/BPD/96952/2013 (to CP), and SFRH/BPD/93164/2013 (to BF)]. The NMR experiments were performed at the National NMR Facility supported by FCT (RECI/BBB-BQB/0230/2012). Mass spectrometry data were obtained by the Mass Spectrometry Laboratory, Analytical Services Unit, Instituto de Tecnologia Química e Biológica. N-terminal sequencing was obtained by the Analytical Laboratory, Analytical Services Unit, Instituto de Tecnologia Química e Biológica, Universidade Nova de Lisboa.

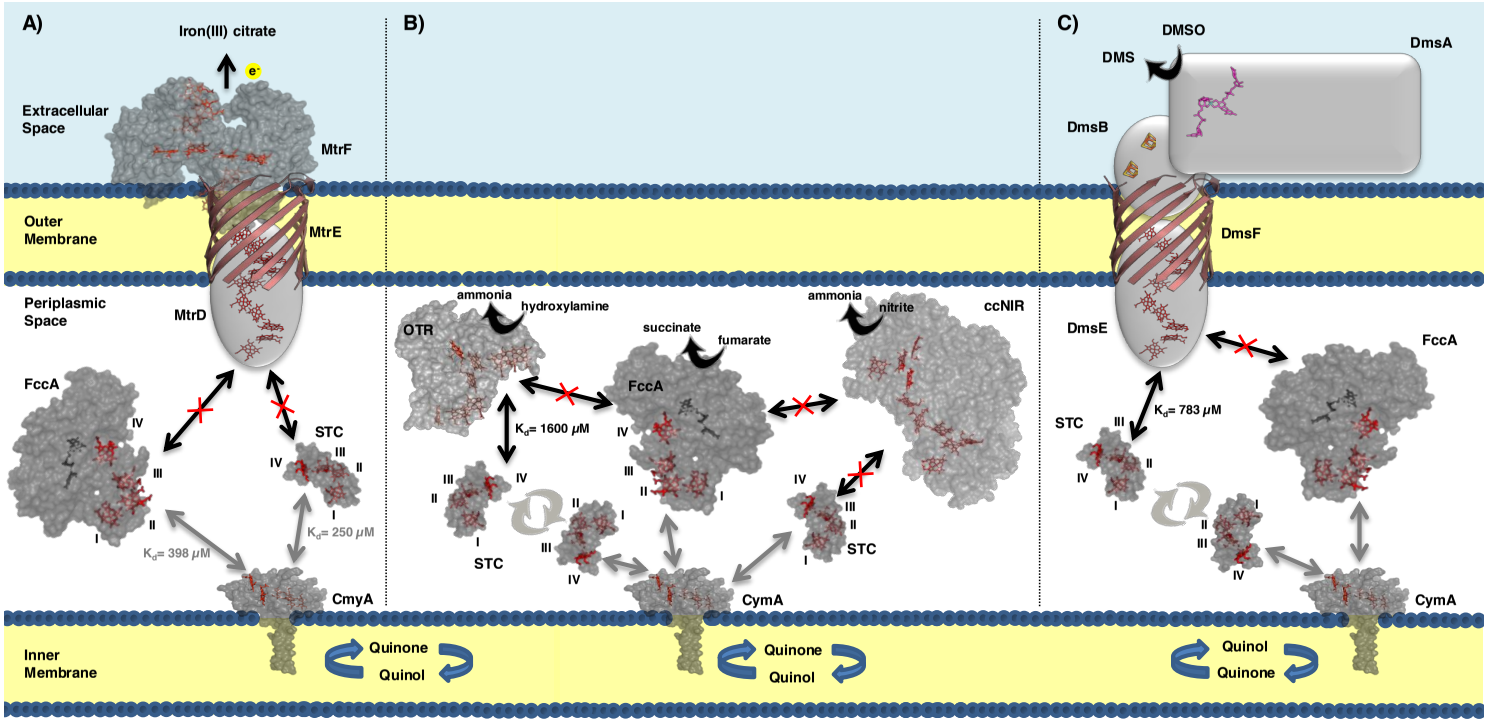

Figure 6. Interactions between the most abundant periplasmic cytochromes (STC and FccA), and outer membrane complex MtrDEF (A), periplasmic nitrite reductases OTR and ccNiR (B) and outer membrane complex DmsEFABGH (C). The arrows in bold indicate the interactions that occur between the cytochromes and point to the possible docking site. Black arrows indicate data from this work and gray arrows indicate data previously reported (Fonseca et al., 2013). The dissociation constants (K_d) corresponding to each interaction are indicated next to their respective arrow. Interactions that were not detected experimentally are represented by a crossed-out arrow. The Roman numerals correspond to the order of heme attachment to the polypeptide chain. Cytochrome representations were made with PyMOL using the structures of STC (PDB code 1M1Q), FccA (PDB code 1D4D), OTR (PDB code 1S3P), and ccNiR (PDB code 3UBR). For CymA the model was made with SWISS-MODEL (Arnold et al., 2006; Kiefer et al., 2009) using as template the structure of NrfH (PDB code 2J7A).

References

Abresch, E. C., Gong, X.M., Paddock, M. L., and Okamura, M. Y. (2009). Electron Transfer from Cytochrome *c*(2) to the Reaction Center: A Transition State Model for Ionic Strength Effects due to Neutral Mutations. *Biochemistry*. 48, 11390–11398. doi: 10.1021/bi901332t

Arnold, K., Bordoli, L., Kopp, J., and Schwede, T. (2006). The SWISS-MODEL Workspace: A Web-based Environment for Protein Structure Homology Modelling. *Bioinformatics*. 22, 195–201. doi: 10.1093/bioinformatics/bti770

Atkinson, S. J., Mowat, C. G., Reid, G. A., and Chapman, S. K. (2007). An Octaheme *c*-type Cytochrome from *Shewanella oneidensis* can Reduce Nitrite and Hydroxylamine. *FEBS Lett*. 581, 3805–3808. doi: 10.1016/j.febslet.2007. 07.005

Banci, L., Pierattelli, R., and Turner, D. L. (1995). Determination of Haem Electronic Structure in Cytochrome *b*5 and Metcyanomyoglobin. *Eur. J. Biochem*. 232, 522–527. doi: 10.1111/j.1432-1033.1995.522zz.x

Bashford, D., and Karplus, M. (1990). pKa's of Ionizable Groups in Proteins: Atomic Detail from a Continuum Electrostatic Model. *Biochemistry*. 29, 10219–10225. doi: 10.1021/bi00496a010

Bashir, Q., Scanu, S., and Ubbink, M. (2011). Dynamics in Electron Transfer Protein Complexes. *FEBS J*. 278, 1391–1400. doi: 10.1111/j.1742-4658.2011.08062.x

Berks, B. C., Ferguson, S. J., Moir, J. W., and Richardson, D. J. (1995). Enzymes and Associated Electron Transport Systems that Catalyse the Respiratory Reduction of Nitrogen Oxides and Oxyanions. *Biochim. Biophys. Acta*. 1232, 97–173. doi: 10.1016/0005-2728(95)00092-5

Burns, J. L., and DiChristina, T. J. (2009). Anaerobic Respiration of Elemental Sulfur and Thiosulfate by *Shewanella oneidensis* MR-1 requires *psrA*, a homolog of the *phsA* gene of *Salmonella enterica* serovar typhimurium LT2. *Appl. Environ. Microbiol*. 75, 5209–5217. doi: 10.1128/AEM.00888-09

Coursolle, D., and Gralnick, J. A. (2010). Modularity of the Mtr Respiratory Pathway of *Shewanella oneidensis* strain MR-1. *Mol. Microbiol*. 77, 995–1008. doi: 10.1111/j.1365-2958.2010.07266.x

Coursolle, D., and Gralnick, J. A. (2012). Reconstruction of Extracellular Respiratory Pathways for Iron(III) Reduction in *Shewanella oneidensis* strain MR-1. *Front. Microbiol*. 3: 56. doi: 10.3389/fmicb.2012.00056

Crowley, P. B., and Ubbink, M. (2003). Close Encounters of the Transient Kind: Protein Interactions in the Photosynthetic Redox

Chain Investigated by NMR spectroscopy. *Acc. Chem. Res*. 36, 723–730. doi: 10.1021/ar0200955

DeLano, W. L. (2003). The PyMOL Molecular Graphics System. San Carlos, CA: DeLano Scientific LLC.

Diaz-Moreno, I., Diaz-Quintana, A., Molina-Heredia, F. P., Nieto, P. M., Hansson, O., De la Rosa, M. A., et al. (2005a). NMR Analysis of the Transient Complex Between Membrane Photosystem I and Soluble Cytochrome *c*6. *J. Biol. Chem*. 280, 7925–7931. doi: 10.1074/jbc.M412422200

Diaz-Moreno, I., Diaz-Quintana, A., Ubbink, M., and De la Rosa, M. A. (2005b). An NMR-based Docking Model for the Physiological Transient Complex Between Cytochrome *f* and Cytochrome *c*6. *FEBS Lett*. 579, 2891–2896. doi: 10.1016/j.febslet.2005.04.031

Einsle, O., and Kroneck, P. M. (2004). Structural Basis of Denitrification. *Biol. Chem*. 385, 875–883. doi: 10.1515/BC.2004.115

Einsle, O., Messerschmidt, A., Huber, R., Kroneck, P. M., and Neese, F. (2002). Mechanism of the Six-electron Reduction of Nitrite to Ammonia by Cytochrome *c* Nitrite Reductase. *J. Am. Chem. Soc*. 124, 11737–11745. doi: 10.1021/ja02 06487

Firer-Sherwood, M. A., Bewley, K. D., Mock, J. Y., and Elliott, S. J. (2011). Tools for Resolving Complexity in the Electron Transfer Networks of Multiheme Cytochromes *c*. *Metallomics*. 3, 344–348. doi: 10.1039/c0mt00097c

Fonseca, B. M., Paquete, C. M., Neto, S. E., Pacheco, I., Soares, C. M., et al. (2013). Mind the Gap: Cytochrome Interactions Reveal Electron Pathways Across the Periplasm of *Shewanella oneidensis* MR-1. *Biochem. J*. 449, 101–108. doi: 10.1042/BJ20121467

Fonseca, B. M., Saraiva, I. H., Paquete, C. M., Soares, C. M., Pacheco, I., Salgueiro, C. A., et al. (2009). The Tetraheme Cytochrome from *Shewanella oneidensis* MR- 1 Shows Thermodynamic Bias for Functional Specificity of the Hemes. *J. Biol. Inorg. Chem*. 14, 375–385. doi: 10.1007/s00775-008-0455-7

Francis, R. T. Jr., and Becker, R. R. (1984). Specific Indication of Hemoproteins in Polyacrylamide Gels Using a Double-staining Process. *Anal. Biochem*. 136, 509–514. doi: 10.1016/0003-2697(84)90253-7

Fredrickson, J. K., Romine, M. F., Beliaev, A. S., Auchtung, J. M., Driscoll, M. E., Gardner, T. S., et al. (2008). Towards Environmental Systems Biology of *Shewanella*. *Nat. Rev. Microbiol.* 6, 592–603. doi:10.1038/nrmicro1947.

Gralnick, J. A., and Newman, D. K. (2007). Extracellular Respiration. *Mol. Microbiol*. 65, 1–11. doi: 10.1111/j.1365-2958.2007.05778.x

Gray, H. B., and Winkler, J. R. (2010). Electron Flow Through Metalloproteins. *Biochim. Biophys. Acta*. 1797, 1563–1572. doi: 10.1016/j.bbabio.2010.05.001

Hartshorne, R. S., Jepson, B. N., Clarke, T. A., Field, S. J., Fredrickson, J., Zachara, J., et al. (2007). Characterization of *Shewanella oneidensis* MtrC: a Cell-surface Decaheme Cytochrome Involved in Respiratory Electron Transport to Extracellular Electron Acceptors. *J. Biol. Inorg. Chem*. 12, 1083–1094. doi: 10.1007/s00775-007-0278-y

Hartshorne, R. S., Reardon, C. L., Ross, D., Nuester, J., Clarke, T.A., and Gates, A. J. (2009). Characterization of an Electron Conduit Between Bacteria and the Extracellular Environment. *Proc. Natl. Acad. Sci. U.S.A.* 106, 22169–22174. doi: 10.1073/pnas.0900086106

Hau, H. H., and Gralnick, J. A. (2007). Ecology and Biotechnology of the Genus *Shewanella*. *Annu. Rev. Microbiol*. 61, 237–258. doi: 10.1146/annurev.micro.61.080706.093257

Heidelberg, J. F., Paulsen, I. T., Nelson, K. E., Gaidos, E. J., Nelson, W. C., Read, T. D., et al. (2002). Genome Sequence of the Dissimilatory Metal ion-reducing bacterium *Shewanella oneidensis*. *Nat. Biotechnol*. 20, 1118–1123. doi: 10.1038/nbt749

Judd, E. T., Youngblut, M., Pacheco, A. A., and Elliott, S. J. (2012). Direct Electrochemistry of *Shewanella oneidensis* Cytochrome *c* Nitrite Reductase: Evidence of Interactions Across the Dimeric Interface. *Biochemistry*. 51, 10175– 10185. doi: 10.1021/bi3011708

Kiefer, F., Arnold, K., Kunzli, M., Bordoli, L., and Schwede, T. (2009). The SWISS-MODEL Repository and Associated Resources. *Nucleic Acids Res*. 37, D387–D392. doi: 10.1093/nar/gkn750

Logan, B. E., and Rabaey, K. (2012). Conversion of Wastes Into Bioelectricity and Chemicals by Using Microbial Electrochemical Technologies. *Science*. 337, 686–690. doi: 10.1126/science.1217412

Lovley, D. R. (2006). Bug Juice: Harvesting Electricity With Microorganisms. *Nat. Rev. Microbiol*. 4, 497–508. doi: 10.1038/nrmicro1442

Marritt, S. J., Lowe, T. G., Bye, J., McMillan, D. G., Shi, L., Fredrickson, J., et al. (2012). A Functional Description of CymA, an Electron-transfer Hub Supporting Anaerobic Respiratory Flexibility in *Shewanella*. *Biochem. J*. 444, 465–474. doi: 10.1042/BJ20120197

Massey, V. (1959). The Microestimation of Succinate and the Extinction Coefficient of Cytochrome *c*. *Biochim. Biophys. Acta*. 34, 255–256. doi: 10.1016/0006- 3002(59)90259-8

Meschi, F., Wiertz, F., Klauss, L., Blok, A., Ludwig, B., Merli, A., et al. (2011). Efficient Electron Transfer in a Protein Network Lacking Specific Interactions. *J. Am. Chem. Soc*. 133, 16861–16867. doi: 10.1021/ja205043f

Mowat, C. G., Rothery, E., Miles, C. S., McIver, L., Doherty, M. K., Drewette, K., et al. (2004). Octaheme Tetrathionate Reductase is a Respiratory Enzyme with Novel Heme Ligation. *Nat. Struct. Mol. Biol.* 11, 1023–1024. doi:10.1038/nsmb827.

Myers, C. R., and Myers, J. M. (1997). Isolation and Characterization of a Transposon Mutant of *Shewanella putrefaciens* MR-1 Deficient

in Fumarate Reductase. *Lett. Appl. Microbiol*. 25, 162–168. doi: 10.1046/j.1472- 765X.1997.00196.x

Myers, C. R., and Nealson, K. H. (1988). Bacterial Manganese Reduction and Growth with Manganese Oxide as the Sole Electron Acceptor. *Science*. 240, 1319–1321. doi: 10.1126/science.240.4857.1319

Myers, J. M., and Myers, C. R. (2000). Role of the Tetraheme Cytochrome CymA in Anaerobic Electron Transport in Cells of *Shewanella putrefaciens* MR-1 With Normal Levels of Menaquinone. *J. Bacteriol*. 182, 67–75. doi: 10.1128/JB.182.1.67-75.2000

Nealson, K. H., and Saffarini, D. (1994). Iron and Manganese in Anaerobic Respiration: Environmental Significance, Physiology, and Regulation. *Annu. Rev. Microbiol*. 48, 311–343. doi: 10.1146/annurev.mi.48.100194.001523

Perkins, J. R., Diboun, I., Dessailly, B. H., Lees, J. G., and Orengo, C. (2010). Transient Protein-protein Interactions: Structural, Functional, and Network Properties. *Structure*. 18, 1233–1243. doi: 10.1016/j.str.2010.08.007

Pessanha, M., Rothery, E. L., Miles, C. S., Reid, G. A., Chapman, S. K., Louro, R. O., et al. (2009). Tuning of Functional Heme Reduction Potentials in *Shewanella* Fumarate Reductases. *Biochim. Biophys. Acta*. 1787, 113–120. doi: 10.1016/j.bbabio.2008.11.007

Pitts, K. E., Dobbin, P. S., Reyes-Ramirez, F., Thomson, A. J., Richardson, D. J., and Seward, H. E. (2003). Characterization of the *Shewanella oneidensis* MR- 1 Decaheme Cytochrome MtrA: Expression in *Escherichia coli* Confers the Ability to Reduce Soluble Fe(III) Chelates. *J. Biol. Chem*. 278, 27758–27765. doi: 10.1074/jbc.M302582200

Richardson, D. J., Butt, J. N., Fredrickson, J. K., Zachara, J. M., Shi, L., Edwards, M. J., et al. (2012). The "Porin-cytochrome" Model for Microbe-to- mineral Electron Transfer. *Mol. Microbiol*. 85, 201–212. doi: 10.1111/j.1365- 2958.2012.08088.x

Rudolph, J. (2007). Inhibiting Transient Protein-protein Interactions: Lessons From the Cdc25 Protein Tyrosine Phosphatases. *Nat. Rev. Cancer*. 7, 202–211. doi: 10.1038/nrc2087

Saffarini, D. A., Blumerman, S. L., and Mansoorabadi, K. J. (2002). Role of Menaquinones in Fe(III) Reduction by Membrane Fractions of *Shewanella putrefaciens*. *J. Bacteriol*. 184, 846–848. doi: 10.1128/JB.184.3.846-848.2002

Schicklberger, M., Sturm, G., and Gescher, J. (2013). Genomic Plasticity Enables a Secondary Electron Transport Pathway in *Shewanella oneidensis*. *Appl. Environ. Microbiol*. 79, 1150–1159. doi: 10.1128/AEM.03556-12

Schwalb, C., Chapman, S. K., and Reid, G. A. (2003). The Tetraheme Cytochrome CymA is Required for Anaerobic Respiration with

Dimethyl Sulfoxide and Nitrite in *Shewanella oneidensis*. *Biochemistry*. 42, 9491–9497. doi: 10.1021/bi034456f

Scott, W., Hünenberger, P., Tironi, I., Mark, A., Billeter, S., Fennen, J., et al. (1999). The GROMOS Biomolecular Simulation Program Package. *J. Phys. Chem. A*. 103, 3596–3607. doi: 10.1021/jp984217f

Shi, L., Lin, J. T., Markillie, L. M., Squier, T. C., and Hooker, B. S. (2005). Overexpression of Multi-heme *c*-type Cytochromes. *Biotechniques*. 38, 297–299. doi: 10.2144/05382PT01

Simon, J. (2002). Enzymology and Bioenergetics of Respiratory Nitrite Ammonification. *FEMS Microbiol. Rev*. 26, 285–309. doi: 10.1111/j.1574-6976. 2002.tb00616.x

Sturm, G., Richter, K., Doetsch, A., Heide, H., Louro, R. O., and Gescher, J. (2015). A Dynamic Periplasmic Electron Transfer Network Enables Respiratory Flexibility Beyond a Thermodynamic Regulatory Regime. *ISME J.*, 1–10. doi:10.1038/ismej.2014.264.

Tsapin, A. I., Vandenberghe, I., Nealson, K. H., Scott, J. H., Meyer, T. E., Cusanovich, M. A., et al. (2001). Identification of a Small Tetraheme Cytochrome *c* and a Flavocytochrome *c* as Two of the Principal Soluble Cytochromes *c* in *Shewanella oneidensis* strain MR1. *Appl. Environ. Microbiol*. 67, 3236–3244. doi: 10.1128/AEM.67.7.3236-3244.2001

Worrall, J. A., Reinle, W., Bernhardt, R., and Ubbink, M. (2003). Transient Protein Interactions Studied by NMR Spectroscopy: The

Case of Cytochrome *c* and Adrenodoxin. *Biochemistry*. 42, 7068–7076. doi: 10.1021/bi0342968

Youngblut, M., Judd, E. T., Srajer, V., Sayyed, B., Goelzer, T., Elliott, S. J., et al. (2012). Laue Crystal Structure of *Shewanella oneidensis* Cytochrome *c* Nitrite Reductase from a High-yield Expression System. *J. Biol. Inorg. Chem.* 17, 647–662. doi:10.1007/s00775-012-0885-0.

Zhang, H., Chobot, S. E., Osyczka, A., Wraight, C. A., Dutton, P. L., and Moser, C. C. (2008). Quinone and Non-quinone Redox Couples in Complex III. *J. Bioenerg. Biomembr*. 40, 493–499. doi: 10.1007/s10863-008-9174-6

Chapter III

Characterization of OmcA Mutants from *Shewanella oneidensis MR*-1 to Investigate the Molecular Mechanisms Underpinning the Electron Transfer Processes Across the Microbe-Electrode Interface

Chapter III is in preparation to be submitted

Neto, S. E., Paquete, C. M., de Melo-Diogo, D., Correia, I. J., Louro, R. O. (2017) Characterization of OmcA Mutants from *Shewanella oneidensis MR*-1 to Investigate the Molecular Mechanisms Underpinning the Electron Transfer Processes Across the Microbe-Electrode Interface

Author contributions:

All experiments described in this chapter were performed by Sónia E. Neto.

Sónia E. Neto contributed to the planning of the experiments and to the writing of the original paper.

Abstract

Electricity production in microbial fuel cells (MFCs) is an emerging green alternative to the usage of for fossil fuels. *Shewanella oneidensis* MR-1 (SOMR-1) is a sedimentary Gram-negative bacterium with a highly versatile metabolism, uniquely suited for the operation in MFCs, due to its ability to link its bioenergetic metabolism through the periplasm to reduce extracellular electron acceptors. OmcA is the most abundant outer-membrane cytochrome of SOMR-1 cells and the major responsible for extracellular electron transfer to terminal electron acceptors and electron shuttles. To investigate electron transfer performed by OmcA towards final acceptors, site directed mutagenesis was used to disturb the axial coordination of hemes. Interactions between OmcA and redox partners such as iron and graphene oxides, and mobile electron shuttles were characterized using NMR and stopped-flow experiments. Results showed that solid electron acceptors do not come into close proximity to the hemes, in agreement with experimentally observed slow electron transfer. In contrast, mutation of the distal axial ligand of heme VII changes the driving force of OmcA towards electron shuttles and reduces the affinity of the FMN:OmcA complex.

Overall, these results reveal a functional specificity of particular hemes of OmcA and provide guidance for the design of mutated SOMR-1 strains optimized for different operational modes of microbial electrochemical devices.

Introduction

It is now well recognized that some microorganisms have the ability to convert chemical energy into electrical current. This occurs when they are inoculated in devices belonging to a vast class of the so-called microbial electrochemical technologies that can have a multitude of applications in industrial processes of low ecological footprint (Wang and Ren, 2013). Although the first reports for microbial electricity production date from early 1910s (Potter, 1911), studies focused on the efficient implementation of devices that use bacteria to produce electricity called microbial fuel cells (MFC) only began in the 60's (Davis and Yarbrough, 1962; Sisler, 1969). The efficiency of MFCs depends on numerous factors, including the electrode material, the architecture of the cell and the bacteria used (Logan, 2007). The first microorganism to show electrical current production in a MFC, without the need of exogenously added mediators was *Shewanella oneidensis* MR-1 (SOMR-1) (Kim et al., 2002). This bacterium is able to use lactate as carbon source and electron donor and the electrode as the electron acceptor (Kim et al., 1999). One of the defining features of SOMR-1 is its ability to use a wide variety of terminal electron acceptors that includes both organic and inorganic compounds, such as oxygen, fumarate, nitrite, nitrate, thiosulfate, sulfur, trimethylamine N-oxide, DMSO, and also soluble and insoluble metallic compounds, for example iron, manganese, uranium, chromium, cobalt, technetium and vanadium (Gralnick and Newman, 2007). Given its ability to grow on electrodes of

different chemical nature including carbon based electrodes, SOMR-1 is of great interest for applications in MFCs (Gralnick and Newman, 2007).

Extracellular electron transfer of SOMR-1 relies on outer-membrane cytochromes that are located at the cell surface. These proteins can reduce directly the solid electron acceptors, or reduce them indirectly using small soluble electron shuttles that are secreted from the cell (Marsili et al., 2008). It was also shown that SOMR-1 has the ability to form outer-membrane extensions called pilli or nanowires, when the cells' reductase activity increases (Gorby et al., 2006) being these extensions decorated with outer-membrane cytochromes (Pirbadian et al., 2014).

Electron shuttles were shown to be essential for extracellular electron transfer in SOMR-1, leading to the increase of current production in MFCs and an increase in the rate of insoluble iron reduction (von Canstein et al., 2008; Ross et al., 2009; Kotloski and Gralnick, 2013). Flavins such as FMN and riboflavin are the most abundant redox mediators secreted by SOMR-1 to the extracellular environment, reaching concentrations in the µM range (von Canstein et al., 2008). Furthermore, SOMR-1 can opportunistically make use of other compounds such as phenazines and humic acids to promote microbial iron reduction (Lovley et al., 1996; Hernandez et al., 2004).

Among SOMR-1 outer-membrane cytochromes, OmcA is the most abundant cytochrome located on the outer surface of SOMR-1 cells (Zhang et al., 2009) and is the major responsible for cellular attachment

to solid surfaces (Xiong et al., 2006). OmcA is a decaheme cytochrome with a lipid anchor in the N-terminus that binds to the outer-membrane, and is part of a porin like complex, MtrCAB-OmcA, which spans through the outer-membrane of the cells (Edwards et al., 2014). OmcA is likely to be reduced by MtrC that in turn is postulated to receive electrons from MtrA, which is inserted in the MtrB porin and contacts the periplasmic space of this Gram-negative bacterium (Richardson et al., 2012). The structure of OmcA indicates that the hemes are organized in a staggered cross arrangement (Figure 1) with an orientation determined by the lipid anchor near the N-terminus (Edwards et al., 2014).

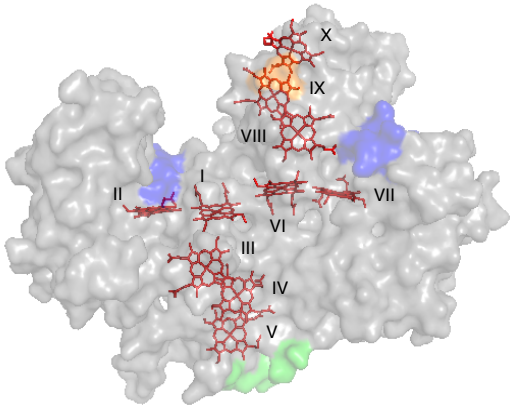

Figure 1. Surface representation of crystal 3D-structure of OmcA (PDB: 4LMH). Hemes are colored in red. Flavin binding domains, hematite binding motif and cytochrome-cytochrome interaction site are represented in blue, orange and green, respectively.

Analysis of the crystal structure of OmcA, lead to the proposal that heme V is near the outer-membrane of SOMR-1, and therefore the heme responsible for the reduction of OmcA by MtrC, via cytochrome-cytochrome interaction (Edwards et al., 2014). Hemes II and heme VII are located near two flavin binding domains (Clarke et al., 2011;

Edwards et al., 2012; Paquete et al., 2014). Although docking studies showed that heme II is the one that presents the lowest energy conformation state for the complex OmcA-FMN (Paquete et al., 2014; Breuer et al., 2015), heme VII is in close proximity to an hydrophobic cleft where flavins dock and to an oxygen regulated disulfide bond that was shown to be important to control the redox activity of outer-membrane cytochromes towards FMN (Edwards et al., 2015). Finally, hemes IX and X were proposed to be responsible for the interaction of OmcA with minerals and metal ions (Edwards et al., 2014) given that they are located near a proposed hematite binding motif with the conserved sequence Ser/Thr-Pro-Ser/Thr (Lower et al., 2008).

In order to explore the proposed functional specificity of the various hemes in OmcA, site-directed mutagenesis was used to change the distal ligand of the heme iron in various hemes of OmcA. Kinetics of electron transfer and interaction studies to soluble and solid electron acceptors were measured and showed that heme VII plays a key role in the interaction of OmcA with soluble electron shuttles. The results open new perspectives on the molecular mechanisms of electron transfer mediated by OmcA and provide guidance for the design of mutated SOMR-1 strains optimized for use in MFCs.

Materials and Methods

Protein Production

The cloning vector pLS147 was kindly provided by Dr Liang Shi from the Pacific Northwest National Laboratory (Richland, WA, USA). This plasmid consists of the commercial available plasmid pBAD202/D-TOPO containing the *omcA* gene that was modified to obtain the soluble version of the protein (Edwards et al., 2014). This construct contains a histidine tag (his-tag) at the C-terminal to facilitate purification of the protein (Edwards et al., 2014). Five mutants of OmcA were constructed with a single mutation in the histidine amino acid that binds the axial position of the iron of the hemes II, V, VII, IX and X, which was substituted to a methionine (mutants H240M, H359M, H576M, H733M and H696M, respectively). All the mutations were performed using site directed mutagenesis (NZYMutagenesis kit from NZYTech, Lda.) using the primers listed in Table 1.

Table 1. Primers used in this study for site directed mutagenesis.

Primer	Sequence (5'-3')
H240M_Fw	CAG AAA GCT TAG CGC TGA TGG GTG GCC GTC GTA TC
H240M_Rev	GAT ACG ACG GCC ACC CAT CAG CGC TAA GCT TTC TG
H359M_Fw	CAC TGA AAA ACC ATC TGC TCA CAT GAG CAG CAC TGA TTG TAT GGC TT
H359M_Rev	AAG CCA TAC AAT CAG TGC TGC TCA TGT GAG CAG ATG GTT TTT CAG TG
H576M_Fw	GGT TGC CAT AAC AAG GAA ATT GTT ATG TAT GAC AAC GGC GTT AAC TGT CA
H576M_Rev	TGA CAG TTA ACG CCG TTG TCA TAC ATA ACA ATT TCC TTG TTA TGG CAA CC
H733M_Fw	CTC CAT CGC AAT TGA TGG AAG CAA TGG GTA ACG ATG ACG ATG ACA
H733M_Rev	TGT CAT CGT CAT CGT TAC CCA TTG CTT CCA TCA ATT GCG ATG GAG
H696M_Fw	AGA AGT ATC TGT CTG ATG CAG CCA AGT CTA TGA TTG AAA CTA ACG GCG GTA TCT TAA AT
H696M_Rev	ATT TAA GAT ACC GCC GTT AGT TTC AAT CAT AGA CTT GGC TGC ATC AGA CAG ATA CTT CT

The constructs were confirmed by DNA sequencing (GATC Biotech, Germany) and used to transform SOMR-1 wild-type using the protocol described in the literature (Myers and Myers, 1997). SOMR-1 strains were grown aerobically at 30°C in Terrific Broth (TB) medium supplemented with 50 µg/mL kanamycin. Gene expression was induced by the addition of 1 mM arabinose at the mid-log phase of growth and the cells were allowed to grow overnight at the same temperature. Cells were separated from the medium by centrifugation at 11,292 *g* for 15 minutes at 4°C. Medium was concentrated in a stirred Amicon pressure cell and loaded onto a HisTrap HP column (GE Healthare) equilibrated with buffer A (20 mM phosphate buffer, 500 mM KCl and 20 mM imidazole, pH 7.6). The loaded sample was washed with buffer A and eluted with buffer B (20 mM phosphate buffer, 500 mM KCl and 300 mM imidazole, pH 7.6). After elution the proteins were washed with

buffer C (20 mM phosphate buffer and 100 mM KCl, pH 7.6) and concentrated to approximately 200 μM. Concentration of the cytochrome was determined by UV-Vis spectroscopy, using a $\varepsilon_{408\ nm}$ of 125,000 $M^{-1}\,cm^{-1}$ per heme, for the oxidized state of the cytochrome. Pure OmcA mutants presented an A_{408}/A_{280} ratio above 5 and a single band a SDS-PAGE.

Graphene Oxide Materials Preparation

Synthesis

Graphite was purchased from Sigma–Aldrich (Sintra, Portugal). Potassium permanganate ($KMnO_4$) was acquired from Acros Organics (Geel, Belgium). Sulfuric acid (H_2SO_4, 96 %) was obtained from Panreac (Darmstadt, Germany). Phosphoric acid (H_3PO_4, 85 %) was purchased from VWR (Carnaxide, Portugal). Double deionized water (0.22 μm filtered, 18.2 MΩ·cm) was used in all experiments.

Graphite oxide was first produced by using a modified version of the improved Hummer's method as previously described elsewhere (doi: 10.2147/IJN.S26812). Briefly, a concentrated mixture of H_2SO_4/H_3PO_4 (9:1 v/v, 67 mL) was slowly poured into a mixture of graphite (0.51 g) and $KMnO_4$ (3.10 g) in an ice bath. Graphite oxidation was then carried out at room temperature, for 4 days, under stirring. Subsequently, the reaction was transferred into a glass apparatus containing 67 mL of ice-cold water and, then, H_2O_2 was added to the mixture until a yellow

colored solution was obtained. The produced material was purified through repeated centrifugations (with HCl (3.7 %) and water), followed by dialysis against water for 5 days, yielding graphite oxide.

Finally, graphene oxide materials with different lateral dimensions were prepared through the exfoliation of graphite oxide by ultrasonication during 6 or 60 min (Vibra-Cell VC600-2, Sonics & Materials, Newtown, USA).

Characterization

Attenuated total reflection Fourier transform infrared (ATR-FTIR) spectroscopy analysis was performed to confirm the successful synthesis of graphene oxide based materials, using a Nicolet iS10 spectrometer (Thermo Scientific Inc., Waltham, USA) in the 4000 to 600 cm^{-1} wavenumber range. UV-Vis-NIR absorption spectroscopy analysis was also performed to identify the characteristic peak of graphene oxide. To accomplish that, aqueous suspensions containing graphene oxide materials (25 $\mu g\ ml^{-1}$) were characterized on an Evolution 201 spectrophotometer (Thermo Scientific Inc., Waltham, USA) in the 200-1000 nm wavelength range. The size distribution of the produced materials was assessed through dynamic light scattering (DLS) using a Zetasizer Nano ZS (Malvern Instruments, Worcestershire, UK) at a scattering angle of 173 °.

NMR Experiments

Experimental Conditions and Sample Preparation

NMR experiments were performed at 25°C on a Bruker Avance II 500 MHz NMR spectrometer equipped with QXI probe for ^{1}H detection and a SEX probe for ^{31}P detection. ^{1}H-1D-NMR experiments were calibrated using the water signal as an internal reference and collected with a water suppression pulse program. ^{31}P-1D-NMR experiments were calibrated using phosphate buffer as an internal reference and collected with proton decoupling.

^{1}H-1D-NMR spectra were collected from the different mutants and compared with the spectrum of OmcA with a his-tag (from now forward called wtOmcA). All experiments were performed at pH 7.6, in buffer C.

Titrations with Soluble and Insoluble Terminal Electron Acceptors

100 µM FMN samples were titrated against increasing amounts of the target OmcA mutant and ^{31}P-1D-NMR spectra were recorded after each addition. FMN samples were prepared in buffer C, and 10 % of $^{2}H_2O$ (99.9 atom %) was added to a final concentration of 100 µM. Samples of OmcA mutants were prepared by adding 10 % $^{2}H_2O$ (99.9 atom %) to the previously prepared samples.

Titration of wtOmcA prepared with 10 % $^{2}H_2O$ (99.9 atom %) was performed with iron (III) oxide nanopowder (<50 nm particle size).

wtOmcA was titrated against increasing amounts of a 10 mM solution of iron oxide (III) prepared in buffer C with 10 % $^{2}H_2O$ (99.9 atom %), and ^{1}H-1D-NMR spectra were collected after each addition. To study the binding of graphene to OmcA, wtOmcA prepared with 10 % $^{2}H_2O$ (99.9 atom %) was incubated with graphene (final concentration of 0.2 mg/mL) and ^{1}H-1D-NMR spectra were collected before and after the addition of graphene.

Data Analysis and Binding Affinities

The NMR spectra were processed and analyzed using Bruker TopSpin 3.2 software. Chemical shifts are reported in parts per million (ppm) using inorganic phosphate or water as internal references, in the case of phosphorus or proton spectra, respectively.

Binding affinities between FMN and OmcA mutants were calculated based on the chemical shift perturbations ($\Delta\delta_{bind}$) of the ^{31}P signal of FMN upon formation of the complex FMN-OmcA (ligand-cytochrome) relative to the molar ratio (R) between the two (R=[Cyt]/[FMN]). Data were fitted with least squares minimization to the following binding model

$$C + nL \rightleftharpoons CL_n$$

using equation 1 that considers a fast exchange regime and corrects for dilution effects (Paquete et al., 2014; Worrall et al., 2003).

$$\Delta\delta_{bind} = \frac{1}{2}\Delta\delta_{bind}^{\infty}\left(A - \sqrt{(A^2 - 4nR)}\right) \quad \textbf{Equation 1}$$

$$A = 1 + nR + \frac{\beta_d([L]_o R + [C]_0)}{[L]_0[C]_0} \quad \textbf{Equation 2}$$

$\Delta\delta_{bind}^{\infty}$ is the maximum chemical shift perturbation of the NMR signal, resulting from the formation of the FMN-OmcA complex and β_d is the macroscopic dissociation constant. These are the two parameters fitted. $[L]_0$ is the initial concentration of FMN, $[C]_0$ is the stock concentration of OmcA and n is the number of binding sites. Only chemical shift perturbations larger than 0.025 ppm were considered significant (Díaz-Moreno et al., 2005).

Kinetic Experiments

Sample Preparation

OmcA mutants were diluted to the desired concentration (≈100 µM) with degassed buffer C. The exact concentration of cytochrome was determined in the reduced state by UV-visible spectroscopy using an ε_{552nm}=30,000 $M^{-1}cm^{-1}$ per heme (Massey, 1959). Stock solutions of the four electron shuttles: anthraquinone 2,6-disulfonate (AQDS), flavin mononucleotide (FMN), riboflavin (RF), and phenazine methosulfate (PMS) were prepared in buffer C. Dilutions of the electron shuttles were prepared in degassed buffer C, and the exact concentrations were determined by UV-visible spectroscopy using the ε values presented in

Table 2. An excess of electron shuttles was used to allow complete oxidation of the cytochromes.

Table 2. ε values of RF, FMN, AQDS and PMS.

Name	ε ($M^{-1}cm^{-1}$) [λ_{max}]	Reference
Riboflavin (RF)	12,500 [445 nm]	(Whitby, 1953)
Flavin mononucleotide (FMN)	12,200 [445 nm]	(Aliverti et al., 1999)
Antraquinone 2,6-disulfonate (AQDS)	5,200 [326 nm]	(Shi et al., 2012)
Phenazine methosulfate (PMS)	26,300 [387 nm]	(Dawson, 1987)

Reduced solutions of OmcA mutants were prepared by the addition of small volumes of a concentrated solution of sodium dithionite that was prepared in buffer C. The concentration of sodium dithionite solution was determine using ε_{314nm}=8,000 $M^{-1}cm^{-1}$ (Dixon, 1971), to make sure that it was not in excess before the experiment. All the experiments were performed inside an anaerobic chamber (M-Braun 150) containing less than 5 ppm of oxygen.

Data Acquisition

Kinetic experiments were performed using a stopped-flow spectrometer (HI-TECH Scientific SF-61 DX2) placed inside an anaerobic chamber (M-Braun 150) and measuring the light absorption changes at 552 nm. At 552 nm, the OmcA UV-Vis spectrum presents a peak in the reduced state that is not present in the oxidized state or in the spectrum of any of the electron shuttles (Table 2) (Paquete et al., 2014).

The temperature of the stopped-flow apparatus was kept at 25 °C using an external circulating water bath. For each OmcA mutant, the fully oxidized and fully reduced states of the cytochromes were calibrated by mixing the protein with potassium ferricyanide or sodium dithionite, respectively. These values were used to normalize the kinetic data in order to plot reduced fraction versus time.

Results and Discussion

OmcA Mutants

OmcA is a decaheme *c*-type cytochrome where all the hemes have bis-histidine coordination. In the oxidized state iron is in the +3 state and the hemes are low-spin paramagnetic. In these conditions, the NMR signals of the methyl substituents at the periphery of the heme appear in the high frequency region of the spectra, well resolved from the main envelope of protein signals. The spectra of native OmcA and wtOmcA (OmcA with his-tag) present the same profile (data not shown), showing that the his-tag does not disturb the environment around the hemes and the folding of the cytochrome.

The mutations at the axial ligand of the hemes of OmcA were chosen to modify the heme reactivity without affecting the overall protein structure. Indeed, substitution of the distal histidine by a methionine allows the heme to retain its low-spin character in the oxidized state and

increases the reduction potential of the targeted heme by up to 200 mV (Mus-Veteaus et al., 1992). ^{1}H-1D-NMR experiments of the five OmcA mutants show that spectral changes are limited to a few signals relative to those found in the spectrum of wtOmcA (Figure 2). These observations indicate that the overall fold of the protein is retained, given the exquisite sensitivity of paramagnetic shifts to structural changes (Louro, 2013). The substitution of the iron axial ligand changes the chemical shift of signals from the mutated heme allowing the assignment of signals that fall in clear spectral regions to specific hemes (Figure 2).

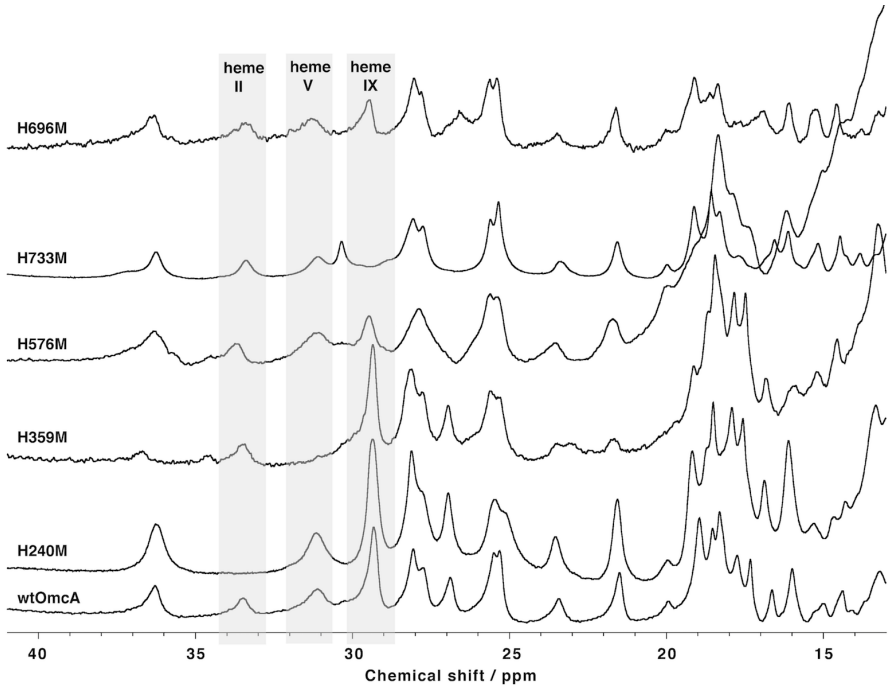

Figure 2. ^{1}H-1D-NMR spectra of OmcA and mutants. The spectrum at the bottom corresponds to OmcA with his-tag. Spectra from H240M, H359M, H576M, H733M and H696M correspond to spectra from mutants of OmcA in the distal axial ligand of hemes II, V, VII, IX and X, respectively. Grey boxes represent the assignment of the signals to specific hemes of OmcA.

Interaction Studies with Soluble Electron Shuttles

Kinetic Studies

Kinetics of oxidation of OmcA by four electron shuttles, (FMN and riboflavin, AQDS and phenazine methosulfate) were studied using stopped-flow as previously described (Paquete et al., 2014). Collectively these four compounds represent the chemical and electrostatic diversity of electron shuttles encountered by outer-membrane cytochromes of SOMR-1 in the environment (Hernandez et al., 2004). FMN and RF are flavins, whereas AQDS is considered a humic acid analogue and PMS is a representative of phenazines. While FMN and AQDS are negatively charged, riboflavin is neutral and PMS is positively charged.

Kinetic traces of oxidation of wtOmcA and OmcA mutants by the various electron shuttles are presented in Figure 3. As observed previously for native OmcA, all electron shuttles oxidize the mutants very fast with PMS achieving full oxidation within the dead-time of the stopped-flow (Paquete et al., 2014). The similar profile of wtOmcA, to native OmcA indicates that the his-tag present at the C-terminal does not affect the reactivity of OmcA towards soluble electron shuttles. With exception of heme VII mutant, all the OmcA mutants have a similar profile to that observed with native OmcA (Paquete et al., 2014). As previously observed, the extent of the oxidation of the protein by each redox shuttle is determined by the value of the reduction potentials of the four electron shuttles, suggesting the establishment of a thermodynamic equilibrium during the reaction between oxidized and reduced species

(see scheme 1) (Paquete et al., 2014). FMN and RF have very similar reduction potentials, and in this specific case oxidize the cytochrome to the same extent. AQDS, which has a slightly higher reduction potential can extract more electrons from OmcA enabling further oxidation of the cytochrome (Figure 3 and Scheme 1). PMS with a reduction potential that is above that of the titration envelope of OmcA (Scheme 1) (Firer-Sherwood et al., 2008; Bodemer et al., 2010), achieves nearly complete oxidation of OmcA.

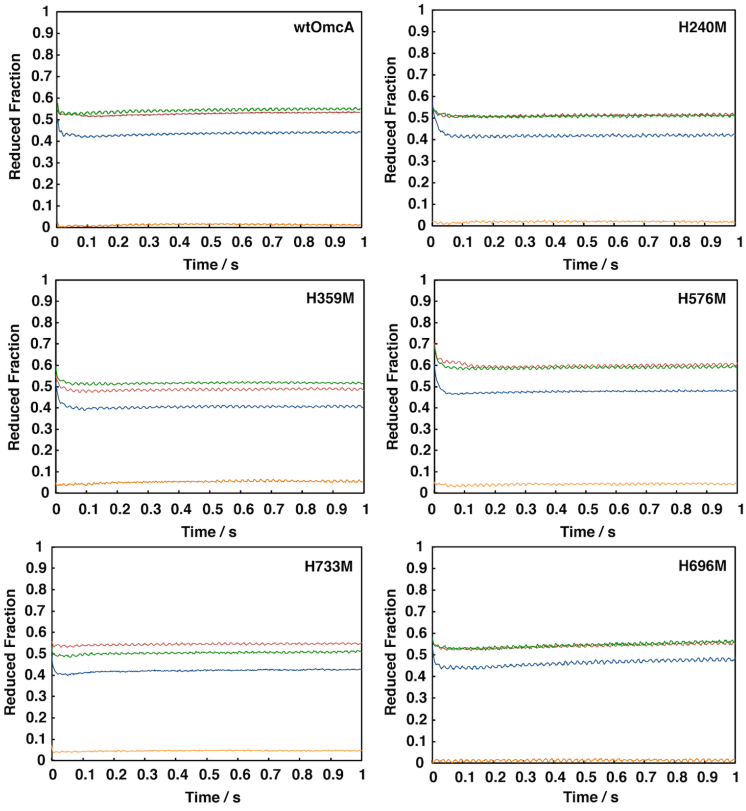

Figure 3. Kinetics traces of oxidation wtOmcA and OmcA mutants H240M, H359M, H576M, H733M and H696M, by RF (red), FMN (green), AQDS (blue) and PMS (orange). The cytochrome concentration was 0.73 µM, 0.61 µM, 0.64 µM, 0.68 µM, 0.69 µM and 0.52 µM for wtOmcA and mutants of hemes II, V, VII, IX and X, respectively.

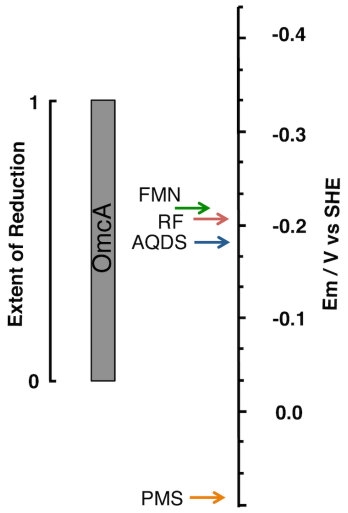

Scheme 1. Schematic representation of the reduction potentials of native OmcA and of the redox shuttles RF, FMN, AQDS and PMS at 25°C pH7, (Prince et al., 1981; Shi et al., 2012).

The kinetic experiments of the mutant of heme VII show that AQDS, FMN and RF are not able to oxidize the protein to the same extent as they do for wtOmcA. Indeed, it shows that this mutant becomes less oxidized by approximately 10%, which is in agreement with approximately one more heme that remains reduced in the decaheme protein OmcA. These data show that the increase in the reduction potential of heme VII by the replacement of the axial histidine by a methionine changed its potential from a value that was below that of FMN, RF and AQDS to a value that is now above, rendering these shuttles unable to extract electrons from heme VII. By contrast, the mutations in the axial ligands of hemes II, V, IX and X do not affect to great degree the final extent of oxidation. This indicates that despite the mutation, the reduction potential of those hemes remained either below or above the potentials of FMN, RF and AQDS.

Binding of FMN Followed by ^{31}P-1D-NMR Spectroscopy

Having studied the electron transfer between the mutants and the redox shuttles, we also explored the effect of the mutations in the binding of FMN to hemes II and VII that are located in the so called flavin binding domains of OmcA. Interaction studies between FMN and OmcA measured using ^{31}P-1D-NMR, revealed a dissociation constant of 29 μM between FMN and OmcA with a stoichiometry of 2:1 (Paquete et al., 2014). The addition of the his-tag did not affect the binding of OmcA to FMN when compared with the native OmcA (data not shown). As previously observed, upon protein binding the phosphorous atom signal shifts position and broadens, which indicates an interaction between FMN and the cytochrome in a fast regime on the NMR time scale (Paquete et al., 2014). Figure 4 shows that, while the interaction of FMN with the mutant of heme II is similar to the wtOmcA, the interaction with the mutant of heme VII is quite distinct. The macroscopic dissociation constants obtained for the interaction of FMN with these mutants are reported in Table 3. As observed for native OmcA, the values of the dissociation constants are in agreement with weak transient interactions, typical of electron transfer reactions between redox proteins such as cytochromes and their physiological partners (Perkins et al., 2010; Bashir et al., 2011). The differences in the binding of the mutant of heme VII when compared to native OmcA are an indication that in addition to the changes in the driving force for electron transfer revealed in the previous section, the chemical environment for FMN recognition around heme VII was modified.

Table 3. Dissociation constants and stoichiometry of binding for FMN with OmcA mutants. Values in parenthesis indicate the standard error of the fitted value determined from the diagonal elements of the covariance matrix.

	β_d (μM)	n	Reference or source
OmcA	29 (11)	2	(Paquete et al., 2014)
OmcA H240M	45 (5)	2	This work
OmcA H576M	137 (26)	2	This work

Our data show that neither the thermodynamics and kinetics of oxidation of OmcA by redox shuttles nor the binding characteristics of FMN were disturbed by the replacement of the distal axial ligand of heme II. In contrast, replacement of the distal axial ligand of heme VII had a significant effect in the overall oxidation by redox shuttles and caused considerable weakening of the binding affinity for FMN. Heme VII was previously postulated to have an important role in the interaction of OmcA with FMN, because it is near a disulfide bond whose redox state was proposed to control changes of OmcA between cytochrome and flavocytochrome states (Edwards et al., 2015). Moreover, next to heme VII there is a hydrophobic cleft, proposed to be important for flavin binding (Edwards et al., 2015) that is only found in MtrC and OmcA outer-membrane cytochromes that bind flavins transiently (Paquete et al., 2014; Breuer et al., 2015; Edwards et al., 2015).

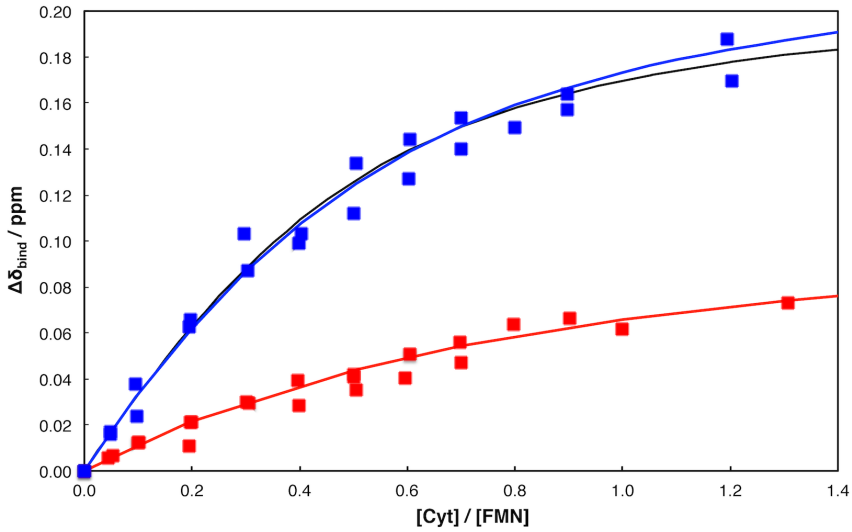

Figure 4. Binding curves of OmcA mutants with FMN. Chemical shift perturbations of the signal of the phosphorous nucleus of FMN are plotted as a function of the molar ratio of the interacting molecules. Binding curves fitted to data obtained using native OmcA (black line) [22]; mutant of heme II (blue data); and mutant of heme VII (red data). The best global fitting for the binding model are represented by the solid lines.

Overall, in the particular case of FMN it was possible to locate a binding site in close vicinity of heme VII. Furthermore, the data indicate that this heme, due to a reduction potential that is close to the potentials of RF, FMN and AQDS, is a prime target for manipulating the redox activity of OmcA.

Interaction with Insoluble Electron Acceptors

In addition to electron transfer mediated by redox shuttles OmcA is involved in strong binding and direct electron transfer to solid conductive surfaces (Xiong et al., 2006). Given this role the interaction of wtOmcA with iron oxides and graphene were investigated by ^{1}H-1D-NMR, looking for perturbations in heme signals upon addition of these

insoluble materials. The position of NMR signals is very sensitive to the chemical environment, and therefore a perturbation would indicate a close proximity of these materials to the hemes of OmcA. This proximity would allow fast direct electron transfer given the strong distance dependence of the rates (Gray and Winkler, 2003). A hematite binding motif was previously identified in OmcA and MtrC (Lower et al., 2008). In OmcA heme IX is found in close proximity to this motif and therefore available to give electrons from a source that would recognize the motif. However, the addition of iron oxide nanoparticles to wtOmcA did not disturb any of the heme signals that are clearly visible outside of the main protein envelope (Figure 5A).

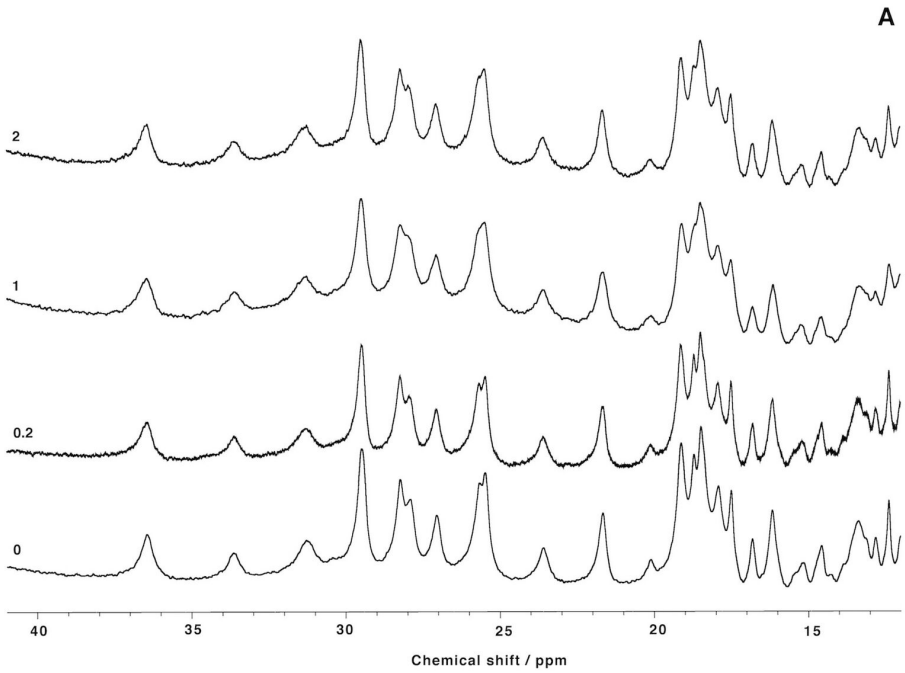

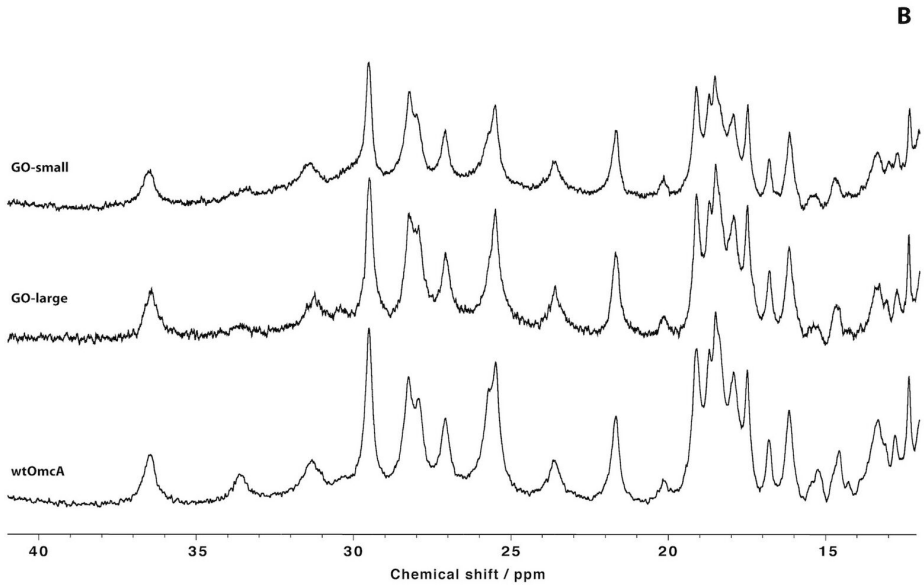

Figure 4. High frequency region of the ^{1}H-1D NMR spectra of wtOmcA, in the presence of increasing amounts of iron oxide, the labels on the left side represent the molar ratio of [iron oxide]/[OmcA] (A); and with and without graphene (B). This region is populated by the heme methyl signals.

Carbon based electrodes of different natures are being proposed for biotechnological applications of organisms such as SOMR-1 (Sanchez et al., 2015). This is a consequence of their chemical and biological inertness in the operating conditions of microbial electrochemical technologies, and their potential for being cheap to produce. Graphene is a carbon based material that in the form of graphene oxide can be prepared as suspensions of nanosized particles with defined dimensions (Huang et al., 2010).

When OmcA interacts with graphene oxides of two different average sizes (Figure 5B), there are small changes in some heme signals and the behavior was the same for both sizes of graphene. However, this change

was due to pH changes caused by the addition of the graphene solution that is only stable at low pH. Indeed, the affected peaks moved back to the original position (without graphene) after returning the pH back to 7.6 (Figure 5B).

The lack of changes in the NMR signals of the hemes shows that the interaction between OmcA and iron oxides or graphene does not occur near the hemes.

This is in agreement with the experimentally observed slow rate of direct electron transfer (Ross et al., 2009). Indeed, it suggests that the main drive for the presence of the hematite binding motif is to ensure a strong anchoring of the protein to solid conductive surfaces, and that facilitation of direct electron transfer played a secondary role. This result supports the importance of soluble electron shuttles for reduction of solid electron acceptors by OMCs (Ross et al., 2009)

Conclusions

Overall our results show that the reduction potential of heme VII in OmcA is below that of RF, FMN and AQDS but sufficiently close to enable it to become higher than the potential of these redox shuttles upon mutation of the distal axial histidine by a methionine. This mutation, in addition to changing the driving force of electron transfer, also inadvertently perturbed one of the binding sites of FMN to OmcA.

This, however, appears to be a local effect given that the vast majority of the paramagnetically shifted signals in the NMR spectrum remained undisturbed. Furthermore, this mutation reduces the affinity of the protein for FMN, increasing the difference to a putative flavocytochrome state with FMN strongly bound. This change actually favors a faster turnover, which cannot be appreciated in our kinetic data given that the oxidation of OmcA is already too fast for confident measurement using stopped-flow. Nonetheless, to better understand the effect of the mutation of the heme VII axial ligand, and the way electrons are taken up by this decaheme cytochrome and then distributed to downstream acceptors, a detailed kinetic and thermodynamic characterization at a microscopic level is required. However, the discrimination of the redox properties of the individual hemes has only been achieved for multiheme cytochromes with up to six centers (Alves et al., 2016; Paquete and Louro, 2014), with the characterization of more complex proteins, such as the decaheme cytochrome OmcA remaining a challenge from the experimental and computational points of view.

The work reported in this study expanded our understanding of electron transfer between OmcA and its soluble and solid redox partners, suggesting that the production of extracellular electron shuttles by SOMR-1 is crucial to sustain enhanced electron transfer rates. Future work should focus on the role of electrostatic and hydrophobic interactions of OmcA with soluble and insoluble electron acceptors, and the control of the redox potentials of the individual hemes to achieve

the desired rates and extent of electron uptake and release. This information will help the rational design of cytochromes with properties tuned-up towards application of SOMR-1 in microbial fuel cells by improving attachment of cells to electrodes and optimizing electron transfer.

References

Aliverti, A., Curti, B., and Vanoni, M. A. (1999). Identifying and Quantitating FAD and FMN in Simple and in Iron-Sulfur-Containing Flavoproteins. *Methods Mol. Biol.* 131, 9–23. doi:10.1385/1-59259-266-X:9.

Alves, M. N., Fernandes, A. P., Salgueiro, C. A., and Paquete, C. M. (2016). Unraveling the Electron Transfer Processes of a Nanowire Protein from *Geobacter sulfurreducens*. *Biochim. Biophys. Acta - Bioenerg.* 1857, 7–13. doi:10.1016/j.bbabio.2015.09.010.

Bashir, Q., Scanu, S., and Ubbink, M. (2011). Dynamics in Electron Transfer Protein Complexes. *FEBS J.* 278, 1391–1400. doi:10.1111/j.1742-4658.2011.08062.x.

Breuer, M., Rosso, K. M., and Blumberger, J. (2015). Flavin Binding to the Deca-heme Cytochrome MtrC: Insights from Computational Molecular Simulation. *Biophys. J.* 109, 2614–2624. doi:10.1016/j.bpj.2015.10.038.

von Canstein, H., Ogawa, J., Shimizu, S., and Lloyd, J. R. (2008). Secretion of Flavins by *Shewanella* Species and Their Role in Extracellular Electron Transfer. *Appl. Environ. Microbiol.* 74, 615–623. doi:10.1128/AEM.01387-07.

Clarke, T. A., Edwards, M. J., Gates, A. J., Hall, A., White, G. F., Bradley, J., et al. (2011). Structure of a Bacterial Cell Surface Decaheme Electron Conduit. *Proc. Natl. Acad. Sci. U. S. A.* 108, 9384–9. doi:10.1073/pnas.1017200108.

Davis, J., and Yarbrough, H. (1962). Preliminary Experiments on a Microbial Fuel Cell. *Science* 137, 615–616.

Dawson, R. (1987). *Data for Biochemical Research, 3rd Edn*. New York, NY: Oxford University Press. doi: 10.1016/0307-4412(87)90110-5

Díaz-Moreno, I., Díaz-Quintana, A., Ubbink, M., and De La Rosa, M. A. (2005). An NMR-Based Docking Model for the Physiological Transient Complex Between Cytochrome *f* and Cytochrome *c*6. *FEBS Lett.* 579, 2891–2896. doi:10.1016/j.febslet.2005.04.031.

Dixon, M. (1971). The Acceptor Specificity of Flavins and Flavoproteins. *Biochim. Biophys. Acta* 226, 269–284. doi:10.1016/0005-2728(71)90094-6.

Edwards, M. J., Baiden, N. A., Johs, A., Tomanicek, S. J., Liang, L., Shi, L., et al. (2014). The X-Ray Crystal Structure of *Shewanella oneidensis* OmcA Reveals New Insight at the Microbe-Mineral Interface. *FEBS Lett.* 588,

1886–1890. doi:10.1016/j.febslet.2014.04.013.

Edwards, M. J., Hall, A., Shi, L., Fredrickson, J. K., Zachara, J. M., Butt, J. N., et al. (2012). The Crystal Structure of the Extracellular 11-heme Cytochrome UndA Reveals a Conserved 10-heme Motif and Defined Binding Site for Soluble Iron Chelates. *Structure* 20, 1275–1284. doi:10.1016/j.str.2012.04.016.

Edwards, M. J., White, G. F., Norman, M., Tome-Fernandez, A., Ainsworth, E., Shi, L., et al. (2015). Redox Linked Flavin Sites in Extracellular Decaheme Proteins Involved in Microbe-Mineral Electron Transfer. *Nat. Sci. Reports* 5: 11677. doi:10.1038/srep11677.

Gorby, Y. A., Yanina, S., McLean, J. S., Rosso, K. M., Moyles, D., Dohnalkova, A., et al. (2006). Electrically Conductive Bacterial Nanowires Produced by *Shewanella oneidensis* Strain MR-1 and Other Microorganisms. *Proc. Natl. Acad. Sci. U. S. A.* 103, 11358–63. doi:10.1073/pnas.0604517103.

Gralnick, J. A., and Newman, D. K. (2007). Extracellular Respiration. *Mol. Microbiol.* 65, 1–11. doi:10.1111/j.1365-2958.2007.05778.x.

Gray, H. B., and Winkler, J. R. (2003). Electron tunneling through proteins. *Q. Rev. Biophys.* 36, 341–372. doi:10.1017/S0033583503003913.

Hernandez, M. E., Kappler, A., and Newman, D. K. (2004). Phenazines and Other Redox-Active Antibiotics Promote Microbial Mineral

Reduction. *Appl. Environ. Microbiol.* 70, 921–928. doi:10.1128/AEM.70.2.921.

Huang, X., Boey, F., and Zhang, H. (2010). A Brief Review on Graphene-Nanoparticle Composites. *Cosmos* 6, 159–166. doi:10.1142/S0219607710000607.

Kim, B. H., Ikeda, T., Park, H. S., Kim, H. J., Hyun, M. S., Kano, K., et al. (1999). Electrochemical Activity of an Fe(III)-Reducing Bacterium, *Shewanella putrefaciens* MR-1, in the Presence of Alternative Electron Acceptors. *Biotechnol. Tech.* 13, 475–478. doi:10.1023/A:1008993029309.

Kim, H. J., Park, H. S., Hyun, M. S., Chang, I. S., Kim, M., and Kim, B. H. (2002). A Mediator-Less Microbial Fuel Cell Using a Metal Reducing Bacterium, *Shewanella putrefaciens*. *Enzyme Microb. Technol.* 30, 145–152. doi:10.1016/S0141-0229(01)00478-1.

Kotloski, N. J., and Gralnick, J. A. (2013). Flavin Electron Shuttles Dominate Extracellular Electron Transfer by *Shewanella oneidensis*. *MBio* 4. doi:10.1128/mBio.00553-12.

Logan, B. E. (2007). “Introduction,” in *Microbial Fuel Cells* (John Wiley & Sons, Inc.), 1–11. doi:10.1002/9780470258590.ch1.

Louro, R. O. (2013). “Chapter 4 – Introduction to Biomolecular NMR and Metals,” in *Practical Approaches to Biological Inorganic Chemistry*, 77–107. doi:10.1016/B978-0-444-56351-4.00004-X.

Lovley, D. R., Coates, J. D., Blunt-Harris, E. L., Phillips, E. J., and Woodward, J. C. (1996). Humic Substances as Electron Acceptors for Microbial Respiration. *Nature* 382, 445.

Lower, B. H., Lins, R. D., Oestreicher, Z., Straatsma, T. P., Hochella, M. F., Shi, L., et al. (2008). In Vitro Evolution of a Peptide with a Hematite Binding Motif that may Constitute a Natural Metal-Oxide Binding Archetype. *Environ. Sci. Technol.* 42, 3821–3827. doi:10.1021/es702688c.

Marsili, E., Baron, D. B., Shikhare, I. D., Coursolle, D., Gralnick, J. A., and Bond, D. R. (2008). *Shewanella* Secretes Flavins that Mediate Extracellular Electron Transfer. *Proc. Natl. Acad. Sci. U. S. A.* 105, 3968–3973. doi:10.1073/pnas.0710525105.

Massey, V. (1959). The Microestimation of Succinate and the Extinction Coefficient of Cytochrome *c*. *Biochim. Biophys. Acta* 34, 255–256. doi:10.1016/0006-3002(59)90259-8.

Mus-Veteaus, I., Dolla, A., Guerlesquin, F., Payan, F., Czjzekii, M., Haser, R., et al. (1992). Site-directed Mutagenesis of Tetraheme Cytochrome *c*3. *J. Biol. Chem.* 267, 16851–16858.

Myers, C. R., and Myers, J. M. (1997). Replication of Plasmids with the p15A Origin in *Shewanella putrefaciens* MR-1. *Lett. Appl. Microbiol.* 24, 221–5. doi:10.1046/j.1472-765X.1997.00389.x.

Paquete, C. M., Fonseca, B. M., Cruz, D. R., Pereira, T. M., Pacheco, I.,

Soares, C. M., et al. (2014). Exploring the Molecular Mechanisms of Electron Shuttling Across the -Microbe/Metal Space. *Front. Microbiol.* 5, 318–330. doi:10.3389/fmicb.2014.00318.

Paquete, C. M., and Louro, R. O. (2014). Unveiling the Details of Electron Transfer in Multicenter Redox Proteins. *Acc. Chem. Res.* 47, 56–65.

Perkins, J. R., Diboun, I., Dessailly, B. H., Lees, J. G., and Orengo, C. (2010). Transient Protein-Protein Interactions: Structural, Functional, and Network Properties. *Structure* 18, 1233–1243. doi:10.1016/j.str.2010.08.007.

Pirbadian, S., Barchinger, S. E., Leung, K. M., Byun, H. S., Jangir, Y., Bouhenni, R. A., et al. (2014). *Shewanella oneidensis* MR-1 Nanowires are Outer Membrane and Periplasmic Extensions of the Extracellular Electron Transport Components. *Proc. Natl. Acad. Sci.* 111, 12883–12888. doi:10.1073/pnas.1410551111.

Potter, M. C. (1911). Electrical Effects Accompanying the Decomposition of Organic Compounds. *Proc. R. Soc. London. Ser. B, Contain. Pap. a Biol. Character* 84, 260–276.

Prince, R. C., Linkletter, S. J., and Dutton, P. L. (1981). The Thermodynamic Properties of Some Commonly used Oxidation-Reduction Mediators, Inhibitors and Dyes, as Determined by Polarography. *Biochim. Biophys. Acta* 635, 132–148.

Richardson, D. J., Butt, J. N., Fredrickson, J. K., Zachara, J. M., Shi, L.,

Edwards, M. J., et al. (2012). The “Porin-Cytochrome” Model for Microbe-to-Mineral Electron Transfer. *Mol. Microbiol.* 85, 201–212. doi:10.1111/j.1365-2958.2012.08088.x.

Ross, D. E., Brantley, S. L., and Tien, M. (2009). Kinetic Characterization of OmcA and MtrC, Terminal Reductases Involved in Respiratory Electron Transfer for Dissimilatory Iron Reduction in *Shewanella oneidensis* MR-1. *Appl. Environ. Microbiol.* 75, 5218–5226. doi:10.1128/AEM.00544-09.

Sanchez, D. V. P., Jacobs, D., Gregory, K., Huang, J., Hu, Y., Vidic, R., et al. (2015). Changes in Carbon Electrode Morphology Affect Microbial Fuel Cell Performance with *Shewanella oneidensis* MR-1. *Energies* 8, 1817–1829. doi:10.3390/en8031817.

Shi, Z., Zachara, J. M., Shi, L., Wang, Z., Moore, D. A., Kennedy, D. W., et al. (2012). Redox Reactions of Reduced Flavin Mononucleotide (FMN), Riboflavin (RBF), and Anthraquinone-2,6-disulfonate (AQDS) with Ferrihydrite and Lepidocrocite. *Environ. Sci. Technol.* 46, 11644–11652. doi:10.1021/es301544b.

Sisler, F. D. (1969). Biochemical Fuel Cell.

Wang, H., and Ren, Z. J. (2013). A Comprehensive Review of Microbial Electrochemical Systems as a Platform Technology. *Biotechnol. Adv.* 31, 1796–1807. doi:10.1016/j.biotechadv.2013.10.001.

Whitby, L. G. (1953). A New Method for Preparing Flavin-Adenine

Dinucleotide. *Biochem. J.* 54, 437–442.

Worrall, J. A. R., Reinle, W., Bernhardt, R., and Ubbink, M. (2003). Transient Protein Interactions Studied by NMR Spectroscopy: The Case of Cytochrome *c* and Adrenodoxin. *Biochemistry* 42, 7068–7076. doi:Doi 10.1021/Bi0342968.

Xiong, Y., Shi, L., Chen, B., Mayer, M. U., Lower, B. H., Londer, Y., et al. (2006). High-Affinity Binding and Direct Electron Transfer to Solid Metals by the *Shewanella oneidensis* MR-1 Outer Membrane *c*-Type Cytochrome OmcA. *J. Am. Chem. Soc.* 128, 13978–13979. doi:10.1021/ja063526d.

Zhang, H., Tang, X., Munske, G. R., Tolic, N., Anderson, G. A., and Bruce, J. E. (2009). Identification of Protein-Protein Interactions and Topologies in Living Cells with Chemical Cross-linking and Mass Spectrometry. *Mol. Cell. Proteomics* 8, 409–420. doi:10.1074/mcp.M800232-MCP200.

Chapter IV

Analysis of the Residual Alignment of a Paramagnetic Multiheme Cytochrome by NMR

Chapter IV has been published in

Neto, S. E., Fonseca, B. M., Maycock, C., Louro R. O. (2014). Analysis of the residual alignment of a paramagnetic multiheme cytochrome by NMR. *Chem Commun (Camb).* 50, 4561-4563.
doi: 10.1039/C3CC49135H

Author contributions:

All experiments described in this chapter were performed by Sónia E. Neto.

Sónia E. Neto contributed to the planning of the experiments and to the writing of the original paper.

Abstract

Residual dipolar couplings measured by NMR spectroscopy reveal that the rhombicity of the electronic structure of low-spin paramagnetic hemes determines their relative contribution towards the preferential orientation of a protein with multiple hemes when placed in a strong magnetic field.

Communication

Multiheme cytochromes *c* are ubiquitous proteins in prokaryotes. They play key roles in the bioenergetic metabolism of sediment and soil organisms that are of great interest for biotechnological processes of low environmental footprint such as bioremediation of metal contaminated soils or energy generation from waste water in microbial fuel cells (Nealson et al., 2002). The structure of many of these proteins is organized as domains linked by peptide segments that can have varying levels of flexibility. This flexibility can be essential for their biological activity (Clarke et al., 2007; Czjzek et al., 2002; Leys et al., 1999; Pokkuluri et al., 2011). The hemes in the cytochromes undergo changes of redox and spin state and often are paramagnetic with one or various unpaired electrons. Hemes with unpaired electrons are magnetically anisotropic (Assfalg et al., 2003; Déméné et al., 2000), and when subjected to external magnetic fields this anisotropy induces a

magnetic moment that is orientation dependent. As a consequence, the whole cytochrome tends to adopt a preferential orientation (Assfalg et al., 2003), making it possible to use nuclear magnetic resonance (NMR) to measure residual dipolar couplings (RDC) between NMR active nuclei in the cytochrome. Residual dipolar couplings can be used to improve the refinement of NMR structures of proteins in solution and to define the range of motions in the case of flexible proteins (Bertini et al., 2004; Prestegard et al., 2004). Very importantly it also provides a means to investigate the dynamics and relative orientation of protein complexes involving weakly interacting partners (Xu et al., 2009). However, the application of RDCs to paramagnetic proteins has been limited thus far to examples containing a single paramagnetic centre, either naturally occurring or added as a covalently attached tag (Banci et al., 1998; Peters et al., 2011).

Recently, a method for the specific labelling with ^{13}C of the methyl substituents at the periphery of the hemes in multiheme proteins was proposed (Fonseca et al., 2012). For low-spin paramagnetic proteins the chemical shift of the heme methyls provide information on the electronic structure of the hemes. This defines the shape and the orientation magnetic susceptibility tensor associated with the unpaired electron without the need of measuring pseudo-contact shifts of nuclei from the protein amino-acids (Louro et al., 1998; Turner et al., 2000; Williams et al., 1985). In paramagnetic multiheme cytochromes the combined effect of the magnetic susceptibility tensors of the various hemes is expected to give rise to

a preferential orientation of the protein in solution when placed in a strong magnetic field. Here, we set out to observe this phenomenon and relate it to the electronic properties of the individual hemes in the Small Tetraheme Cytochrome (STC) from the metal reducing bacterium *Shewanella oneidensis* MR-1. Heme methyls are not convenient to explore residual dipolar couplings due to rotational averaging, but the C-H bond of the heme *meso* substituents provides an appropriate handle to measure the RDCs that result from the preferential orientation of the cytochrome (Erbil et al., 2009). Therefore, we modified our heme labelling strategy to specifically label with ^{13}C the *meso* carbons of hemes *c* in STC from *S. oneidensis* MR-1. An *E. coli* JM109 strain (LS542) auxotrophic for the heme precursor δ-aminoluvelinic acid (δ-ALA) (Fonseca et al., 2012), was transformed with the pEC86 plasmid containing the *ccm* gene cluster necessary for aerobic cytochrome *c* maturation and with the pET21a-STC(D2N) expression plasmid encoding for the STC(D2N).

This is a mutant of the STC cytochrome that does not disturb the structure but is interesting for functional studies described elsewhere (Qian et al., 2011). The cells were grown in a medium supplemented with 5-^{13}C-δ-ALA to produce cytochrome with the hemes labelled in the *meso* carbons (Figure 1).

The assignment of the *meso* signals was made using NMR experiments collected at 500 MHz and 800 MHz using 0.5 mM

protein samples prepared in 500 μL of D_2O (99.9 atom %) and buffered with 10 mM potassium phosphate at pH 7.6 (Figure 2).

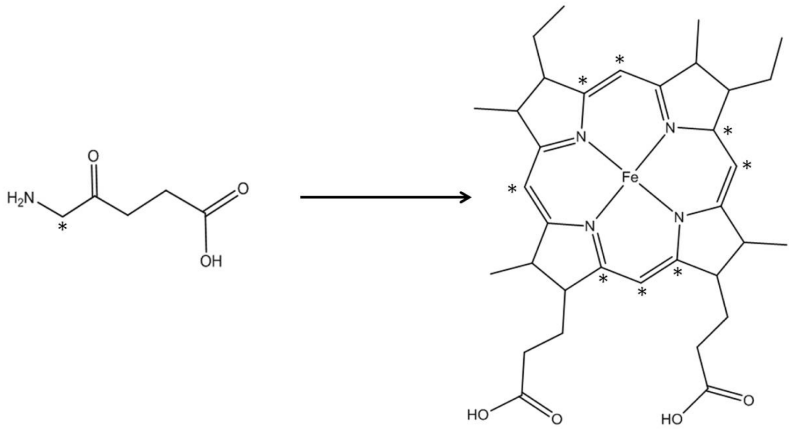

Figure 1. Outcome of heme biosynthesis using 5-^{13}C-δ-ALA showing the position of the labelled carbon atoms in the porphyrin ring.

The assignment of the heme *meso* carbons and protons is reported in Table 1.

Table 1. Assignment of the heme *meso* carbon and proton signals obtained from 2D ^{1}H-^{13}C HMQC collected at 500 MHz, 25°C. Some signals could not be confidently assigned due to overlap with the protein envelop in the HMQC spectra (Figure 2). Heme substituents are numbered according to IUPAC-IUBMB nomenclature.

Heme Substituent	Heme I		Heme II		Heme III		Heme IV	
	^{1}H	^{13}C	^{1}H	^{13}C	^{1}H	^{13}C	^{1}H	^{13}C
5^{1}	7.92	34.4	---	---	---	---	-0.18	41.3
ΔRDC	20.9		---		---		-7.0	
10^{1}	---	---	-2.68	17.1	-6.99	61.9	---	---
ΔRDC	---		10.5		-1.7		---	
15^{1}	9.68	4.9	4.3	-1.1	13.93	-7.9	5.58	-13.5
ΔRDC	16.6		-1.0		-		3.6	
20^{1}	1.95	46.5	-2.91	35.1	2.23	-8.2	-1.00	46.1
ΔRDC	3.0		---		16.0		6.2	

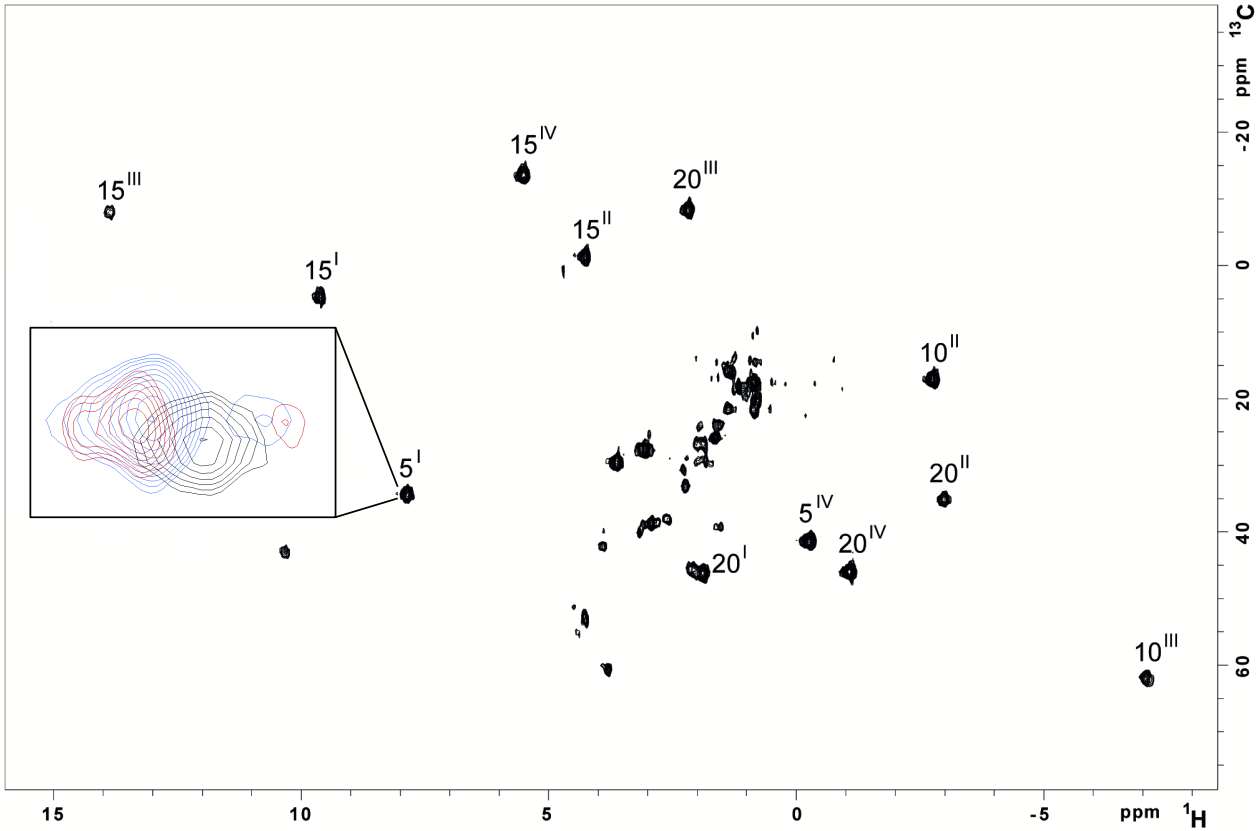

Figure 2. 2D ^{1}H-^{13}C HMQC from STC of *S. oneidensis* MR-1 at pH 7.6 and 25°C, acquired with proton-carbon decoupling, with the assigned *mesos* labelled using the IUPAC-IUBMB nomenclature with superscripts to designate the heme in roman numbers, ordered according to the sequence of attachment to the polypeptide chain. The inset zooms in the signal of the spectrum (black) and superimposed with the signals of 2D ^{1}H-^{13}C HMQC spectra from the same sample acquired at 500 MHz (red) and 800 MHz (blue), without decoupling. Split peaks in this paramagnetic protein have asymmetric intensity as reported in the literature (Tolman et al., 1995).

When a molecule is partially oriented in a strong magnetic field, residual dipolar couplings between magnetic nuclei separated by a known distance such as a C-H bond can be measured and provide information about the orientation of the bond with respect to the magnetic susceptibility tensor. Because macromolecules can have sizable diamagnetic magnetic anisotropy (Bertini et al., 2005), we chose to measure the field dependent changes in dipolar coupling for the C-H pair of the meso groups of the hemes of STC(D2N) at 500 MHz and 800 MHz. In this case ΔRDC equals the difference in observed signal splitting at the two field strengths (Assfalg et al., 2003). The experimental ΔRDC of the heme *meso* groups were used to fit the five parameters that describe the orientation (Euler angles) and anisotropy ($\Delta\boldsymbol{\chi}_{\boldsymbol{ax}}^{\boldsymbol{mol}}$ and $\Delta\boldsymbol{\chi}_{\boldsymbol{rh}}^{\boldsymbol{mol}}$) of the molecular alignment tensor relative to the X-ray structure of STC (PDB ID: 1M1Q) using Equation 1.

$$\Delta\boldsymbol{RDC} = -\frac{\mathbf{1}}{\mathbf{4\pi}}\frac{\boldsymbol{\gamma_H\gamma_C h}}{\mathbf{4\pi^2 r_{HC}^3}}\boldsymbol{S}\left[\Delta\boldsymbol{\chi}_{\boldsymbol{ax}}^{\boldsymbol{mol}}(\mathbf{3}\boldsymbol{cos^2\theta}-\mathbf{1})+\frac{\mathbf{3}}{\mathbf{2}}\Delta\boldsymbol{\chi}_{\boldsymbol{rh}}^{\boldsymbol{mol}}(\boldsymbol{sin^2\theta cos2\phi})\right]$$

Equation 1

Where $\Delta\boldsymbol{\chi}_{\boldsymbol{ax}}^{\boldsymbol{mol}}$ and $\Delta\boldsymbol{\chi}_{\boldsymbol{rh}}^{\boldsymbol{mol}}$ represent the axial and rhombic components of the molecular alignment tensor, respectively, and $\boldsymbol{\theta}$ and $\boldsymbol{\phi}$ correspond to the polar coordinates of the vector defined by the C-H bond in the frame of the molecular alignment tensor. Of the 12 mesos that could be confidently assigned in the spectra 10 had signals that provided reliable measurements of RDC at both field strengths. The fit is shown in Figure 3, showing overall good agreement between the

experimental RDCs and those calculated on the basis of the X-ray structure. The axial and rhombic components of the tensor calculated considering the order parameter S equal to 1 yield the values -6.8 x 10^{-31} m^{-3} and 4.6 x 10^{-31} m^{-3}, respectively. The Euler angles for the protein were 83, -57 and -116 degrees, for α, β and γ, respectively.

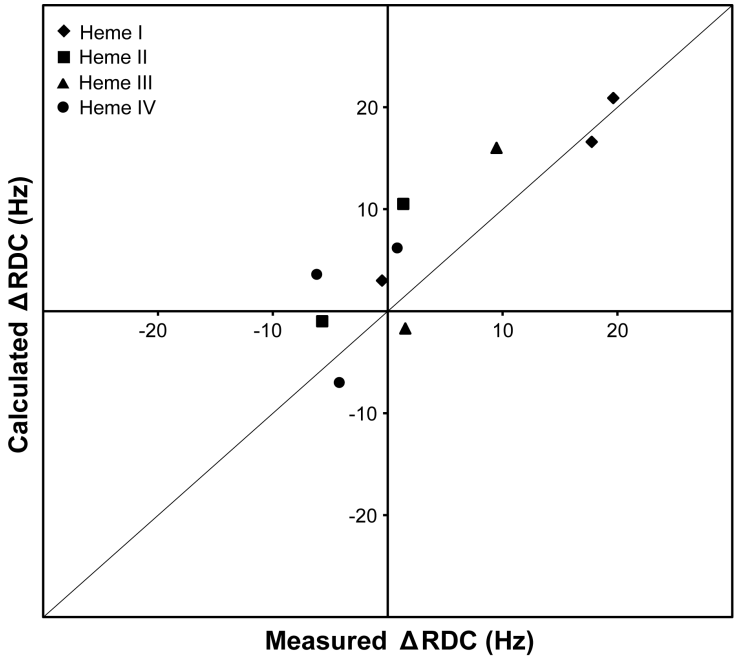

Figure 2. Correlation between experimental ΔRDCs and those calculated using the coordinates of the crystal structure of STC from *S. oneidensis* MR-1 (PDB ID: 1M1Q).

We then set out to relate the molecular alignment tensor with the magnetic susceptibility tensors of the four hemes. When the iron is in octahedral coordination the zz direction of the magnetic susceptibility tensor is nearly perpendicular to the heme plane. In

monoheme cytochromes the zz axis of the magnetic susceptibility tensor has very similar direction to the zz axis of the molecular alignment tensor (Assfalg et al., 2003). However in multiheme cytochromes, such as STC, each of the hemes will exert a force to orient the cytochrome so that its magnetic zz axis aligns with the external field. To determine the contribution of the magnetic susceptibility tensors of each of the four hemes to the overall molecular alignment tensor we calculated the normal of the plane of each of the hemes, and considered this to represent the direction of the zz axis of the magnetic susceptibility tensor of each heme. Considering equal contribution from each heme towards the overall molecular orientation, the average direction was found to make an angle of 10.7 degrees with the direction of the zz axis of the molecular alignment tensor. Although this reveals good agreement between the two axes, the four hemes may have different contributions. The four hemes of STC are known to be different with respect to their electronic structure as revealed by the energy splitting of their molecular orbitals (Fonseca et al., 2009), which relate with the rhombicity of the g-tensor (Gordon et al., 2000; Louro et al., 2002). In the absence of zero field splitting, a condition typically found in low spin hemes (Bertini et al., 2002), the magnetic susceptibility tensor and the g-tensor are directly related (Bertini and Luchinat, 1996). Therefore, we used the value of the rhombic energy splitting determined previously (Fonseca et al., 2009) to weigh the contribution of each heme towards defining the orientation of the cytochrome. The calculated orientation showed a deviation of 7.2

degrees with the orientation of the zz axis of the molecular alignment tensor, and makes an angle of 10.0 degrees with the vector obtained in the non-weighted calculation (Figure 4). Therefore, our results show that using the energy splitting of the heme frontier molecular orbitals to scale the contribution of the magnetic susceptibility of each heme towards the overall molecular alignment, improves the agreement with the molecular alignment tensor. In the particular case of the relative orientation of the hemes of STC, the zz direction of the overall magnetic susceptibility tensor calculated by both approaches turns out not to be very different, but this outcome depends on the protein shape, the relative orientation of the hemes, and the electronic structure of the hemes.

Methods

D-ALA Synthesis

The method reported by Wang et al (Wang and Scott, 1997) was used to synthesize 5-^{13}C-δ-ALA. The nature of the final product was confirmed by 1D-NMR (Figure 5) and the overall yield of the reaction was 67%, in agreement with the literature. Analytical data of 5-^{13}C-δ-ALA, ^{1}H-NMR (D_2O) δ: 2.66 (m, 2H), 2.83 (m, 2H), 4.06 (dd, 2H, J= 143 Hz); ^{13}C-NMR (D_2O) δ: 47.0 (s).

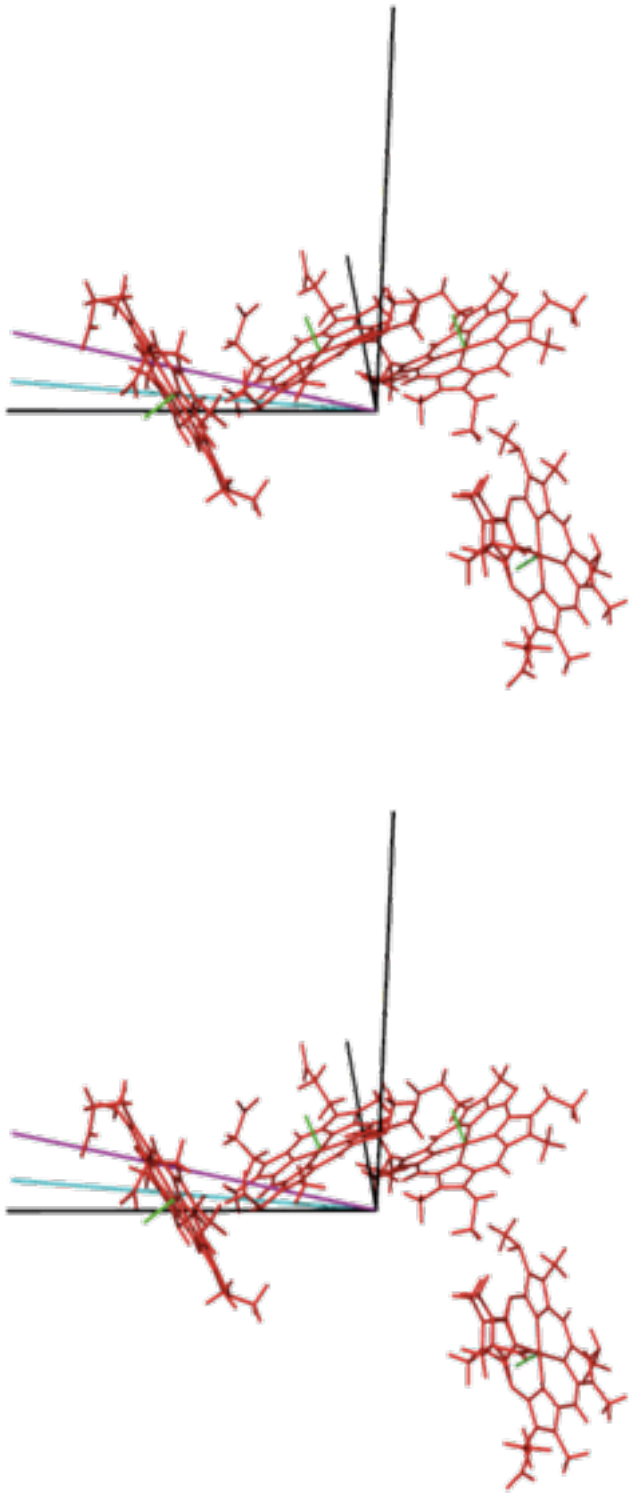

Figure 4. Stereo cross-eyed view of the hemes in the PDB structure 1M1Q of STC (red) and the normal to the heme planes calculated as detailed in the supplementary materials (green). The molecular alignment tensor is showed in black, and the overall magnetic susceptibility tensors calculated with and without scaling the contribution of each heme are showed in cyan and pink respectively.

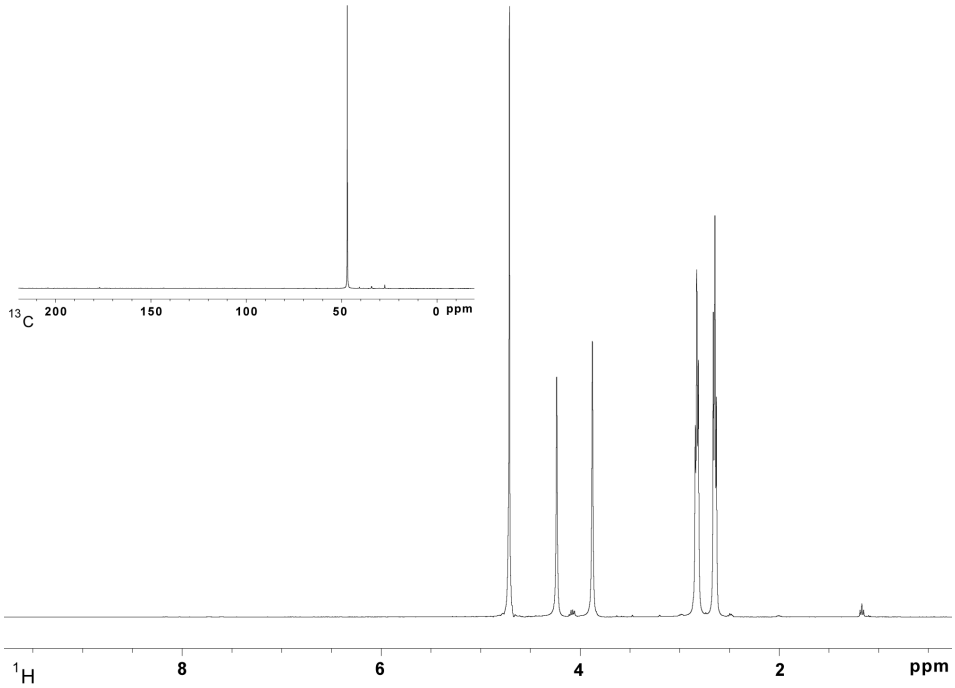

Figure 5. ^{1}H-1D-NMR spectrum from synthesized ^{13}C-5-δ-ALA. The inset shows the ^{13}C-NMR spectrum with the single peak corresponding to the labelled carbon of the molecule.

Cell Growth and Protein Purification

Cells of *E. coli* LS542 strain were grown in Lysogeny Broth (LB) supplemented with 5-^{13}C-δ-ALA 50 mg/L to ensure the biosynthesis of STC labelled in the heme rings. 10 mg/L ampicilin and 34 mg/L chloramphenicol were added to the growth medium to maintain selective pressure for the pET21a-STC (D2N) and pEC86 plasmids, respectively. Cells were allowed to grow for 20 hours at 30 ˚C and 180 rpm, in 500 mL *Erlenmeyer* flasks filled with one-fifth of the total volume and were harvested by centrifugation at 4 °C, 10000 X *g*,

for 10 min. Cell pellet was ressuspended in a extraction solution (30 mL/L of culture), containing 500 mM sucrose, 200 mM Tris pH 8.0, 0.5 mM EDTA and 100 mg/L lysozyme, incubated in ice for 30 min with gentle stirring, and ultra centrifuged at 4 ˚C, 138000 x *g*, for 1 hour. The supernatant was dialyzed against 10 mM Tris-HCl pH 7.6, over-night, and concentrated. Protein purification was performed as described previously (Fonseca et al., 2012). The final yield of pure protein was 1.3 mg/L.

NMR Experiments

Protein samples (0.5 mM) were freeze-dried and dissolved in 500 μL of D_2O (99.9 atom %) and contained 10 mM potassium phosphate buffer (pH 7.6). The pH value reported is a direct reading without correction for the isotope effect. The assignment of the *meso* carbons and protons was made using a set of NMR experiments performed at 25 °C on a Bruker Avance II 500 MHz NMR spectrometer equipped with a QXI or a TXI probe, and at a Avance III 800 MHz spectrometer, equipped with a QXI probe. 2D-^{1}H-^{13}C heteronuclear multiple quantum correlation (HMQC) spectra were obtained without proton-carbon decoupling. The spectra collected at 500 MHz were acquired with 2048 points covering a spectral width of 20 kHz in the ^{1}H dimension and 256 increments with time-proportional phase incrementation (TPPI) to give a spectral width of 37.7 kHz in the ^{13}C dimension, with 64 scans. The spectra collected at 800 MHz were acquired with 2048 points covering a spectral width of

32 kHz in the ^{1}H dimension and 512 increments with time-proportional phase incrementation (TPPI) to give a spectral width of 80.5 kHz in the ^{13}C dimension. ^{1}H nuclear Overhauser effect spectroscopy (NOESY) spectra were acquired with 25 ms of mixing time, 2048 points in the direct dimension and 400 increments with time-proportional phase incrementation (TPPI) in the indirect dimension, both covering a spectral width of 39.7 kHz with 400 scans. All NMR experiments were calibrated using the water signal as an internal reference. The Bruker TopSpin program (Bruker BioSpin, Wissembourg, France) and Sparky (T. D. Goddard and D. G. Kneller, SPARKY 3, University of California, San Francisco) were used to visualize and analyze the NMR spectra.

Heme Plane Determination

In order to determine the normal to each of the hemes of STC, the average plane for each heme was defined by minimizing the distance to the coordinates of the iron and the pyrrole nitrogen atoms extracted from the pdb file (PDB ID: 1M1Q). The normal to this plane was considered the normal of the heme.

Conclusions

Our data show that it is possible to extract RDCs from the heme *meso* protons of multiheme cytochromes that are sufficiently precise to define

a molecular alignment tensor in a cytochrome containing a single structural domain. This opens the opportunity to explore the dynamics in solution of multidomain cytochromes and heme enzymes for which the X-ray structures have been reported by comparing the observed with the expected RDCs. Alternatively, it provides geometric restraints for the relative orientation of hemes in multiheme proteins and enzymes for which structures are not available but for which the electronic structure of the individual hemes can be determined from NMR or EPR data.

Acknowledgements

This work is part of a collaboration under COST Action CM1003. This work was supported by Fundação para a Ciência e a Tecnologia (FCT) – Portugal (Grant PEst-OE/EQB/LA0004/2011). The NMR experiments were performed at the National NMR Facility (CERMAX) supported by Fundação para a Ciência e a Tecnologia (FCT) (RECI/BBB-BQB/0230/2012).

The authors are grateful to Dr. Ivo H. Saraiva for helpful discussions. The *E. coli* strain LS542 used in this study was provided by Dr. Liang Shi and the plasmids pET21a-STC (D2N) and pEC86, used in this work were provided by Dr. Ming Tien and Dr. Linda Thöny-Meyer, respectively.

References

Assfalg, M., Bertini, I., Turano, P., Mauk, A. G., Winkler, J. R., and Gray, H. B. (2003). ^{15}N-^{1}H Residual Dipolar Coupling Analysis of Native and Alkaline-K79A *Saccharomyces cerevisiae* Cytochrome *c*. *Biophys. J.* 84, 3917–3923.

Banci, L., Bertini, I., Huber, J. G., Luchinat, C., and Rosato, A. (1998). Partial Orientation of Oxidized and Reduced Cytochrome *b*5 at High Magnetic Fields: Magnetic Susceptibility Anisotropy Contributions and Consequences for Protein Solution Structure Determination. *J. Am. Chem. Soc.* 120, 12903–12909.

Bertini, I., Del Bianco, C., Gelis, I., Katsaros, N., Luchinat, C., Parigi, G., et al. (2004). Experimentally Exploring the Conformational Space Sampled by Domain Reorientation in Calmodulin. *Proc. Natl. Acad. Sci.* 101, 6841–6846. doi:10.1073/pnas.0308641101.

Bertini, I., and Luchinat, C. (1996). "Chapter I: Introduction," in *Coordination Chemical Reviews*, 1–28.

Bertini, I., Luchinat, C., and Parigi, G. (2002). Magnetic Susceptibility in Paramagnetic NMR. *Prog. Nucl. Magn. Reson. Spectrosc.* 40, 249–273. doi:10.1016/S0079-6565(02)00002-X.

Bertini, I., Luchinat, C., Parigi, G., and Pierattelli, R. (2005). NMR Spectroscopy of Paramagnetic Metalloproteins. *Chembiochem* 6, 1536–1549. doi:10.1002/cbic.200500124.

Clarke, T. A., Cole, J. A., Richardson, D. J., and Hemmings, A. M. (2007). The Crystal Structure of the Pentahaem *c*-type Cytochrome NrfB and Characterization of its Solution-State Interaction with the Pentahaem Nitrite Reductase NrfA. *Biochem. J.* 406, 19–30. doi:10.1042/BJ20070321.

Czjzek, M., ElAntak, L., Zamboni, V., Morelli, X., Dolla, A., Guerlesquin, F., et al. (2002). The Crystal Structure of the Hexadeca-Heme Cytochrome Hmc and a Structural Model of Its Complex with Cytochrome *c*3. *Structure* 10, 1677–1686.

Déméné, H., Tsan, P., Gans, P., and Marion, D. (2000). NMR Determination of the Magnetic Susceptibility Anisotropy of Cytochrome *c*' of *Rhodobacter Capsulatus* by $^{1}J_{HN}$ Dipolar Coupling Constants Measurement: Characterization of Its Monomeric State in Solution. *J. Phys. Chem.* 104, 2559–2569.

Erbil, W. K., Price, M. S., Wemmer, D. E., and Marletta, M. A. (2009). A Structural Basis for H-NOX Signaling in *Shewanella oneidensis* by Trapping a Histidine Kinase Inhibitory Conformation. *Proc. Natl. Acad. Sci.* 106, 19753–19760. doi:10.1073/pnas.0911645106.

Fonseca, B. M., Saraiva, I. H., Paquete, C. M., Soares, C. M., Pacheco, I., Salgueiro, C. A., et al. (2009). The Tetraheme Cytochrome from *Shewanella oneidensis* MR-1 Shows Thermodynamic Bias for Functional Specificity of the Hemes. *J. Biol. Inorg. Chem.* 14, 375–385. doi:10.1007/s00775-008-0455-7.

Fonseca, B. M., Tien, M., Rivera, M., Shi, L., and Louro, R. O. (2012). Efficient and Selective Isotopic Labeling of Hemes to Facilitate the Study of Multiheme Proteins. *Biotechniques* 1–7. doi:10.2144/000113859.

Gordon, E. H. J., Pike, A. D., Hill, A. E., Cuthbertson, P. M., Chapman, S. K., and Reid, G. A. (2000). Identification and Characterization of a Novel Cytochrome *c*3 from *Shewanella frigidimarina* that is Involved in Fe(III) Respiration. *Biochem. J.* 349, 153–158.

Leys, D., Tsapin, A. S., Nealson, K. H., Meyer, T. E., Cusanovich, M. A., and van Beeumen, J. J. (1999). Structure and Mechanism of the Flavocytochrome *c* Fumarate Reductase of *Shewanella putrefaciens* MR-1. *Nat. Struct. Biol.* 6, 1113–1117.

Louro, R. O., Correia, I. J., Brennan, L., Coutinho, I. B., Xavier, A. V., and Turner, D. L. (1998). Electronic Structure of Low-Spin Ferric Porphyrins: ^{13}C NMR Studies of the Influence of Axial Ligand Orientation. *J. Am. Chem. Soc.* 120, 13240–13247. doi:10.1021/ja983102m.

Louro, R. O., Pessanha, M., Reid, G. A., Chapman, S. K., Turner, D. L., and Salgueiro, C. A. (2002). Determination of the Orientation of the Axial Ligands and of the Magnetic Properties of the Haems in the Tetrahaem Ferricytochrome from *Shewanella frigidimarina*. *FEBS Lett.* 531, 520–524.

Nealson, K. H., Belz, A., and McKee, B. (2002). Breathing Metals as a Way of Life: Geobiology in Action. *Antonie Van Leeuwenhoek* 81, 215–222.

Peters, F., Maestre-Martinez, M., Leonov, A., Kovačič, L., Becker, S., Boelens, R., et al. (2011). Cys-Ph-TAHA: a Lanthanide Binding Tag for RDC and PCS Enhanced Protein NMR. *J. Biomol. NMR* 51, 329–337. doi:10.1007/s10858-011-9560-y.

Pokkuluri, P. R., Londer, Y. Y., Duke, N. E. C., Pessanha, M., Yang, X., Orshonsky, V., et al. (2011). Structure of a Novel Dodecaheme Cytochrome *c* from *Geobacter sulfurreducens* Reveals an Extended 12 nm Protein with Interacting Hemes. *J. Struct. Biol.* 174, 223–233. doi:10.1016/j.jsb.2010.11.022.

Prestegard, J. H., Bougault, C. M., and Kishore, A. I. (2004). Residual Dipolar Couplings in Structure Determination of Biomolecules. *Chem. Rev.* 104, 3519–3540. doi:10.1021/cr030419i.

Qian, Y., Paquete, C. M., Louro, R. O., Ross, D. E., LaBelle, E., Bond, D. R., et al. (2011). Mapping the Iron Binding Site(s) on the Small Tetraheme Cytochrome of *Shewanella oneidensis* MR-1. *Biochemistry* 50, 6217–6224. doi:10.1021/bi2005015.

Tolman, J. R., Flanagan, J. M., Kennedy, M. A., and Prestegard, J.H. (1995). Nuclear Magnetic Dipole Interactions in Field-oriented Proteins: Information for Structure Determination in Solution. *Proc. Natl. Acad. Sci.* 92, 9279-9283.

Turner, D. L., Brennan, L., Messias, A. C., Teodoro, M. L., and Xavier, A. V. (2000). Correlation of Empirical Magnetic Susceptibility Tensors and Structure in Low-Spin Haem Proteins. *Eur. Biophys. J.* 29, 104–112.

Wang, J., and Scott, A. I. (1997). An Efficient Synthesis of δ-Aminolevulinic Acid (ALA) and Its Isotopomers. *Tetrahedron Lett.* 38, 739–740.

Williams, G., Clayden, N. J., Moore, G. R., and Williams, R. J. P. (1985). Comparison of the Solution and Crystal Structures of Mitochondrial Cytochrome *c*. *J. Mol. Biol.* 183, 447–460.

Xu, X., Keizers, P. H. J., Reinle, W., Hannemann, F., Bernhardt, R., and Ubbink, M. (2009). Intermolecular Dynamics Studied by Paramagnetic Tagging. *J. Biomol. NMR* 43, 247–254. doi:10.1007/s10858-009-9308-0.

Chapter V

Concluding Remarks

The ability of exoelectrogenic microorganisms to transfer electrons to external insoluble substrates has been the focus of interest of several research teams in the last years (White et al., 2016). *Shewanella* and *Geobacter* have been widely used as model organisms in these studies (Debabov, 2008) to understand how electron transfer pathways are assembled from inside of the cells to the final extracellular electron acceptors. The key players in electron transfer pathways in these two microorganisms are multiheme *c*-type cytochromes that efficiently create redox chains reaching from the cytoplasmic membrane, across the periplasmic space and outer-membrane cytochromes to deliver electrons to insoluble electron acceptors (Bewley et al., 2013).

The work developed in this thesis is focused on clarifying the electron transfer pathways assembled by *Shewanella oneidensis* MR-1 (SOMR-1), either in the periplasmic space towards soluble electron acceptors, such as nitrite, or in the extracellular environment towards insoluble compounds like iron, DMSO or electrode materials (Gralnick and Newman, 2007).

The two most abundant cytochromes found in the periplasmic space of SOMR-1 are STC and FccA (Meyer et al., 2004). These proteins establish two non-communicating electron transfer pathways for the reduction of insoluble compounds, working as an electron carriers (Fonseca et al., 2013).

The work developed in this thesis showed that STC plays a key role in SOMR-1 metabolism, shuttling electrons between several redox partners, by charging and discharging electrons, using the same heme

for both processes. Moreover, competitive binding assays showed that STC and FccA compete for the same docking site of MtrA, a cytochrome that is part of an outer-membrane complex involved in extracellular iron reduction, or at least bind to it in closely related locations (Alves et al., 2015).

Among outer-membrane cytochromes identified in SOMR-1 (Bücking et al., 2012), the emphasis of the work reported in this thesis was towards OmcA, the most abundant cytochrome in the outer-membrane of SOMR-1 (Zhang et al., 2009).

OmcA is able to reduce electron shuttles (indirect electron transfer) and solid electron acceptors directly. Indirect electron transfer is the primary mechanism for the reduction of final substrates (Stolz et al., 2006; Marsili et al., 2008; Kotloski and Gralnick, 2013), using FMN and riboflavin as the major endogenous electron shuttles. Two flavin binding domains were identified in OmcA near heme II and heme VII (Paquete et al., 2014).

The work of this thesis shows that the binding domain near heme VII is affected by changes in the axial ligand of that heme, and that the thermodynamic equilibrium of the electron transfer between OmcA and the electron shuttles is also affected. Furthermore, binding studies of OmcA with solid electron acceptors supported the importance of indirect electron transfer with redox shuttles.

In order to assemble a method that would facilitate the structural characterization of multiheme cytochromes, a strategy was developed

that allows the assessing of the heme architecture inside the cytochrome using NMR. Four heme substituents that define the orientation in space of the heme plane were labelled with ^{13}C and residual dipolar couplings were measured. This method showed for the first time that it is possible to obtain geometric restraints for the relative orientation of multiple hemes in multiheme cytochromes using data obtained from NMR and EPR.

Ultimately, the work described in this thesis contributes to a deeper insight about the electron transfer pathways that occur in SOMR-1. This information is important to guide the rational design of cytochromes tuned-up towards applications of SOMR-1 in microbial electrochemical technologies, providind the opportunity to develop more efficient and sustainable devices using exoelectrogenic organisms.

References

Alves, M. N., Neto, S. E., Alves, A. S., Fonseca, B. M., Carrêlo, A., Pacheco, I., et al. (2015). Characterization of the Periplasmic Redox Network that Sustains the Versatile Anaerobic Metabolism of *Shewanella oneidensis* MR-1. *Front. Microbiol.* 6, 1–10. doi:10.3389/fmicb.2015.00665.

Bewley, K. D., Ellis, K. E., Firer-Sherwood, M. A., and Elliott, S. J. (2013). Multi-Heme Proteins: Nature's Electronic Multi-Purpose Tool. *Biochim.*

Biophys. Acta 1827, 938–948. doi:10.1016/j.bbabio.2013.03.010.

Bücking, C., Piepenbrock, A., Kappler, A., and Gescher, J. (2012). Outer-Membrane Cytochrome-Independent Reduction of Extracellular Electron Acceptors in *Shewanella oneidensis*. *Microbiology* 158, 2144–2157. doi:10.1099/mic.0.058404-0.

Debabov, V. G. (2008). Electricity from Microorganisms. *Microbiology* 77, 123–131. doi:10.1134/S002626170802001X.

Fonseca, B. M., Paquete, C. M., Neto, S. E., Pacheco, I., Soares, C. M., and Louro, R. O. (2013). Mind the Gap: Cytochrome Interactions Reveal Electron Pathways Across the Periplasm of Shewanella oneidensis MR-1. *Biochem. J.* 449, 101–108. doi:10.1042/BJ20121467.

Gralnick, J. A., and Newman, D. K. (2007). Extracellular Respiration. *Mol. Microbiol.* 65, 1–11. doi:10.1111/j.1365-2958.2007.05778.x.

Kotloski, N. J., and Gralnick, J. A. (2013). Flavin Electron Shuttles Dominate Extracellular Electron Transfer by *Shewanella oneidensis*. *MBio* 4. doi:10.1128/mBio.00553-12.

Marsili, E., Baron, D. B., Shikhare, I. D., Coursolle, D., Gralnick, J. A., and Bond, D. R. (2008). *Shewanella* Secretes Flavins that Mediate Extracellular Electron Transfer. *Proc. Natl. Acad. Sci.* 105, 3968–3973. doi:10.1073/pnas.0710525105.

Meyer, T. E., Tsapin, A. I., Vandenberghe, I., de Smet, L., Frishman, D., Nealson, K. H., et al. (2004). Identification of 42 Possible Cytochrome *c*

Genes in the *Shewanella oneidensis* Genome and Characterization of Six Soluble Cytochromes. *Omi. A J. Integr. Biol.* 8, 57–77. doi:10.1089/153623104773547499.

Paquete, C. M., Fonseca, B. M., Cruz, D. R., Pereira, T. M., Pacheco, I., Soares, C. M., et al. (2014). Exploring the Molecular Mechanisms of Electron Shuttling Across the -Microbe/Metal Space. *Front. Microbiol.* 5, 318–330. doi:10.3389/fmicb.2014.00318.

White, G. F., Edwards, M. J., Gomez-Perez, L., Richardson, D. J., Butt, J. N., and Clarke, T. A. (2016). *Mechanisms of Bacterial Extracellular Electron Exchange*. 1st ed. Elsevier Ltd. doi:10.1016/bs.ampbs.2016.02.002.

Zhang, H., Tang, X., Munske, G. R., Tolic, N., Anderson, G. A., and Bruce, J. E. (2009). Identification of Protein-Protein Interactions and Topologies in Living Cells with Chemical Cross-linking and Mass Spectrometry. *Mol. Cell. Proteomics* 8, 409–420. doi:10.1074/mcp.M800232-MCP200.

Appendix 1

Supplementary Figure of Chapter I

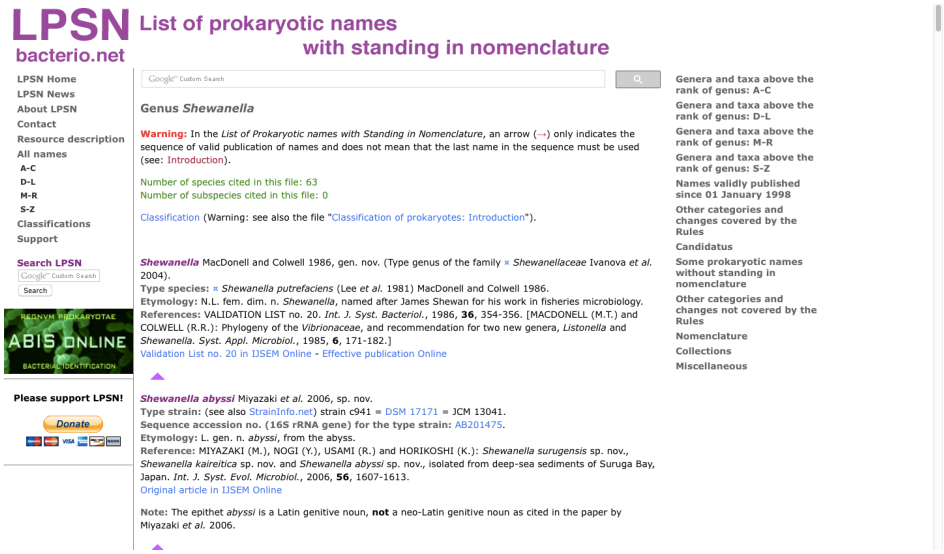

Figure 1. Print screen of the LPSN webpage (**http://www.bacterio.net**) acquired in 23th September 2016.

Appendix 2

Supplementary Figure of Chapter II

Figure 1. STC represented with hemes ordered sequentially from top to bottom showing hemes II, III and IV exposed at the surface. The image was prepared with PyMOL using PDB code 1M1Q.